Effects of Resolvin D1 on Blood-Brain Barrier Disruption Induced by Angiotensin II

by

Ecem AYVAZ GÖLCÜK

A Dissertation Submitted to the Graduate School of Sciences and Engineering in Partial Fulfillment of the Requirements for the Degree of

Doctor of Philosophy

in

Cellular and Molecular Medicine

KOÇ ÜNİVERSİTESİ

July, 2025

Effects of Resolvin D1 on Blood-Brain Barrier Disruption Induced by Angiotensin II

Koç University

Graduate School of Sciences and Engineering

This is to certify that I have examined this copy of a doctoral dissertation by

Ecem Ayvaz Gölcük

and have found that it is complete and satisfactory in all respects, and
that any and all revisions required by the final
examining committee have been made.

Committee Members:

_____

Professor Mehmet Kaya (Advisor)

_____

Professor Bülent Ahıshalı

_____

Professor Helene Girouard

_____

Professor Sacit Karamürsel

_____

Professor Shilpa Buch

Date: 14 July 2025

To my beloved parents and my soulmate ♡

ABSTRACT

Effects of Resolvin D1 on Blood-Brain Barrier Disruption Induced by Angiotensin II

nomen

Doctor of Philosophy in Cellular and Molecular Medicine

July 14, 2025

Chronic hypertension is a major contributor to cerebrovascular dysfunction and the progression of neurodegenerative disease through disruption of the blood-brain barrier (BBB) and neurovascular unit (NVU). Although hypertension can be controlled by antihypertensive medications, therapeutic approaches cannot fully ameliorate the damage to the cardiovascular and cerebrovascular structures. Specialized pro-resolving mediators such as Resolvin D1 (RvD1) have emerged as a promising candidate for improving neuroinflammation and restoring BBB integrity under hypertensive conditions.

In this study, we investigated the therapeutic potential of RvD1 in attenuating BBB disruption induced by chronic hypertension. An in vitro BBB model was established using mouse brain microvascular endothelial cells (bEnd.3) and following Ang (Angiotensin) II and/or RvD1 administration, cell viability, transendothelial electrical resistance (TEER), paracellular permeability of sodium fluorescein (NaFl), and expression of claudin-5, caveolin-1 (Cav-1), and major facilitator superfamily domain 2a (Mfsd2a) were assessed. In parallel, chronic hypertension was induced in mice via Ang II (1000 ng/kg/min) infusion using osmotic mini pumps. Then, hypertensive animals were intraperitoneally treated with RvD1 (3 μg/kg/day) for 5 days. BBB integrity was evaluated via quantification of Alexa Fluor 594 conjugated bovine serum albumin (BSA) leakage and, claudin-5, Cav-1, and Mfsd2a expressions. In addition, Prussian blue staining was performed to assess microvascular damage, and glial fibrillary acidic protein (GFAP) immunofluorescence staining was conducted to evaluate astrogliosis.

Ang II administration resulted in a significant decrease in cell viability and TEER values, accompanied by an increase in NaFl permeability ($p<0.01$). Furthermore, Ang II caused alterations in the paracellular pathway by decreasing claudin-5 and in the transcellular pathway by increasing Cav-1 and decreasing Mfsd2a expression ($p<0.001$). RvD1 treatment remarkably increased TEER values ($p<0.001$), reduced NaFl permeability ($p<0.001$), downregulated Cav-1 ($p<0.01$), and upregulated claudin-5 ($p<0.05$) and Mfsd2a expressions ($p<0.001$) in Ang II-treated cells. In vivo, subcutaneous Ang II-infusion elevated arterial blood pressure, increased Alexa Fluor 594-conjugated BSA leakage, exacerbated microhemorrhages, and astrogliosis as evidenced by increased GFAP intensity in the brain ($p<0.01$). In addition, Cav-1 was upregulated ($p<0.0001$) along with the downregulation of claudin-5 ($p<0.01$) and Mfsd2a ($p<0.05$) in these animals. Following RvD1 administration, arterial blood pressure and BBB permeability of Alexa Fluor-594 conjugated tracer were decreased, and microhemorrhage burden was reduced along with the attenuation of reactive astrocytes ($p<0.01$). Moreover, RvD1

restored tight junctions by increasing claudin-5, and reversed transcytotic shift by decreasing Cav-1 ($p<0.0001$) and increasing Mfsd2a expressions ($p<0.0001$).

In conclusion, our results demonstrate that RvD1 protects BBB integrity under hypertensive conditions. Thus, RvD1 can be a promising therapeutic agent against hypertension-associated cerebrovascular pathologies.

ÖZETÇE

Doktora Tez Başlığı
Discipulus nomen
Hücresel ve Moleküler Tıp, Doktora
14 Temmuz 2025

Kronik hipertansiyon, kan-beyin bariyerinin (KBB) ve nörovasküler ünitenin (NVU) bütünlüğünü bozarak serebrovasküler disfonksiyon ve nörodejeneratif hastalıkların ilerlemesinde önemli bir rol oynar. Antihipertansif ilaçlarla hipertansiyon kontrol altına alınabilse de mevcut tedavi yaklaşımları kardiyovasküler ve serebrovasküler yapılarda oluşan tüm hasarı geri döndüremez. Rezolvin D1 (RvD1) gibi özel çözümleyici aracılar, hipertansif koşullar altında nöroenflamasyonu azaltma/ortadan kaldırma ve KBB bütünlüğünü yeniden sağlama potansiyeli taşıyan umut verici adaylar arasında yer almaktadır.

Bu çalışmada, RvD1'in kronik hipertansiyona bağlı KBB bozulmasını hafifletmedeki terapötik etkisi araştırılmıştır. Fare beyin mikrovasküler endotel hücreleri (bEnd.3) kullanılarak oluşturulan in vitro KBB modelinde hücre canlılığı, transendotelyal elektrik direnci (TEER), sodyum flöresin (NaFl) geçişi ve klaudin-5, kaveolin-1 (Cav-1) ile majör taşıyıcı süper ailesi alan içeren protein 2a (Mfsd2a) protein miktarları tespit edildi. Çalışmanın in vivo kısmında, ozmotik mini pompalar aracılığıyla uygulanan anjiyotensin II (Ang II, 1000 ng/kg/dk) infüzyonu ile kronik hipertansiyon modeli geliştirildi. Bu modele sahip farelere 5 gün boyunca periton içi enjeksiyon yoluyla RvD1 (3 μg/kg/gün) uygulandı. KBB bütünlüğü; Alexa Fluor-594 ile konjuge edilmiş sığır serum albümininin (BSA) sızıntısı, klaudin-5, Cav-1 ve Mfsd2a proteinlerinin kantifikasyonu ile değerlendirildi. Ek olarak, beyindeki mikrovasküler hasarın belirlenmesi amacıyla Prusya mavisi ve astrositozun incelenmesi içinse glial fibriler asidik protein (GFAP) immünofloresan boyaması yapıldı.

Ang II uygulanması, hücre canlılığında ve TEER değerlerinde anlamlı bir azalmaya yol açarken, NaFl geçirgenliğinde artışa neden oldu ($p<0.01$). Ayrıca, Ang II, Cav-1 düzeyini artırarak, klaudin-5 ile Mfsd2a protein miktarlarını azaltarak hem paraselüler hem de transelüler yolakları bozmuştur ($p<0.001$). RvD1 tedavisi, Ang II ile uyarılan hücrelerde TEER değerlerini artırdı ($p<0.001$), NaFl geçirgenliğini azalttı ($p<0.001$), Cav-1 ifadesini baskıladı ($p<0.01$) ve klaudin-5 ($p<0.05$) ile Mfsd2a düzeylerini yükseltti ($p<0.001$). In vivo deney sonuçları incelediğinde, subkutan Ang II infüzyonunun arteriyel kan basıncının yükselmesine, Alexa Fluor-594 ile konjugat BSA sızıntısının, mikrokanama oluşumunun ve GFAP protein miktarının artışına neden olduğu tespit edildi ($p<0.01$). Ek olarak, Ang II, Cav-1 düzeyini yükseltirken ($p<0.0001$), klaudin-5 ($p<0.001$) ve Mfsd2a ($p<0.05$) miktarlarını düşürdü ve geçirgenliği arttırarak KBB bütünlüğünün bozulmasına yola açtı. RvD1 uygulanmasının ardından, arteriyel kan basıncı ve floresan konjugat albümin geçirgenliğinin azaldığı, mikrokanamaların

yatıştırıldığı ve reaktif astrosit aktivitesini baskılandığı gözlendi ($p<0.01$). Ayrıca RvD1 tedavisi, klaudin-5 protein miktarını artırarak sıkı bağlantı bütünlüğünü iyileştirmesinin yanı sıra, Cav-1 protein miktarını azaltıp ($p<0.0001$) Mfsd2a'nınkini artırarak ($p<0.0001$) Ang II'nin yol açtığı KBB hasarının azaltılmasını sağladı.

Sonuç olarak, bu çalışmadan elde edilen veriler RvD1'in hipertansiyon koşullarında KBB bütünlüğünü koruyabildiğini göstermektedir. Bu nedenle RvD1, hipertansiyonla ilişkili serebrovasküler patolojilere karşı potansiyel bir terapötik ajan olarak değerlendirilebilir.

ACKNOWLEDGMENTS

I would like to express my profound gratitude to my advisor, Professor Mehmet Kaya, for his invaluable guidance, constructive feedback, and continuous support throughout my PhD journey. His experience and wisdom were essential to the successful completion of this thesis.

I am also deeply thankful to Professor Bülent Ahıshalı for his extensive knowledge and critical questioning brainstorms, which remarkably enriched my research.

My sincere appreciation also goes to Professor Hélène Girouard and her research team. During my one-year stay at Université de Montréal, she made me feel like a valued member of the team. Her insightful suggestions and encouraging feedback helped shape the direction of this project.

I would like to express my heartfelt thanks to Diane Vallerand for her generous support, broad expertise, and unwavering patience throughout all the challenges I faced.

I am truly thankful to my jury members, Professor Sacit Karamürsel and Professor Shilpa Buch, for their time and valuable comments for refining this thesis.

Moreover, I would like to acknowledge the generous financial support of the Scientific and Technological Research Institution of Turkey (TUBITAK) through the 2214A International Research Fellowship Programme for PhD Students. Spending a year in Montreal was not only a milestone in my academic career as a young scientist but also a deeply personal journey of growth, independence, and cultural discovery across the continents.

I am especially grateful to Elif Sude Duran, Ece Üresin, and Oğuz Çağlar for their friendship, support, and contribution to my work. I also acknowledge the contributions of former members of the MK Lab.

I wish to thank my lovely friends Zeynep Arslantürk and Nazım Berk Demircan for their friendship over more than a decade. Our friendship has been a source of comfort, laughter, and strength throughout the years. Even though we have followed different career paths and sometimes lived in different cities, they have always made me feel supported and wholehearted. I can’t imagine any New Year’s Eve without our joyful and unforgettable celebrations.

I would like to express my heartfelt thanks to Dr. Duygu Aydemir for her unwavering support, valuable advice, and sincere friendship over the past five years. Her scientific guidance and the knowledge she generously shared have had a lasting impact on both my research and personal development.

Furthermore, I would also like to thank my dear friends from ITU- Berkehür Abaylı, Fatih Şekerci, Nazlı Dilara Erdoğdu, Sıla, and Umut Gerlevik. From undergraduate days to the very different corners of the world, we have always supported each other. Even though we moved to different countries, our bond has never faded.

My deepest gratitude goes to my parents, Derya and Aydın Ayvaz; this is more than a simple appreciation because they are the unofficial owners of this thesis. Without their devotion, encouragement, and endless support, I could have never imagined becoming a PhD. During the most difficult and frustrating moments of my life, they were always there to lift me up. Always be by my side, no matter what.

One of the heartfelt thanks goes to my beloved soulmate, Dr. Mert Gölcük, the one who walked with me through every chapter of this journey. Together, we have overcome a pandemic, a wedding, a qualifier exam, and now a PhD dissertation. This is yet another milestone in our journey, overcoming a long-distance relationship. Whenever I felt lost, you were always there to motivate me. When I was down, you found a way to cheer me up. When I felt like giving up, you reminded me of my strength. Be my forever best friend, playmate, and my other half.

Finally, I would like to express my deepest gratitude to myself. Navigating the long and demanding journey of this thesis required resilience, patience, and a commitment to move forward despite moments of doubt and discouragement. Throughout the five years, I have learned not only to overcome scientific challenges but also to grow stronger in the face of professional adversity. These challenges shaped my strength and taught me to believe in myself. Reaching this point stands as a proud reminder to myself that determination and an unwavering stance can carry you forward.

TABLE OF CONTENTS

ABSTRACT **4**
ÖZETÇE **6**
ACKNOWLEDGMENTS **8**
TABLE OF CONTENTS **10**
LIST OF TABLES **12**
LIST OF FIGURES **13**
ABBREVIATIONS **15**
CHAPTER 1 INTRODUCTION **1**
1.1 The Neurovascular Unit 1
1.2 Endothelial Cells and Blood-Brain Barrier 2
1.2.1 Junctional complexes 3
1.2.2 Transport pathways across the blood-brain barrier 4
1.3 Circumventricular organs 8
1.4 Pericytes 8
1.5 Astrocytes 9
1.6 Microglia 10
1.7 Neurons 11
1.8 Hypertension and Its Impact on the Neurovascular Unit Cells 11
1.8.1 Overview of Hypertension 11
1.8.2 Hypertension-Induced Damage to the Neurovascular Unit Cells 13
1.8.2.1 Neuroinflammation 13
1.8.2.2 Endothelial Dysfunction and Oxidative Stress 15
1.8.2.3 Cognitive Impairment 16
1.8.3 Hypertensive Animal Models 17
1.9 Specialized Pro-Resolving Mediators 18
1.9.1 Inflammation and Resolution 18
1.9.2 Overview of Specialized Pro-Resolving Mediators and Resolvin D1 19
1.10 Hypothesis 21
CHAPTER 2 MATERIALS **23**
CHAPTER 3 METHODS **26**
3.1 In vitro experimentation 26
3.1.1 In-vitro blood-brain barrier model using transwell 27
3.1.2 Angiotensin II and Resolvin D1 administration 27
3.1.3 CellTiter Glo Luminescent Cell Viability Assay 27
3.1.4 Trans-endothelial electrical resistance measurement and sodium-fluorescein

permeability assay 27
3.1.5 Immunofluorescence staining of proteins involved in transcellular and paracellular transport 28
3.2 In vivo experimentation 28
3.2.1 Angiotensin II-induced hypertension model 29
3.2.2 Non-invasive arterial blood pressure measurement 29
3.2.3 Resolvin D1 administration 30
3.2.4 Assessment of the BBB permeability 30
3.2.5 Microhemorrhage detection 30
3.2.6 Immunofluorescence staining of proteins involved in transcellular and paracellular transport 31
3.2.7 Glial fibrillary acidic protein immunofluorescence staining 31
3.3 Statistical analysis 32
CHAPTER 4 RESULTS 33
4.1 In vitro experimentation 33
4.1.1 Dose-dependent effects of Angiotensin II 33
4.1.2 Dose-dependent effects of Resolvin D1 upon Angiotensin II disruption 34
4.1.3 Immunofluorescence staining 35
4.2 In vivo experimentation 37
4.2.1 Non-invasive blood pressure measurements 37
4.2.2 Microhemorrhage detection using Prussian blue 38
4.2.3 Assessment of the BBB permeability using bovine serum albumin Alexa-Fluor 594 conjugate administration 39
4.2.4 Immunofluorescence staining of junctional and transport proteins Claudin-5 Immunofluorescence Staining 41
4.2.5 Mfsd2a Immunofluorescence staining 42
4.2.6 Caveolin-1 Immunofluorescence Staining 43
4.2.7 Astrogliosis assessment using GFAP 44
CHAPTER 5 DISCUSSION 46
CHAPTER 6 CONCLUSION 52
BIBLIOGRAPHY 53

LIST OF TABLES

Table 2.1: Cell line used in experiments..... 23
Table 2.2: List of chemicals used in experiments..... 23
Table 2.3: List of antibodies used in experiments. 24
Table 2.4: List of devices..... 24
Table 2.5: List of laboratory equipment used in experiments. 25

LIST OF FIGURES

Figure 1.1: Schematic representation of the NVU (created with biorender.com).... 2

Figure 1.2: Transport systems across the blood-brain barrier (adapted from (Ohtsuki et al., 2007)) 5

Figure 1.3: The renin-angiotensin system pathway..... 12

Figure 1.4: Specialized Pro-resolving mediators produced from arachidonic acid, eicosapentaenoic acid, and docosahexaenoic acid (Sousa & Barbosa, 2023) 19

Figure 3.1 Representative workflow of in vitro experiments (created with biorender.com)..... 26

Figure 3.2 Schematic representation of in vivo experiment workflow (created with biorender.com)..... 29

Figure 4.1 Dose-dependent effects of ANG II on bEnd.3 cells by conducting CTG assay, TEER, and NaFl permeability assay. Bars represent mean ± SD (p<0.01, *** p<0.001, **** p<0.0001).. 33**

Figure 4.2 Dose-dependent effects of 25, 50, 75 ng/mL RvD1 upon Ang II administration to bend.3 cells by performing CTG assay, TEER, and NaFl permeability assay. Bars represent mean ± SD (*p<0.05, **p<0.01, *** p<0.001, **** p<0.0001). 34

Figure 4.3 Representative images and quantitative fluorescence intensity analysis of claudin-5 in bEnd.3 cells. Bars represent mean ± SD (*p<0.05, *** p<0.001, **** p<0.0001). 35

Figure 4.4. Representative images and the fluorescence intensity analysis of Cav-1 in bEnd.3 cells. Bars represent mean ± SD (p<0.01, ****p<0.0001)..... 36**

Figure 4.5. Representative images and the quantitative analysis of Mfsd2a in bEnd.3 cells. Bars represent mean ± SD (*p<0.001, ****p<0.0001) 36**

Figure 4.6. Systolic, diastolic, and mean arterial blood pressure changes among the experimental groups at day 0, 5, 10, and 15. Bars represent mean ± SD (n = 14-15 mice per group; *p<0.05, **p<0.01, ***p<0.001, ****p<0.0001). 37

Figure 4.7. Systolic, diastolic, and mean arterial blood pressure changes in all animal groups over the experiment period. Data is represented as mean ± standard deviation; n=14-15/group, *p<0.05, **p<0.01, ***p<0.001, ****p<0.0001). 38

Figure 4.8. Microhemorrhage detection revealed by Prussian blue staining. Representative coronal sections show Prussian blue-positive deposits (blue) in each group. Quantification of Prussian blue-positive area per section. Bars represent mean ± SD (n = 7–8 mice per group; *p<0.05, **p<0.01, ***p<0.001) 38

Figure 4.9. Left panel. Mouse brain p222 from the Allen brain atlas. Center panel. Quantification of Alexa Fluor 594-positive pixels within the cerebral cortex of 4

experimental groups. Right panel. Representative images for Alexa Fluor 594-conjugated BSA (red color) content in the cerebral cortex. Bars represent mean ± SD (n=5/group, ****p<0.0001). 39

Figure 4.10: Left panel. Mouse brain p273 from the Allen brain atlas. Upper right panel. Quantification of Alexa Fluor 594 positive pixels within the cerebral cortex and representative images for Alexa Fluor 594 conjugated BSA (red color) content. Lower right panel. Quantification of Alexa Fluor 594 positive pixels within the hippocampal region and representative images for Alexa Fluor 594 conjugated BSA. Bars represent mean ± SD (n=5/group; **p<0.01, ****p<0.0001) 40

Figure 4.11: Left panel. Mouse brain p376 from the Allen brain atlas. Center panel. Quantification of Alexa Fluor 594-positive pixels within the brains of 4 experimental groups. Right panel. Representative images for Alexa Fluor 594 conjugated BSA (red color) content. Bars represent mean ± SD (n = 5 mice per group; ****p<0.0001) 41

Figure 4.12: Claudin-5 immunofluorescence staining and quantitative analysis. Bars represent mean ± SD (n=5 mice/group; **p<0.01, ****p<0.0001) 42

Figure 4.13: Mfsd2a immunofluorescence staining and quantitative analysis. Bars represent mean ± SD (n=5/group; *p<0.05, ****p<0.0001). 43

Figure 4.14: Caveolin-1 immunofluorescence staining and quantitative analysis. Bars represent mean ± SD (n=5/group, ****p<0.0001). 44

Figure 4.15: GFAP immunofluorescence staining and quantitative analysis. Bars represent mean ± SD (n=7-8/group, **p<0.01, ***p<0.001). 45

ABBREVIATIONS

BBB	Blood-Brain Barrier
TNF-α	Tumor Necrosis Factor Alpha
2K1C	Two-Kidney, One-Clamp
ABC	ATP-Binding Cassette
ACE	Angiotensin-Converting Enzyme
ACKR1	Atypical Chemokine Receptor 1
ALS	Amyotrophic Lateral Sclerosis
Ang	Angiotensin
ANOVA	Analysis Of Variance
AP	Area Postrema
AT1R	Angiotensin Type 1 Receptor
AT2R	Angiotensin Type 2 Receptor
BCRP	Breast-Cancer Resistance Protein
BSA	Bovine Serum Albumin
CBF	Cerebral Blood Flow
CCL2	C-C Motif Ligand-2
CMT	Carrier-Mediated Transcytosis
CNS	Central Nervous System
CSF	Cerebrospinal Fluid
CSVD	Cerebral Small Vessel Disease
CTG	Celltiter Glo
CVO	Circumventricular organs
DBP	Diastolic Blood Pressure
DHA	Docosahexaenoic Acid
DMEM	Dulbecco's Modified Eagle's Medium
DOCA	Deoxycorticosterone Acetate
EAATs	Excitatory Amino Acid Transporters
eNOS	Endothelial Nitric Oxide Synthase
EPA	Eicosapentaenoic Acid
FBS	Fetal Bovine Serum
GFAP	Glial Fibrillary Acidic Protein
Glut1	Glucose Transporter 1
H0	Null Hypothesis
IL	Interleukin
JAM	Junctional Adhesion Molecule
KUTTAM	Koç University Research Center for Translational Medicine

LAT1	Large Neutral Amino Acid Transporter
LIF1	Leukemia Inhibitory Factor 1
L-NAME	L-N^G-Nitro arginine methyl ester
LRP1	Lipoprotein Receptor-Related Protein 1
MCP-1	Monocyte Chemoattractant Protein-1
ME	Median Eminence
Mfsd2a	Major Facilitator Superfamily Domain-Containing Protein 2a
MMP	Matrix Metalloproteinase
MS	Multiple Sclerosis
NGS	Normal Goat Serum
NO	Nitric Oxide
NOX2	NADPH Oxidase 2
NTS	Nucleus Of the Solitary Tract
NVU	Neurovascular Unit
PDGFRβ	Platelet-Derived Growth Factor Receptor Beta
PFA	Paraformaldehyde
P-gp	P-Glycoprotein
PICALM	Phosphatidylinositol Binding Clathrin Assembly Protein
PVN	Paraventricular Nucleus
RMT	Receptor-Mediated Transcytosis
RNS	Reactive Nitrogen Species
ROS	Reactive Oxygen Species
RVLM	Rostral Ventrolateral Medulla
SHRs	Spontaneous Hypertensive Rats
SPMs	Specialized Pro-Resolving Mediators
TEER	Trans Endothelial Electrical Resistance
TLR4	Toll-Like Receptor 4
VEGF	Vascular Endothelial Growth Factor
WHO	World Health Organization
ZO	Zonula Occludens

CHAPTER 1
INTRODUCTION

The brain serves as the primary control center of the body, managing cognitive skills, motor functions, and sensory adaptation. The vital functions of the brain are mainly maintained by the blood-brain barrier (BBB). The brain homeostasis is affected by alterations in vascular morphology, cerebral blood flow (CBF), and disruptions in the elements of the neurovascular unit (NVU) (Rowsthorn et al., 2023). The loss of BBB integrity leads to cerebrovascular diseases, such as epilepsy and cerebral small vessel disease (CSVD). Disruptive damage within the small cerebral vessels is associated with chronic hypertension, stroke, and neurodegenerative diseases (Mogi, 2024; Presa et al., 2020).

1.1 The Neurovascular Unit

The main structural and functional unit of the brain is the NVU, which is responsible for providing nutrition and energy supply, clearing the metabolites, cellular trafficking, and maintaining brain homeostasis and dynamic blood flow (Iadecola, 2017). The NVU is established by the morphological and molecular interactions of endothelial cells with pericytes, astrocytes, and neurons (Figure 1; Abbott et al., 2010a; Weiss et al., 2009).

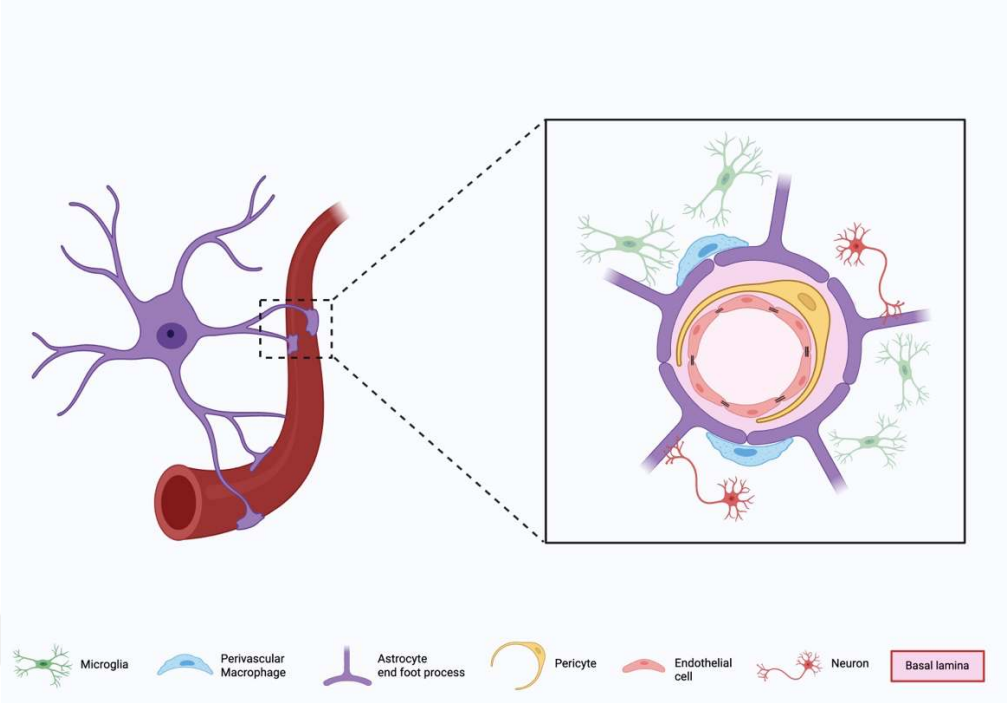

Figure 1.1: Schematic representation of the NVU (created with biorender.com).

1.2 Endothelial Cells and Blood-Brain Barrier

The BBB is a compartment constituted by blood microvessel endothelial cells that separates the brain and blood circulation. The BBB not only protects brain parenchyma from blood-borne biological molecules such as hormones, neurotransmitters, xenobiotics, and neurotoxic compounds or circulating cells such as leukocytes, neutrophils and lymphocytes, but also provides essential nutrients to the brain via component-specific transporters, maintains ionic balance and neural homeostasis (Abbott, 2002; Abbott & Romero, 1996; Hawkins & Davis, 2005). Endothelial cells need to interact with NVU cells, like pericytes, astrocytes, and neurons, to develop and maintain their BBB characteristics.

The first attempt to demonstrate the existence of the BBB was made by Paul Ehrlich (Ehrlich, 1885). Ehrlich injected a dye into the blood circulation to track the staining pattern in the entire body. Interestingly, all organs were stained except the brain and spinal cord. Afterward, Goldmann administered trypan blue to the cerebrospinal fluid (CSF) instead of the blood circulation (Goldmann, 1912). Therefore, all the brain cells were stained this time, but trypan blue could not enter the blood circulation and stained the peripheral organs. These experiments provided evidence for the existence of a

selective barrier that controls the substance exchange between blood and brain parenchyma.

Brain microvessel endothelial cells have a more compact lining than peripheral endothelial layers (Abbott & Romero, 1996). Brain microvascular endothelial cells are interconnected with junctional complexes, which include tight and adherens junctions. Tight junctions (TJs) restrict paracellular passage and provide high trans endothelial electrical resistance (TEER) across the cell layer (Helms et al., 2016). Brain endothelial cells have high electrical resistance and act as a physical barrier, but they also exhibit efflux and metabolic barrier properties with special transporter systems and drug-metabolizing enzymes. Barrier-type endothelial cells have no fenestrae, which limit the passage of substances, and they lack pinocytotic activity for transcytotic transport (Petty & Lo, 2002). These cells have special transporter systems that pump toxic molecules back into the blood or facilitate the passage of substances like glucose or amino acids. Besides, lipophilic molecules use transcellular pathways, and specialized transporter systems deliver nutrients and essential metabolites. Barrier-type endothelial cells have a high number of mitochondria correlated with high energy demand compared to peripheral-type endothelial cells (Abbott et al., 2010b). TJ complexes control paracellular transport between endothelial cells and maintain cell polarity by separating apical and basolateral membranes. The tightness of the endothelial cell layer can be evaluated by TEER and permeability assays using hydrophilic tracer molecules ranging from low- to high- molecular weights, including sodium fluorescein (NaFl; 376 Da), lucifer yellow (444 Da), dextrans of various molecular weights (4, 10, 20, 40, and 70 kDa), horseradish peroxidae (44 kDa), Evans blue-bound albumin (69 kDa), Alexa Fluor conjugated albumin and immunoglobulins G (150 kDa) (Scalisi et al., 2021).

1.2.1 Junctional complexes

Adherens and TJs physically work together to limit paracellular permeability and crosstalk, thereby maintaining the integrity of the barrier-type endothelial cell by supporting TJ formation and mechanical organization. Adherens junctions are transmembrane proteins connected with scaffolding proteins called catenin within the cytoplasm and provide cell-cell adhesion between the endothelial cell layers (Cerutti & Ridley, 2017).

TJs are located closer to the apical side of the intercellular cleft and are responsible for sealing the paracellular passage between neighboring endothelial cells. Claudins,

occludin, and junctional adhesion molecule (JAM) protein families form TJs (Lampugnani, 2012; Martìn-Padura et al., 1998).

Claudins are the major protein family that constitutes TJs with 27 different isoforms. Claudin-5 is ubiquitously expressed in all vasculatures and plays a key role in assembling TJs and BBB regulation (Ohtsuki et al., 2007). Claudin 1, 3, and 12 (molecular weight 21-25 kDa) are found in the barrier-type microvessel endothelial cells, but their expression levels are lower compared to claudin-5 (Komarova et al., 2017; Wolburg et al., 2003). One of the most significant studies highlighting the critical role of claudin-5 in TJ formation demonstrated that claudin-5 knockout is lethal due to excessive BBB permeability, which leads to detrimental developmental defects (Nitta et al., 2003).

Occludin is a 65 kDa tetraspan transmembrane protein that regulates paracellular permeability through its phosphorylation and ubiquitination (Furuse et al., 1993). Occludin's sealing role is still disputable in the literature. However, it has been clearly known that occludin content is lower in non-brain endothelial cells, and this enlightened the role of occludin in TJ assembly in barrier-type endothelial cells (Persidsky et al., 2006). Data from in vivo and in vitro studies show that occludin-knockout mice develop various histological abnormalities such as chronic inflammation, brain microvessel calcification and growth retardation but its BBB remain intact. These results reveal that further studies are required to elucidate the exact mechanism of occludin's role in the regulation of TJs and BBB integrity (Cong & Kong, 2020).

The zonula occludens (ZO) family consists of cytoplasmic scaffolding proteins with three members: ZO-1, ZO-2, and ZO-3 (Haskins et al., 1998; Jesaitis & Goodenough, 1994; Stevenson et al., 1986). This protein family connects TJ proteins with actin filaments to enhance barrier properties (Fanning et al., 1998; Nasdala et al., 2002; Tornavaca et al., 2015). Numerous studies have shown that paracellular permeability increases with ZO-1 downregulation under hypoxia and inflammatory conditions (Ma et al., 2013; Moskal & Michalak, 2025; Yu et al., 2023). Furthermore, ZO-1 knockout mice could not survive during the embryonic period (Chen et al., 2019). Therefore, ZO-1 plays a crucial role in forming functional TJs and facilitating communication between TJs and intracellular signaling.

1.2.2 Transport pathways across the blood-brain barrier

Since the transport of substances across the BBB is limited, alternative pathways are necessary to fulfill the metabolic requirements of the brain by supplying nutrients and

removing waste products through blood flow (Langen et al., 2019). These alternative pathways include passive diffusion, solute carriers/transporters, transcytosis, ABC efflux transporters, and monocellular cell migration via diapedesis (Figure 2).

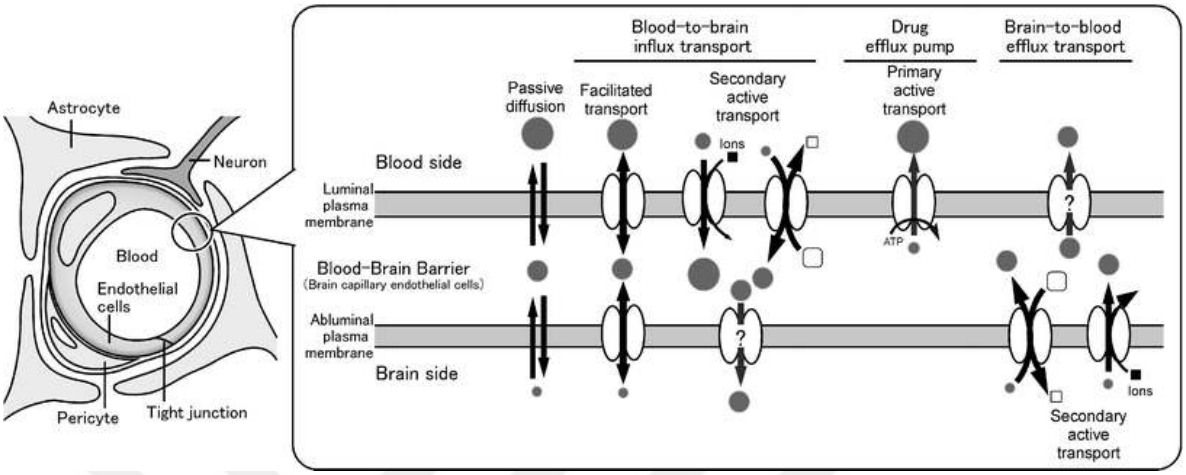

Figure 1.2: Transport systems across the blood-brain barrier (adapted from (Ohtsuki et al., 2007)**)**

Lipid-soluble, non-polar molecules, or blood gases such as carbon dioxide and oxygen, move down their concentration gradients via passive diffusion. However, molecules essential for neural homeostasis and brain nutrition include water-soluble and polar substances such as glucose, amino acids, hormones, ions, and nucleotides, as well as hydrophobic molecules like fatty acids, which require specific transporters located on either the apical or basolateral surface of the endothelial membrane to facilitate passage across the BBB, (Abbott et al., 2010b). One of the most crucial transporters is glucose transporter 1 (Glut1), which delivers glucose from the blood to the brain through the BBB. Glut-1 deficiency results in lethal embryonic abnormalities, barrier disruption, and insufficient amyloid beta clearance, all of which contribute to Alzheimer's disease (Langen et al., 2019; Yazdani et al., 2019). Large neutral amino acid transporter (LAT1) is highly abundant in endothelial cells and facilitates the uptake of amino acids into the brain (Singh & Ecker, 2018). In addition to utilizing gradient differences, some efflux transporters consume energy to remove neurotoxic compounds from the brain parenchyma. For example, excitatory amino acid transporters (EAATs), located on the abluminal side of the BBB, are responsible for transporting excitotoxic amino acids, such as glutamate and aspartate, out of the brain (Zaragozá, 2020).

Carrier-mediated transcytosis (CMT) is driven by the solute carrier proteins, which are

specialized to facilitate the transport of vital nutrients such as glucose, amino acids, and fatty acids into the parenchyma (Liu et al., 2025a).

Receptor-mediated transcytosis (RMT) is one of the most selective pathways that provides the passage of large essential molecules across the BBB endothelial cells (Ayloo & Gu, 2019). Peptides and growth factors act as ligands and bind to highly selective receptors. Receptor-ligand interaction initiates the endocytosis via clathrin-coated vesicles. Internalized vesicles are degraded, recycled, or delivered to the brain parenchyma (Pulgar, 2019; Sweeney et al., 2019a). This shuttle mechanism is also used to deliver therapeutic reagents to the targeted brain regions. In "Trojan horse strategies", a specific drug molecule is conjugated to the ligands, which can bind to the luminal receptors like transferrin, insulin, and low-density lipoprotein receptor-related protein 1 (LRP1) to bypass the highly selective endothelial barrier (Liu et al., 2025b; Pardridge, 2023).

Receptor-mediated transcytosis relies on two types of vesicular pathways: clathrin- and caveolin-mediated transcytosis. Clathrin-mediated transcytosis is driven by the vesicles coated by the polymer structure of clathrin proteins on the cytoplasmic surface of the membrane (Kadlecova et al., 2017). Clathrin-coated vesicle formation is triggered by the ligand-receptor binding, like LRP1 and phosphatidylinositol binding clathrin assembly protein (PICALM), which is employed in the amyloid-ß protein clearance (Ando et al., 2022; Siddiqui et al., 2022).

Caveolae-mediated transcytosis occurs via flask-shaped invaginations within the membrane called caveolae. Cholesterol, sphingolipids, and caveolin-1 (Cav-1) proteins are highly abundant in the structure of caveolae (Zhou et al., 2021). In contrast to clathrin-mediated endocytosis, caveolar transcytosis is mostly receptor-independent and provides nonselective transport of large proteins across the endothelial cells, such as albumin (Sorets et al., 2020). Under physiological conditions, caveolae formation is suppressed for the tight regulation of the BBB using major facilitator superfamily domain-containing protein 2a (Mfsd2a) (Andreone et al., 2017; Eser Ocak et al., 2020). In pathological conditions or neurological diseases such as ischemia, atherosclerosis, multiple sclerosis (MS), and hypertension, caveolae formation is increased and causes BBB impairment due to high infiltration of substances from blood to the brain (Iadecola, 2013; Jasmin et al., 2007; Puddu et al., 2023; Wang et al., 2018; Yang et al., 2025).

Major facilitator superfamily domain-containing protein 2a is a membrane transport protein that is highly expressed in the brain microvascular endothelial cells, mainly in

the capillary side. Specifically, Mfsd2a regulates the lipid metabolism and the transport of essential omega-3 fatty acids such as docosahexaenoic acid (DHA) to the brain parenchyma (Zhao & Zlokovic, 2014). Genetically modified experimental results revealed that Mfsd2a gene ablation causes DHA deficits and BBB impairment through increased levels of caveolae-mediated transcytosis within the brain (Ben-Zvi et al., 2014; Chow & Gu, 2017). Accordingly, Mfsd2a negatively regulates the caveolae-mediated transcytosis by regulating Cav-1 expression, contributes to the restricted lipid transport, and protects BBB integrity (Betsholtz, 2014).

Multiple ATP-binding cassette (ABC) transporters, especially P-glycoprotein (P-gp), breast-cancer resistance protein (BCRP), and other multidrug-resistance-associated proteins (MRPs), are highly expressed at the luminal side of the barrier-type endothelial cell membranes (Miller, 2015). ABC transporters restrict the transport of blood-driven substances, endogenous metabolites, and xenobiotics, including targeted therapeutic drugs, by pumping them back into the bloodstream (Baltira et al., 2024). Although these ATP-driven efflux pumps hamper the drug delivery to the brain, they lead to the emergence of drug resistance. Hence, ABC transporters are the major obstacle in the treatment of neurodegenerative diseases such as dementia, epilepsy, and Alzheimer's disease (Mohi-ud-Din et al., 2022; Zlokovic, 2011).

Barrier-type endothelial cells are also responsible for metabolic barrier functions through special enzymes such as cytochrome P450, gamma-glutamyl transferase, and alkaline phosphatase (Abbott, 2013). These enzymes are predominantly located on the luminal surface of the barrier endothelial cells and are responsible for metabolizing drugs and neurotoxic compounds within the bloodstream (Kadry et al., 2020). Like ABC transporters, metabolic barrier activity also challenges the brain-targeting therapies by limiting the drug delivery across the BBB. Cytochrome P450 metabolizes most anti-epileptic drugs, and this causes drug-resistant epilepsy (Ghosh et al., 2010).

Brain parenchyma is highly privileged against the entry of pathogens and immune cells from the bloodstream. Unlike peripheral endothelial cells, barrier-type endothelial cells present a unique receptor, atypical chemokine receptor 1 (ACKR1), which transports chemokines across the blood microvessels (Marchetti et al., 2022). Diapedesis, or the movement of immune cells, is strictly limited across the BBB. Mononuclear cells can only enter the brain parenchyma during embryonic development through the endothelial cells and subsequently develop into central nervous system (CNS) resident immune cells, known as microglia. However, under pathological conditions such as MS or autoimmune

encephalomyelitis, the disruption of TJs, along with tumor necrosis factor alpha (TNF-α) and matrix metalloproteinase (MMP) activation, leads to the infiltration of pro-inflammatory cytokines and other immune cells into the brain via paracellular transport (Mapunda et al., 2022; Song et al., 2015).

1.3 Circumventricular organs

Circumventricular organs (CVOs) are special brain regions distributed along the third and fourth ventricles. Their microvessels are highly permeable, and their endothelial cells have fenestrations, which increase the permeability (Kaur & Ling, 2017). Unlike endothelial cells of the BBB, they lack TJs such as claudin-5, occludin, and ZO-1, which maintain the barrier integrity (Pfau et al., 2024). CVOs are divided into two categories: sensory and secretory CVOs. Sensory CVOs, comprised of the three main regions, which are the subfornical organ, organum vasculosum of the lamina terminalis, and area postrema (Yao et al., 2025). These sensory CVOs control the osmolarity, secretion of hormones such as angiotensin II (Ang II), cytokines, and adjust thirst, blood pressure, and body temperature. In contrast, secretory CVOs include the median eminence (ME), neurohypophysis, pineal gland, and subcommissural organ, which release neurohormones such as vasopressin, oxytocin, and melatonin directly into the bloodstream (Morita & Miyata, 2012).

1.4 Pericytes

Pericytes are specialized mural cells embedded within the basal lamina of capillaries, making close contact with endothelial cells through N-cadherin and connexin 43 hemichannels, also known as “peg-and-socket” junctions. These junctions modulate nutrient transport and signal transduction (Liebner et al., 2018). Platelet-derived growth factor receptor beta (PDGFRβ) is consistently expressed on pericytes and serves as a marker for identifying them, facilitating their survival, proliferation, and attachment to blood vessels. Impaired PDGFRβ signaling within the brain contributes to hypertension, Alzheimer’s disease, and MS (Li & Fan, 2023; Miners et al., 2019).

Pericytes resemble smooth muscle cells surrounding the arteries by regulating the vessel diameter through vasoconstriction and vasodilation in response to neuronal stimulation and metabolic requirements (Dalkara & Alarcon-Martinez, 2015). In addition to their roles in structural and vascular tone modulation, pericytes help maintain BBB integrity by stabilizing endothelial cells, suppressing transcytosis, and limiting the

filtration of immune cells into the brain. Loss or dysfunction of pericytes leads to BBB breakdown, increased permeability, and the entry of blood-borne neurotoxic molecules, resulting in neuronal degeneration, which contributes to the pathogenesis of Amyotrophic Lateral Sclerosis (ALS), Alzheimer's disease, dementia, stroke, and traumatic brain injury (TBI) (Li & Fan, 2023).

Animal models with ablated pericytes exhibited hypoperfusion, compromised BBB integrity, and disrupted neurovascular coupling. Additionally, the absence of pericytes causes vascular instability in both peripheral and cerebral microvessels, resulting in hypertension and insufficient blood flow regulation. The loss of pericytes exacerbates oxidative stress and inflammation, leading to vascular and neuronal damage (Kisler et al., 2017; Santos et al., 2019).

1.5 Astrocytes

Astrocytes are the most abundant glial cells in the CNS and are essential components of the NVU, playing crucial roles in the development and maintenance of the BBB. They participate in the formation and stabilization of the vascular network during developmental stages (Cheslow & Alvarez, 2016). Astrocytes ensheathe the endothelial-pericyte complex with their end feet, providing physical support and modulating the integrity of TJs by secreting signaling molecules. Signaling molecules secreted by astrocytes, such as Sonic hedgehog, glial-derived neurotrophic factor, and angiopoietin-1, enhance TJ protein expression by increasing TEER values and reducing paracellular transport across the BBB. Barrier-type endothelial cells secrete leukemia inhibitory factor 1 (LIF1), which upregulates glial fibrillary acidic protein (GFAP) expression and leads to astrocyte differentiation (Engelhardt & Liebner, 2014). Astrocytes also regulate water homeostasis via Aquaporin-4 and Kir4.1 potassium channels within their end feet (Gu, 2016). Additionally, astrocytes play a critical role in the clearance of excess glutamate from the synaptic cleft through their specialized transporters, such as excitatory amino acid transporters, which help maintain neuronal homeostasis (Durkee & Araque, 2019). Impaired clearance mechanism promotes excitotoxicity by the excessive glutamate accumulation, and this causes progression of several neurological diseases such as ALS, Alzheimer's disease, and epilepsy (Andersen et al., 2022).

Under certain pathologies, the integrity of endothelial TJs is disrupted, allowing the passage of albumin-like proteins into the parenchyma. Following the entrance of blood-

borne substances, astrocytes undergo reactive gliosis and have dual behavior in regulating the BBB. In the first scenario, reactive astrocytes begin to secrete sonic hedgehog protein, which increases BBB integrity and inhibits immune cell migration (Wang et al., 2021). In another scenario, reactive astrocytes release pro-inflammatory molecules like interleukin (IL)-1β, IL-6, and vascular endothelial growth factor (VEGF), and these substances trigger infiltration of immune cells into the brain by deteriorating BBB integrity (Nagata & Yamasaki, 2024). Activated astrocytes can also trigger the activation of microglia and neuronal damage. Astrogliosis is highly correlated with the severity of BBB damage in chronic brain disorders/diseases such as dementia, Alzheimer's disease, and TBI (Alvarez et al., 2013; Zhang et al., 2023).

1.6 Microglia

During brain angiogenesis, peripheral macrophages migrate into the brain and become resident immune cells called microglia. Under physiological conditions, microglia have a ramified structure to survey the parenchyma against pathogens and protect it from infections (McConnell & Mishra, 2022; Prinz et al., 2019). However, microglia get activated under pathological conditions such as hypertension. Upon activation, microglia turn into their pro-inflammatory phenotype, which secretes pro-inflammatory cytokines, leading to neuroinflammation and cerebrovascular damage (L. Liu et al., 2020).

Angiotensin II plays the primary role in the emergence of hypertension. Under a hypertensive state, elevated blood pressure activates the microglial pro-inflammatory response through the interaction of Ang II receptors on microglia, and thereby, this contributes to neuroinflammation (Zhang et al., 2021). Althammer et.al. revealed that hypertension-related neuroinflammation can be alleviated through the Ang II receptor blockage, resulting in the recovery of BBB integrity (Althammer et al., 2024).

Activated microglia secrete inflammatory mediators such as TNF-α, IL-1β, and IL-6 (Bajwa & Klegeris, 2022; Jurga et al., 2020). Additionally, those microglia with an inflammatory phenotype induce the release of MMPs. Released cytokines and MMPs by activated microglia trigger the microgliosis and neuroinflammation, causing endothelial dysfunction, TJ disruption, and consequently BBB damage (Prado et al., 2021; Ribeiro Vitorino et al., 2023). Moreover, activation of microglia also increases the production of reactive oxygen (ROS) and nitrogen species (RNS) which trigger oxidative and nitrosative stress, tight junctional protein disruption and BBB impairment (Sorriento et al., 2018; Valko et al., 2007; Wang et al., 2025).

In the light of clinical evidence, hypertension-induced neuroinflammation and BBB impairment increase the risk of cerebrovascular diseases, cognitive impairment, and emerging neurodegenerative diseases (Colombari et al., 2025; Wang et al., 2022a).

1.7 Neurons

Neurons are the principal component of the NVU but have no direct contact with endothelial cells in the adult brain; instead, they release several signal molecules and neurotransmitters to influence the barrier-type endothelial cells. Neurons are vital for communication throughout the CNS, the regulation of CBF, and neurovascular coupling (Schaeffer & Iadecola, 2021). During the late embryonic and postnatal phases, while astrocytes are still not fully developed, neurons establish close interactions with endothelial cells, contributing to the formation of the BBB (Langen et al., 2019). Neurons stimulate CBF through secreted neurotransmitters, such as glutamate, which initially activate astrocytes to release nitric oxide and then trigger the downstream pathways for vasodilation (Schaeffer & Iadecola, 2021; Zhao et al., 2022).

Neurons and brain microvascular endothelial cells provide positive feedback to each other for the development and maintenance of BBB integrity and regulation of neuronal homeostasis (Lacoste et al., 2014). However, when the BBB is damaged in pathological conditions, neuronal homeostasis is disrupted by neurotoxic proteins and inflammatory molecules entering the brain parenchyma from circulation, causing neurodegeneration. In the progression of Alzheimer's Disease, BBB impairment results in the accumulation of amyloid-beta proteins within the parenchyma. Protein aggregation causes neuronal injury and cognitive decline (Yue & Man Hoi, 2023). As for epilepsy, BBB integrity is compromised due to the hyperexcitable behavior of neurons, which induces neuroinflammation and neuronal death (van Vliet et al., 2007).

1.8 Hypertension and Its Impact on the Neurovascular Unit Cells

1.8.1 Overview of Hypertension

According to the World Health Organization (WHO), arterial hypertension is one of the significant consequences of cardiovascular diseases and increases the tendency to ischemia and stroke in the brain (Williams et al., 2018). Hypertension is defined as a chronic condition characterized by elevated arterial blood pressure on the vessel wall, and this pressure is measured as systolic blood pressure (SBP) ≥ 140 mmHg and diastolic

blood pressure (DBP) ≥ 90 mmHg (Hansen et al., 2022).

The renin-angiotensin system (RAS) is a complex system that regulates blood pressure, extracellular volume, and cardiovascular function through the interaction of nervous and endocrine systems. RAS comprises multiple peptides such as angiotensinogen, renin, and Ang II (Figure 3) (Lavoie & Sigmund, 2003). The peptides of RAS are found in the brain, kidney, and heart, and impairments in tissue-specific RAS cause cardiovascular diseases and other pathological conditions. Renin cleaves the Angiotensinogen into the Ang I (Santos et al., 2018). Ang I undergoes further cleavage by angiotensin-converting enzyme (ACE) to produce Ang II. Moreover, Ang II is converted to Ang III and IV by aminopeptidase A and N cleavage, respectively (te Riet et al., 2015).

Circulating Ang II stimulates various downstream pathways by binding its receptors, type 1 receptor (AT1R) and type 2 receptor (AT2R) (Baraldi et al., 2015). Interaction between Ang II and AT1R leads to the emergence of chronic hypertension by increasing blood pressure, whereas with AT2R, Ang II mediates vasodilatation, leading to blood pressure decrease, and anti-inflammatory response (Assersen et al., 2020; Elsaafien et al., 2020). AT2Rs are dominantly expressed by the GABAergic neurons in the cardiovascular control centers in the brain, which inhibit the sympathic nerve activation and decrease blood pressure (de Kloet et al., 2016).

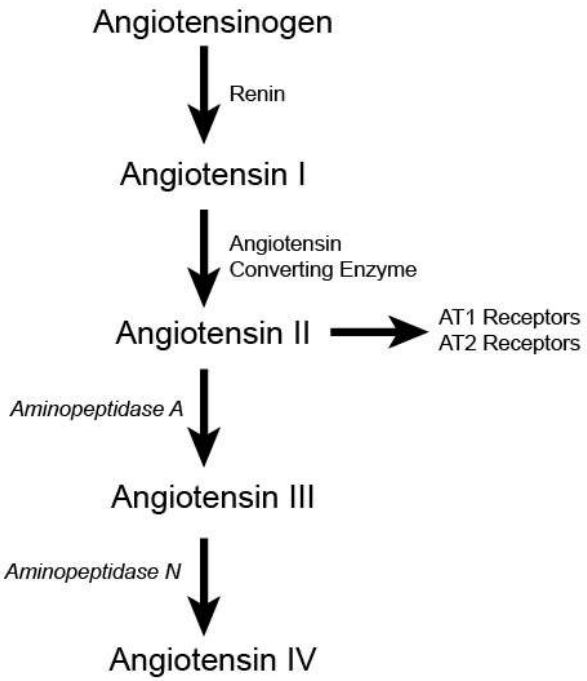

Figure 1.3: The renin-angiotensin system pathway

AT1Rs are predominantly found in the autonomic brain regions, such as the paraventricular nucleus (PVN), the nucleus of the solitary tract (NTS), the area postrema (AP), and the rostral ventrolateral medulla (RVLM) (Braga et al., 2011). AT1Rs are G-protein-coupled receptors and are located on the cell membrane. Ang II/AT1R interaction activates downstream targets, including inositol triphosphate, vasoconstriction, sodium and water reabsorption, and aldosterone secretion, which increase blood pressure (Miller & Arnold, 2019). Activation of the AT1R causes an elevation in sympathetic activity, which stimulates neuroinflammation through the activation of microglia and the secretion of pro-inflammatory cytokines. Furthermore, the hypertension-related inflammatory state causes BBB impairment by increasing permeability across the endothelial barrier (Haspula & Clark, 2018).

Chronic hypertension has a cardiovascular impact on the body and becomes a significant risk factor for the brain's blood microvessels (Daugherty, 2021). In the literature, researchers have focused on the mechanical, structural, and molecular changes in the walls of the brain microvessels in chronic hypertensive conditions (Iadecola et al., 2016). High blood pressure leads to decreased blood flow, endothelial dysfunction, increased oxidative stress, microhemorrhages, and brain edema. These structural and functional alterations in the endothelial cells of the brain microvasculature pave the way for brain atrophy and dementia (Daugherty, 2021; Iadecola et al., 2016; Ishida et al., 2006; Kerkhofs et al., 2020; Loewenstein & Rabbat, 2021; Shekhar et al., 2017).

1.8.2 Hypertension-Induced Damage to the Neurovascular Unit Cells

1.8.2.1 Neuroinflammation

Neurogenic hypertension contributes to the upregulation of pro-inflammatory cytokine and chemokine secretion, such as TNF-α, IL-1β, IL-6, C-C motif ligand-2 (CCL2), and downregulation of the anti-inflammatory cytokines production, like IL-10 (Haspula & Clark, 2018; Koizumi et al., 2025). Constitutive activation of inflammatory pathways exacerbates immune cell migration into the brain, leading to neuroinflammation by activating microglia and astrocytes. Those glial cells get activated and secrete pro-inflammatory cytokines like TNF-α, IL-1β, and IL-6 (Shi et al., 2010). Notably, the inhibition of microglial activation in transgenic mice has been shown to lower blood pressure and decrease the levels of TNF-α and IL-1β in the PVN of the hypertensive mice

(Liu et al., 2023; Santisteban et al., 2015).

Inhibition of Toll-like receptor 4 (TLR4) in the PVN reduces the pro-inflammatory cytokine production and upregulates the anti-inflammatory cytokines (Dange et al., 2015). Additionally, TLR4 is mostly expressed in microglia and promotes neuroinflammation by activating TLR4 through the Ang II/AT1R interaction (Biancardi et al., 2016; Lee et al., 2013). A TLR4 inhibitor called TAK242 administration inhibits the microglial activation and protects BBB integrity in the spontaneous hypertensive rats (SHRs) (Biancardi et al., 2016). In another study, TLR4/ NF-κB inhibition suppressed astrogliosis, reduced pro-inflammatory cytokine release, and mitigated neuroinflammation (Xue et al., 2025). Microglial activation contributes to the increased production of ROS, which further exacerbates BBB impairment and neuroinflammation (Mowry et al., 2021; Yao et al., 2013).

In addition to microglia, astrocytes play a crucial role in the emergence of neuroinflammation and hypertension by amplifying signals from the RAS (Sofroniew, 2015). Astrocytes regulate neurotransmitter clearance, maintenance of BBB integrity, and synaptic transmission. Under hypertensive conditions, astrocytes become reactive, which is called astrogliosis. Astrogliosis is characterized by cellular hypertrophy and upregulation of the GFAP (Silver & Miller, 2004; Verkhratsky & Nedergaard, 2018). Activated astrocytes promote neuroinflammation by triggering inflammatory pathways, such as NF-κB and JAK/STAT3 (Wang et al., 2013; Wanner et al., 2013). Additionally, the upregulation of pro-inflammatory cytokines, such as IL-1β and TNF-α, and the monocyte chemoattractant protein-1 (MCP-1), along with the downregulation of anti-inflammatory cytokines, including IL-10, exacerbates neuroinflammation (Lee et al., 2023; Norden et al., 2014; Xanthos & Sandkühler, 2014). In transgenic mice, astrocyte-derived IL-10 is overproduced and therefore attenuates inflammation by converting surrounding microglia into an anti-inflammatory state (Shanaki-Bavarsad et al., 2022). Moreover, Ang II stimulation elevates ROS production and induces mitochondrial dysfunction. Astrocytes also release VEGF-A that enhances immune cell infiltration and downregulates the TJ proteins. Consequently, those factors compromise the BBB integrity and promote sympathoexcitation by disrupting neuron-astrocyte interaction (Argaw et al., 2012; Stern et al., 2016). Severe neuroinflammation enhances sympathetic activity and elevates blood pressure by damaging cardiovascular regulatory brain regions like PVN (Wei et al., 2024a; Winklewski et al., 2015).

Accumulated data have shown that glial cells have key roles in the emergence of

hypertensive pathogenesis through the regulation of oxidative stress and neuroinflammation (Poulet et al., 2006; Wang et al., 2022b; Wei et al., 2024b). Immune cell recruitment through the compromised BBB upregulates inflammatory cytokine secretion. This feed-forward loop of microglial and astrocyte activation, immune cell migration, and elevated blood pressure through neuronal overactivation leads to chronic hypertension (Wang et al., 2022).

1.8.2.2 Endothelial Dysfunction and Oxidative Stress

Oxidative stress is a critical mediator that disrupts BBB integrity and induces hypertension through the activation of AT1Rs. Endothelial nitric oxide synthase (eNOS) produces nitric oxide (NO), which is an essential molecule for vasodilation and vascular integrity (Forstermann & Sessa, 2012). Additionally, neuronal NO contributes to the regulation of memory, cognition, and brain plasticity (Wigner et al., 2022). Nitric oxide mediates vascular smooth muscle relaxation via activating c-GMP downstream pathways and regulates CBF. The release of neuronal potassium into the interstitial area triggers hyperpolarization within the endothelial junctions and facilitates the relaxation of smooth muscle cells (Kraehling & Sessa, 2017; Longden et al., 2017). In the hypertensive state, an impaired NO/ROS balance with enhanced vasoconstriction and inflammation contributes to endothelial dysfunction. Ang II interacts with its receptor, AT1R, on endothelial cells and leads to the decreased expression of sirtuin-3. Dikalov et. al suggest that the localization of sirtuin-3 decreased, ROS production increased, and these alterations led to mitochondrial oxidative stress (Dikalov et al., 2014). On the other hand, Ang II activates the NADPH oxidase 2 (NOX2) on the endothelial membrane. NOX2 generates superoxide radicals, which cause mitochondrial damage, exacerbate oxidative stress, and ultimately activate cell death mechanisms (Ajoolabady et al., 2024; Pueyo et al., 2000). Increased oxidative stress activates the NF-κB pathway and thereby increases the release of pro-inflammatory cytokines. Overall, oxidative stress and AT1R activation compromise BBB integrity by disrupting TJ proteins such as claudin-5, occludin, ZO-1, and enhancing extravasation of plasma proteins (Takata et al., 2021). Consequently, hyperactivated sympathetic stimulation, elevated ROS, and inflammatory mediators led to hypertension-related neurotoxicity and brain injury (Biswas, 2016; Nozoe et al., 2008).

Additionally, astrocytes and microglia regulate the ROS production and antioxidant mechanisms. Hypertension-induced microglial activation exacerbates ROS production, sympathoexcitation, and inflammation, which causes BBB impairment (Gowrisankar &

Clark, 2016; Wu et al., 2012).

Overall, excessive ROS production, lower levels of NO, and elevated oxidative stress levels cause endothelial dysfunction, hypertension, and end-organ damage. In the therapeutic field, antioxidants are the potential candidates to revert the oxidant production to its physiological level and alleviate the inflammation upon hypertensive-induced organ damage (Amponsah-Offeh et al., 2023).

1.8.2.3 Cognitive Impairment

Clinical studies have demonstrated that midlife hypertension is highly correlated with late-life cognitive impairment, dementia, and stroke predisposition (Clark et al., 2019; Iadecola & Gottesman, 2019).

Hypertension causes the impairment of NVU elements by disrupting the functionality of the endothelial cells, astrocytes, and neurons. Consequently, alterations in BBB and NVU cells lead to neuroinflammation, uncontrolled oxidative stress, cognitive dysfunction, and ultimately, neurodegenerative diseases like ischemia, Alzheimer's disease, and dementia.

Hypertension-induced endothelial dysfunction contributes to cognitive decline by impairing vasodilation, leading to the emergence of brain microhemorrhages and lesions. Patients with hypertension-related BBB dysfunction may lead to brain injury and cerebral small vessel disease (Muñoz Maniega et al., 2017; Nezu et al., 2015; Sargurupremraj et al., 2020; Solé-Guardia et al., 2025)

Under physiological conditions, clearance of amyloid-beta from the brain is primarily driven by LRP1, which is expressed in barrier endothelial cells. One of the recent studies demonstrated that hypertension downregulates the LRP1 expression and thereby accelerates the accumulation of amyloid plaques (Sweeney et al., 2019). Moreover, AQP4 channels, which are mainly located in astrocytic end-feet, serve the removal of metabolic waste products within the brain. Hypertension diminishes the rate of CBF and impairs the glymphatic clearance mechanism of toxic products such as amyloid-beta peptides and phosphorylated tau (Harrison et al., 2020; Pajewski et al., 2022; Rasmussen et al., 2022).

Uncontrolled blood pressure increase contributes to the amyloid plaque accumulation within the brain (Cifuentes et al., 2015). Amyloid deposition causes one of the major neurodegenerative diseases, Alzheimer's disease. In Ang II-induced hypertensive mouse models, elevated blood pressure has been reported to promote amyloid beta tangle

formation, increase microhemorrhage burden, exacerbate cognitive decline, and thereby lead to the emergence of neurodegenerative diseases such as Alzheimer's disease (Faraco et al., 2016; Gannon et al., 2024; Ungvari et al., 2021). Increased blood pressure is also correlated with white matter hyperintensities, cortical atrophy, reduced volume in the hippocampus and prefrontal cortex, which are critical regions for cognition (de Montgolfier et al., 2020; Faraco et al., 2016; Solé-Guardia et al., 2025). Moreover, impaired vascular autoregulation and insufficient cerebral perfusion result in neuronal injury. Altered neuronal homeostasis elicits cognitive deficits, problematic executive daily tasks, and slower motor functions (Baggeroer et al., 2024; Cheon, 2022).

1.8.3 Hypertensive Animal Models

Hypertensive animal models are widely used for investigating the complex pathology underlying hypertension. Acute hypertensive models can be established in a short time, but the changes in blood pressure are transient. This pattern allows investigating the immediate responses upon the stimulation, such as baroreceptor activity, and acute endothelial changes (Xu & Sved, 2002). One of the common models is acute intraperitoneal or intravenous administration of vasoactive agents such as adrenaline, phenylephrine, noradrenaline, or Ang II (Rajanathan et al., 2022; Zubcevic et al., 2017). These models reveal the underlying mechanisms associated with acute oxidative stress, eNOS uncoupling, and sympathetic nervous system activation (Zhang et al., 2004).

Chronic models represent the long-term pathophysiological hypertensive mechanisms within the human body, especially vascular remodelling, inflammation, and BBB impairment (Lerman et al., 2019). The Ang II infusion model is one of the most studied models in the hypertensive research field. Subcutaneous placement of the Ang II-filled osmotic minipumps provides constitutive infusion and induces chronic hypertension (Atis et al., 2022; Yang et al., 2021). This model is also suitable for investigating the vascular oxidative stress and immune cell infiltration into the brain regions (Lu et al., 2020; Sumitomo-Ueda et al., 2010).

Another well-studied model is a genetic model called SHR. Progressive cardiac hypertrophy and alterations in the structure of blood microvessels are developed in this model (Nabika et al., 2012). SHRs represent the early symptoms of hypertension, endothelial dysfunction, and cerebrovascular damage. Mostly, SHRs are used to model the hypertension-related neurodegeneration and cognitive decline (Leong et al., 2015).

Other models, such as the DOCA-Salt model, combine deoxycorticosterone acetate (DOCA) with high-salt intake and nephrectomy. This model leads to reduced renal oxygen levels, elevated oxygen consumption, disrupted tubular transport mechanisms (Kuczeriszka & Wąsowicz, 2022) (Kuczeriszka & Wąsowicz, 2022). However, the DOCA-salt model is widely applied to large animals like pigs, sheep, and primates (Basting & Lazartigues, 2017). In another experimental model, L-NAME (L-N^G-Nitro arginine methyl ester) is administered to increase vascular tone, induce endothelial dysfunction, and cause hypertension by inhibiting all major NOS isoforms (eNOS, nNOS, and iNOS) (Paulis et al., 2008).

The L-NAME model is often studied in metabolic syndrome, aging-related disorder/disease, and BBB integrity (Kalayci et al., 2005; Kaya et al., 2003; Kopincová et al., 2012). Goldblatt developed a unique hypertension model that constricts one of the renal arteries, called the "two-kidney, one-clamp (2K1C) model (Goldblatt et al., 1934). This model is used to understand the volume-pressure control in various species such as rats, dogs, and rabbits (Johnson et al., 2002).

1.9 Specialized Pro-Resolving Mediators

1.9.1 Inflammation and Resolution

Inflammation is a biological response triggered by exposure to pathogens or toxic substances. This process, acute inflammation, aims to eliminate the destructive effects of stimuli, clear out the metabolic waste, and initiate tissue repair. A typical inflammation has three stages: initiation, resolution, and post-resolution.

The initiation phase of inflammation leads to the production of pro-inflammatory mediators, such as cytokines, chemokines, and prostaglandins, as well as the recruitment of neutrophils (Alfaro et al., 2022). Neutrophils neutralize and help remove the initiator stimuli. At the end of the initiation phase, macrophages eliminate the apoptotic neutrophils, and specialized pro-resolving mediators (SPMs), such as resolvins and lipoxins, are released to initiate resolution (Serhan et al., 2024; Soliman et al., 2025). During the resolution phase, monocyte-derived macrophages clear pro-inflammatory mediators and promote the transition of macrophages into an anti-inflammatory phenotype (Woodburn et al., 2021). In the post-resolution phase, acute inflammation is alleviated by the release of anti-inflammatory cytokines, such as IL-10 and TGF-β, as well as the recruitment of adaptive immune cells (Massagué & Sheppard, 2023;

Panigrahy et al., 2021). However, under certain pathological conditions, inflammatory cytokine secretion and macrophage activation drive the acute stage inflammation into the chronic phase (Zhang et al., 2023). Chronic inflammation causes tissue damage, vascular remodeling and dysfunction (Lopez-Candales et al., 2017). This impairment provokes various autoimmune, cardiovascular, metabolic, and neurodegenerative disorders/diseases, such as hypertension, atherosclerosis, diabetes, and Alzheimer's disease (Dash et al., 2025).

1.9.2 Overview of Specialized Pro-Resolving Mediators and Resolvin D1

Specialized pro-resolving mediators are lipid-derived molecules synthesized from polyunsaturated fatty acids such as arachidonic acid, eicosapentaenoic acid (EPA), and DHA, and are essential contributors to the acute inflammation's resolution phase (Serhan, 2014). SPMs are endogenous mediators that are classified into 4 families: lipoxins, resolvins, protectins, and maresins (Figure 4, Sousa & Barbosa, 2023). Those SPM families are involved in the augmentation of the innate immune system response, clearance of pathogens, and protection of specific organs (Serhan & Levy, 2018). Rather than suppressing the immune system, using SPMs as immunoresolvents has the potential to be a promising therapeutic approach.

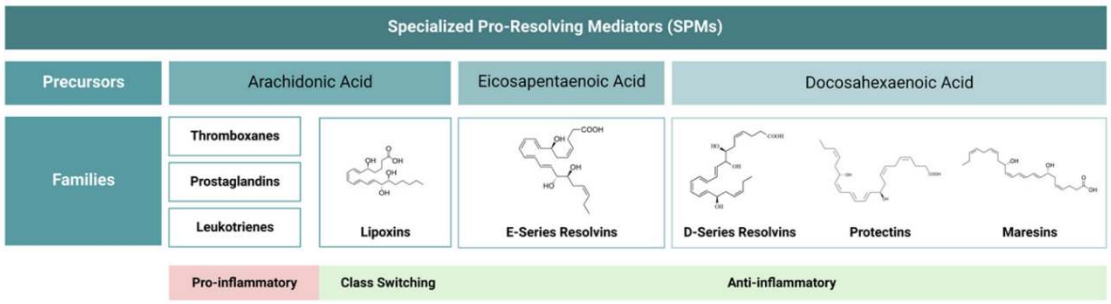

Figure 1.4: Specialized Pro-resolving mediators produced from arachidonic acid, eicosapentaenoic acid, and docosahexaenoic acid (Sousa & Barbosa, 2023)

Resolvins are divided into D- and E-series, which are derived from DHA and EPA, respectively. Resolvin (RvD) family has specific G-protein coupled receptors named ALX/FPR2, GPR32, and ChemR23 (Arita et al., 2005; Krishnamoorthy et al., 2010; Serhan et al., 2002, 2004, 2008; Shalini et al., 2018). It binds through ALX/FPR2 receptor on the cell membrane, regulates the specific miRNAs in the NF-κB pathway, and helps to induce resolution of the inflammatory conditions (Recchiuti et al., 2011; Rey et al., 2016a).

RvD1 exhibits its biological effects through binding to G-protein-coupled receptors: ALX/FPR2 and GPR32. RvD1 binding to its receptors leads to suppression of the NF-κB pathway, downregulation of NLRP3 inflammasome and pro-inflammatory gene expression, and reduction of leukocyte adhesion molecules like ICAM-1. In addition, RvD1 receptors induce anti-inflammatory cytokine release and anti-inflammatory macrophage polarization (Wei et al., 2021a). RvD1-loaded gelatin methacrylate therapy facilitates the resolution of inflammation by decreasing pro-inflammatory cytokines and promoting the release of anti-inflammatory molecules in periodontitis (Xing et al., 2024).

Under pathological conditions, resolvins can suppress IL-6, IL-1β, and TNF-α production, and alleviate inflammation by increasing prostaglandin D2 synthesis upon LPS-induced microglial activation (Gao et al., 2017; Rey et al., 2016b). In TBI, aspirin-triggered RvD1 improves motor and cognitive damage; RvE1 increases post-traumatic sleep in mouse models (J. L. Harrison et al., 2015). Terrando et al reported that RvD1 improved brain inflammation, activated gliosis, synaptic dysfunction, and memory deficits after surgery-induced cognitive decline by modulating IL-6 and TNF-α (Terrando et al., 2013). RvD1 induces the phagocytosis of amyloid plaques and helps to resolve the unfolded protein response in patients with mild cognitive impairment (Olivera-Perez et al., 2017). Furthermore, RvD1 administration preserved the mitochondrial function of the astrocytes, lowered excessive ROS production, inhibited apoptotic stimulation, and attenuated cognitive impairment following TBI (Ren et al., 2020).

RvD1 limits the neutrophil infiltration, suppresses both microgliosis and astrogliosis, and decreases the TNF-α, IL-6, and IL-1β gene expression via inhibition of the TLR4/NF-kB pathway (Bisicchia et al., 2018; Rey et al., 2016b; Yanoshita et al., 2025). In subarachnoid hemorrhage models, RvD1 notably improves the neurological score, reduces brain edema, and ameliorates BBB impairment by reducing the neutrophil recruitment, microglial and astrocytic activation, and pro-inflammatory mediators (Liu et al., 2021). Mechanistically, RvD1 administration significantly reduced Evans blue extravasation, inhibited NLRP3 inflammasome activation, downregulated the MMP-9 levels, and upregulated anti-inflammatory protein complexes such as A20 with TJ proteins such as claudin-5, occludin, and ZO-1 (Wei et al., 2021). Hence, these results highlight the neuroprotective and anti-inflammatory properties of RvD1.

In neuropathic pain models, RvD1 alleviates neuroinflammation by reducing brain-derived neurotrophic factor production in activated microglia (Bo et al., 2025). One of

the recent studies showed that RvD1 treatment alleviates neuroinflammation by decreasing pro-inflammatory cytokine expression in the hippocampus and attenuates the cognitive impairment in diabetic rats with cognitive deficiency (Sun et al., 2021). Moreover, combinatorial therapy using RvD1 and exercise significantly decreased neuronal apoptosis and enhanced neuroplasticity by activating the BDNF/PI3K/Akt signaling pathway. Thereby, RvD1 contributes to the attenuation of inflammation-induced BBB disruption and improvement of the neurological outcomes (Xiaoyu et al., 2024).

Additionally, RvD1 also shows restorative effects in ischemic conditions. A recent study demonstrated that RvD1 administration inhibited apoptotic pathways, mitigated the inflammation, and prevented ischemic damage in Wistar albino rats (Chen et al., 2020). After receiving Belimumab therapy, RvD1 plasma levels of systemic lupus erythematosus patients significantly increased. Additionally, the disease progression was attenuated and their response to therapy was improved (Wang et al., 2025). Chen et al. elucidated that serum RvD1 levels in acute ischemic stroke patients serve as a prognostic biomarker for neurofunctional recovery. Their results showed that lower serum levels of RvD1 were associated with severe clinical outcomes and inadequate resolution, which causes compromised BBB integrity and uncontrolled neuroinflammation (Chen et al., 2023).

In hypertension, RvD1 has been widely used as a novel therapeutic candidate to alleviate the symptoms and secondary injuries. A recent study highlighted that RvD1 decreases both systolic and diastolic blood pressure in Ang II-induced hypertensive mice. Additionally, RvD1 administration inhibits the proliferation of vascular smooth muscle cells, reduces aorta thickness and collagen deposition, which are the major hallmarks of hypertension-related vascular pathology (Wei et al., 2024a).

Overall, the accumulated data suggest that RvD1 is a promising therapeutic candidate by targeting vascular remodeling, activated inflammatory pathways, and brain homeostasis, particularly in metabolic and neurologic pathologies.

1.10 Hypothesis

The impact of anti-hypertensive drugs on BBB integrity has been extensively investigated. However, the underlying mechanistic explanations for their protective effects on the BBB integrity remain limited (Kalayci et al., 2005; Mamo et al., 2017). We suggest that RvD1 could play a crucial role in protecting BBB integrity, particularly

in chronic hypertensive conditions. Nevertheless, the specific effects of RvD1 on endothelial cell function in barrier-type brain microvessels are not clear yet. Due to its small lipophilic nature, RvD1 can easily cross the BBB. Thus, RvD1 could alleviate the effects of systemic inflammation on BBB endothelial cells and suppress oxidative processes and neuroinflammation within the brain.

The expected findings of this study will have the potential to shed light on the underlying mechanisms and treatment of secondary disorders related to hypertension. The protective or preventive effects of RvD1 on disrupted BBB integrity may serve as a precursor to protect the brain, a significant target organ in hypertensive patients worldwide. Moreover, if RvD1 can effectively reduce both the influx of substances from the blood into the brain and the production of cytokines and oxidative agents by intrinsic brain mechanisms, it may have the potential to prevent the onset of various neurodegenerative disorders/diseases, including hypertension.

Overall, we hypothesized that RvD1 ameliorates BBB disruption induced by chronic hypertension. The corresponding null hypothesis (H_0) is that RvD1 has no significant effect on the hypertension-related BBB impairment.

CHAPTER 2
MATERIALS

Cell lines, chemicals, antibodies, laboratory equipment, and devices are listed in Tables 2.1, 2.2, 2.3, and 2.4.

Cell Line

Table 2.1: Cell line used in experiments.

Name	Type	Brand	CAT #
bEnd.3	Endothelial cell	ATCC	CRL-2299

Chemicals

Table 2.2: List of chemicals used in experiments.

Name	Brand	CAT #
Alexa-Fluor 594 conjugated bovine serum albumin	Invitrogen	A13101
Angiotensin II	Sigma Aldrich	A9525
Bovine Serum Albumin	Capricorn Scientific	BSA-1T
CellTiter-Glo Luminescent Cell Viability Assay	Promega	G7570
cOmplete, Mini, EDTA-free Protease Inhibitor Cocktail	Roche	11836170001
DMEM High Glucose	Multicell	319-005
DMSO	Sigma	6195067
DPBS	Biowest	L0615-500
Ethanol	ISOLAB	64-17-5
Fetal Bovine Serum	Biowest	S181H-500
Fluorescein Sodium Salt	Sigma Aldrich	F6377
Glycerol	Sigma Aldrich	49782
Hoechst 33342	Thermo Fisher	62249
L-Glutamine	Biowest	6194078
Normal Goat Serum	Sigma Aldrich	P9416

Nuclear fast red	Sigma Aldrich	N3020
Paraformaldehyde	Sigma Aldrich	158127
Penicillin-Streptomycin	Biowest	L0018-100
Pepsin	MP Biomedical	195367
Potassium ferrocyanide	BioShop	PFC232
Resolvin D1	Cayman Chemical	10012554
Triton X-100	Fisher Bioreagent	BP151-100
Trypan Blue	Thermo Fisher Scientific	6195080
Trypsin-EDTA (0.25 % v/v)	Wisent Bioproducts	325-043-EL

Antibodies

Table 2.3: List of antibodies used in experiments.

Name	**Brand**	**CAT #**
Caveolin-1 (D46G3) Rabbit mAb	Cell Signaling	3267
Claudin 5 (4C3C2) Mouse mAb	Invitrogen	35-2500
GFAP (GA5) Mouse mAb	Millipore	MAB3402
Goat anti-Mouse IgG Secondary Antibody, Alexa Fluor™ 488	Invitrogen	A11029
Goat anti-Rabbit IgG Secondary Antibody, Alexa Fluor™ 488	Invitrogen	A11008
Mfsd2a (E8U2O) Rabbit mAb	Cell Signaling	80302
Mfsd2a Rabbit Polyclonal Antibody	Invitrogen	PA5-21049

Table 2.4: List of devices

Name	**Brand**	**Model**
Brightfield Inverted Microscope	Nikon	ECLIPSE Ti2
CODA Noninvasive Blood Pressure Device	Kent Scientific	CODA-HT4
Confocal Microscope	Leica	TCS SP8
Cryostat	Leica	CM1950
Microplate reader	Biotek	Synergy H1
Millicell Voltohmmeter	Merck Millipore	ERS-2
Mini osmotic pump	ALZET	1004
Slide Scanner	Zeiss	AxioScan 8
Vibratome	Leica	VT1000S
Voltohmmeter	EVOM	EVM-MT-03-02

Laboratory Equipment

Table 2.5: List of laboratory equipment used in experiments.

Name	**Brand**
24-well Plate	Sarstedt
24-well TC Inserts, 0.4 μm	Sarstedt
TC Petri dish, 10 cm	Sarstedt
96-well Black Sided Bottom Plate	Costar
96-well Plate	Sarstedt
Centrifugation	Thermo Fisher Scientific
Biosafety Cabinet	Labconco
Coverslips	Thermo Fisher Scientific
Superfrost Slides	Thermo Fisher Scientific
S220 pH Meter	Mettler Toledo
Synergy H1 Microplate Reader	Bio Tek Instrument
T75 Flask	Sarstedt
TC Incubator	Eppendorf

CHAPTER 3
METHODS

3.1 In vitro experimentation

Mouse brain microvessel endothelial cells (bEnd.3- ATCC CRL-2299) were cultured in Dulbecco's modified Eagle's medium (DMEM; 4.5 g/L; Wisent Inc, Saint-Jean-Baptiste, Quebec, Canada) supplemented with 10 % heat-inactivated fetal bovine serum (FBS), 1 % penicillin-streptomycin, and 1 % L-glutamine. The cells were kept in a humidified 37°C incubator containing 10 % CO2. Once reaching 85-90% confluency, the cells were subcultured using 0.25% trypsin/EDTA. All experiments were performed with bEnd.3 cell line between passages 6 and 9, and the cells were controlled for mycoplasma contamination by KUTTAM. A representative workflow of in vitro experiments is shown in Figure 1.

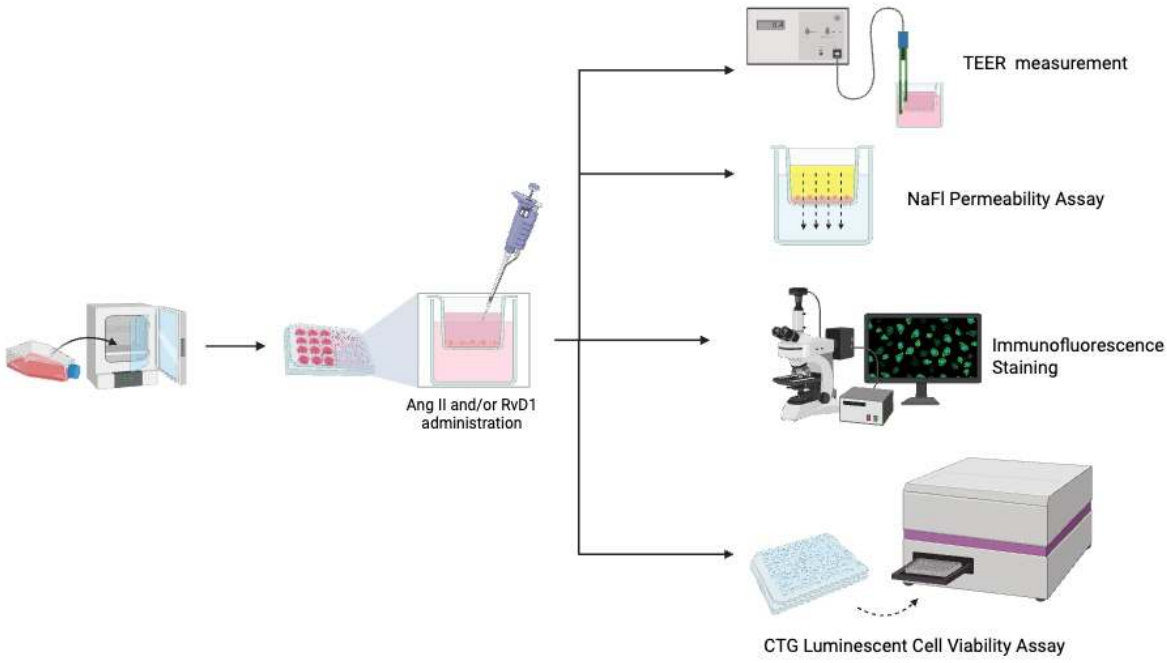

Figure 3.1 Representative workflow of in vitro experiments (created with biorender.com)

3.1.1 In-vitro blood-brain barrier model using transwell

An in vitro culture model was established using bEnd.3 to investigate Ang II and/or RvD1. Confluent bEnd.3 cells were seeded onto transwells with 0.4 μm pore size (Sarstedt AG & Co. KG, Germany) compatible with 24-well plates. bEnd.3 cells were seeded into the luminal side and incubated in a transwell system for 3 days to construct a proper BBB model. Experimental groups were assigned as:

- Control (untreated)
- Ang II (10 nM) treatment
- RvD1 (50 ng/mL) treatment
- Ang II (10 nM) and RvD1 (50 ng/mL) co-treatment

3.1.2 Angiotensin II and Resolvin D1 administration

bEnd.3 cells were seeded into 24-well transwell constructs and incubated for 24 hours to allow attachment to the surface. After 24 hours, 3 different doses of Ang II (10, 100, 1000 nM) were administered. Following 1-hour Ang II administration, 3 different doses of RvD1 (25, 50, 75 ng/mL) were added to the culture media. At the end of 24 hours of exposure, cells were washed with PBS and fixed with 4 % PFA for immunocytochemistry, or cell lysates were harvested to perform western blot.

3.1.3 CellTiter Glo Luminescent Cell Viability Assay

bEnd.3 cells were seeded into black-sided clear bottom 96-well plate for the CellTiter Glo (CTG) luminescent cell viability assay. Following Ang II and/or RvD1 treatment, CTG reagent was added to the culture medium, and the plate was incubated for 10 minutes at room temperature. Luminescence was subsequently measured using a BioTek Synergy H1 microplate reader.

3.1.4 Trans-endothelial electrical resistance measurement and sodium-fluorescein permeability assay

Paracellular permeability of bEnd.3 monolayers on a transwell were evaluated by measuring TEER values and a hydrophilic small fluorescent tracer, NaFl leakage (MW: 376 Dalton).

TEER measurements were performed using an EVOM™ Manual Meter (EVM-MT-03-

02, World Precision Instruments, USA) and STX4 EVOM™ electrode with removable blades. The recorded TEER values were multiplied by the membrane area ($\Omega \cdot cm^2$), which is 0.33 cm^2.

Following the Ang II and/or RvD1 treatments, the culture media in both compartments were removed. The luminal compartment was filled with 100 µL NaFl (10 µg/mL) prepared in 1X PBS, and the abluminal compartment was filled with PBS alone. After 1-hour NaFl incubation, samples were collected from the lower compartment. The absorbance of the samples was measured at 485 nm excitation and 530 nm emission using black-sided clear-bottom 96-well plates.

3.1.5 Immunofluorescence staining of proteins involved in transcellular and paracellular transport

bEnd.3 cells were seeded onto autoclaved sterile glass coverslips and cultured until reaching 85-90 % confluency. Following Ang II and RvD1 administrations, the cells were fixed with 4 % PFA and permeabilized with a 0.1 % Triton-X-PBS solution. After 1 hour of blocking, primary antibodies were added as follows: claudin-5 (1:100, Thermo Fisher, 35-2500), caveolin-1 (1:500, Cell Signalling Technology, #3267), and Mfsd2a (1:50, Thermo Fisher, PA5-21049) overnight at 4°C. The next day, the coverslips were incubated with secondary antibodies for 1 hour at room temperature (1:1000; A11034, Alexa Fluor™ 488 goat anti-rabbit IgG secondary antibody, and 1:1000; A11029, Alexa fluor™ 488 goat anti-mouse IgG secondary antibody). Coverslips were mounted on slides using Hoechst 33342 (1 µg/µL) prepared in PBS/Glycerol solution. The slides were visualized using Leica DMI8 confocal microscopy, and image analysis was performed using FIJI (2.14.0/1.54p, NIH, USA).

3.2 In vivo experimentation

In this study, 10- to 12-week-old Balb/c male mice were used. The experiments were performed with four groups: sham, Ang II, RvD1, and Ang II plus RvD1. Each group consisted of four subgroups, resulting in a total of 80 mice. All animal experiments were conducted at Koç University Research Center for Translational Medicine, (KUTTAM) and the study received approval from the Local Animal Ethics Committee of Koç University (Reference number: 2021.HADYEK.020). A summarized version of the in vivo experimental design is shown in Figure 2.

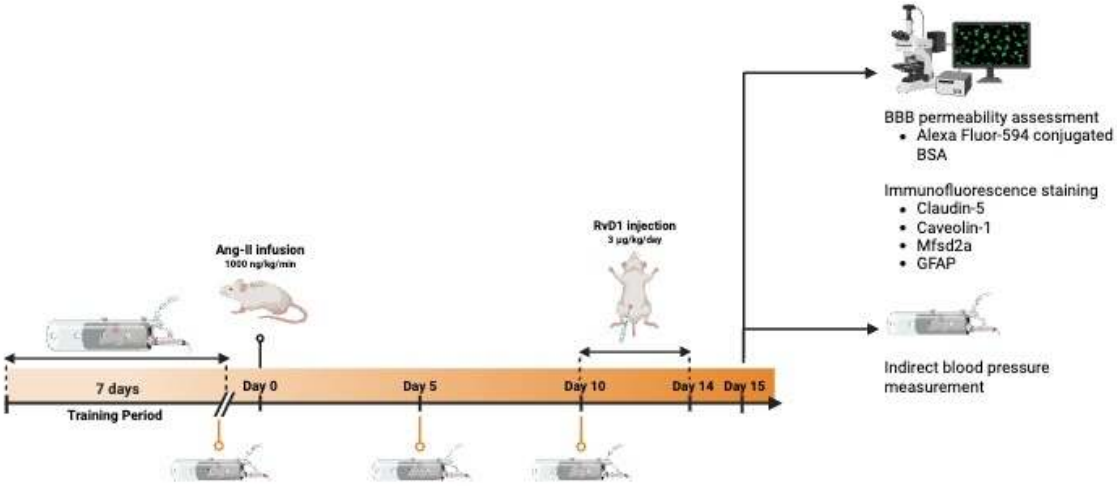

Figure 3.2 Schematic representation of in vivo experiment workflow (created with biorender.com)

3.2.1 Angiotensin II-induced hypertension model

Animals were anesthetized with 2.5 % isoflurane, and the surgical region was shaved before implantation. Alzet mini-osmotic pumps (Model 1004, 0.11 µL/h, 28 days; Durect Co, Cupertino, CA) were filled with Ang II (1000 ng/kg/min; Sigma Chemical Co., St. Louis, MO, USA) dissolved in saline. After placing the pump in the correct position within the pocket, a subcutaneous incision was sutured using 4.0 silk sutures and allowed to infuse for 15 days.

3.2.2 Non-invasive arterial blood pressure measurement

Animals were habituated to the restrainer for 5 consecutive days before pump implantation, and blood pressure measurements were recorded around 8-9 a.m. using the CODA High Throughput non-invasive blood pressure system (Kent Scientific Corporation, CT, USA). The tail temperature was measured with a laser thermometer and maintained at 32-35°C using a heating platform during the recording of blood pressure. Blood pressure measurements were repeated on days 0, 5, 10, and 15 and were analyzed using 2-way repeated measures analysis of variance (ANOVA) to compare the effects of both the Ang II-infusion time and RvD1 treatment, followed by Tukey's post hoc multiple comparisons test using GraphPad Prism (version 10.5.0, GraphPad Software, USA). Data were expressed as mean± standard deviation (SD).

3.2.3 Resolvin D1 administration

Starting from the 10th day after the Alzet pump implantation, RvD1 (3 µg/kg/day, Cayman Chemical, #10012554) was intraperitoneally injected for five consecutive days in 200 µL sterile saline (Olivares-Silva et al., 2021).

3.2.4 Assessment of the BBB permeability

A 100 µL solution of 1 % Alexa-Fluor 594 conjugated bovine serum albumin (BSA; Invitrogen, Thermo Fisher Scientific, #A13101) was intravenously administered under 2.5 % isoflurane anesthesia. Following, the circulation of Alexa-Fluor 594 conjugated BSA throughout the body was allowed for an hour. Under deep anesthesia using ketamine (300 mg/kg) and xylazine (20 mg/kg), the thoracic cavity was opened, and the perfusion needle was placed into the left ventricle. Transcardiac perfusion was performed by administering a bolus of 50 mL physiological saline (0.9 %) solution for about 20-30 seconds, followed by 200 mL of fixative solution containing 4 % paraformaldehyde (PFA) in 1X phosphate buffer (pH 7.4) for 15 minutes. Following decapitation, the brains were kept in a fixative solution for 4 hours and transferred to a 30 % sucrose solution until they sank. Brains were snap-frozen with dry ice and stored at -80°C until cryosectioning. Coronal cryosections (15 µm) were cut using a cryostat (Leica CM 1950, Germany) at levels of the cerebral cortex (P222, P273, P376) and the hippocampus (P273) of the Allen Mouse Brain atlas (https://mouse.brain-map.org). The sections were mounted in glycerol/phosphate-buffered saline (PBS; 1:1) containing Hoechst 33342 (1 µg/mL; Thermo Fisher Scientific, MA, USA) for nuclear staining. Images were acquired with confocal microscopy (2 TCS SP8), and 10 non-overlapping areas from the cerebral cortex and hippocampus were taken under a 40X objective with the same detector and laser settings. Quantitative analysis was performed using FIJI (2.14.0/1.54p, NIH, USA) by measuring the integrated density of the images. Quantified analysis was performed in FIJI (ImageJ v2.14.0) by measuring the integrated density of the 594 positive signals as referred to by (Low et al., 2024).

3.2.5 Microhemorrhage detection

Brains were removed and immersed in 4 % PFA solution for 24 hours post-fixation. Then, vibratome (VT1000S, Leica) was used to take 40-micron free-floating sections. The sections were mounted on SuperFrost™ positively charged slides and left to dry for

1 hour. Afterwards, the slides were immersed in 5 % potassium ferrocyanide (PFC232, BioShop) and 10 % HCl for 20 minutes, then Nuclear Fast Red (ready-to-use, N3020, Sigma-Aldrich) for 15 minutes as a counterstain. Sections were dehydrated with ethanol, cleared in xylene and mounted with DPX mounting medium (Electron Microscopy Sciences). Each slide has 3 consecutive serial sections. The whole slide was scanned by the Zeiss AxioScan 8 scanner. For the quantitative analysis, the iron-positive blue area (pixel) was normalised to the section area using FIJI (ImageJ v2.14.0).

3.2.6 Immunofluorescence staining of proteins involved in transcellular and paracellular transport

Mice were terminally anesthetized with overdoses of ketamine (300 mg/kg, i.p.) / xylazine (20 mg/kg, i.p.). The thoracic cavity was opened, and then the mice were perfused with cold PBS and 4 % PFA, as described in the "Assessment of the BBB permeability" section. The brains were preserved at -80°C until cryosectioning. 15-micron coronal sections were mounted on SuperFrost™ positively charged slides. For antigen retrieval, slides were boiled in sodium-citrate buffer (1X, Abcam, ab93678) in a microwave for 10 minutes. Then, the sections were permeabilized for 10 minutes in 0.1 % PBS-Triton X-100. and blocked in PBS containing 10 % normal goat serum (NGS) for 1 hour at room temperature. Primary antibody solutions for claudin-5 (1:100, Invitrogen, #35-2500), caveolin-1 (1:2000, Cell Signaling, #3267), and Mfsd2a (1:600, Cell Signaling, #80302) overnight at 4°C. Next, secondary antibodies, Alexa Fluor™ 488 488-conjugated goat anti-Rabbit (1:1000, Thermo Fischer, A11034) or Alexa Fluor™ 488-conjugated goat anti-mouse (1:1000, Thermo Fisher, A11029), were used for 1 hour at room temperature. Slides were coverslipped using Hoechst mounting medium (1:1 PBS/Glycerol). 10 non-overlapping fields were captured with a confocal microscope (Leica TCS SP8) using a 40X objective. Quantitative analysis was performed using FIJI (ImageJ v2.14.0), measuring the integrated density of the images.

3.2.7 Glial fibrillary acidic protein immunofluorescence staining

Mice were deeply anesthetized with pentobarbital (100 mg/kg, i.p.). The thoracic cavity was opened to perform transcardiac perfusion with 50 mL of cold PBS. Following perfusion, the brains were post-fixed for 24 hours in 4 % PFA, and then coronal floating

sections (40 μm) were cut using a Leica Vibratome (VT1000S). After PBS and dH_2O wash, sections were incubated with pepsin (1 mg/mL; MP Biomedicals, #195367) for 10 minutes at a 37 ˚C incubator for antigen retrieval and blocked for 1 hour in 0.1 % TritonX and 5 % BSA in PBS at room temperature. The sections were incubated in 488 conjugated glial fibrillary acidic protein (GFAP; 1:500, Millipore, #MAB3402x) antibody overnight at room temperature on a shaker, followed by mounting with Fluoromount G. Whole-slide images were acquired with Zeiss AxioScan 8. For each animal, 3 consecutive serial sections were selected and mounted on the same slide. Quantitative analysis was performed with the following metrics: mean fluorescence intensity, GFAP-positive area (pixel), and GFAP-positive area normalized to total section area using FIJI (Image J v2.14.0).

3.3 Statistical analysis

All data are shown as mean ± standard deviation (SD). Statistical analyses were performed using GraphPad Prism (version 10.5.0, GraphPad Software, USA). The normal distribution of data was evaluated by the Shapiro-Wilk test. Multiple comparisons among the experimental groups were assessed via a non-parametric Kruskal-Wallis test followed by Dunn's multiple comparisons test. For blood pressure measurement, a 2-way repeated measures ANOVA with Bonferroni correction was used. P-values less than 0.05 were considered statistically significant ($p<0.05$). Significance asterisks were indicated in the figures as: $p<0.05$ (*), $p<0.01$ (**), $p<0.001$ (***), $p<0.0001$ (****). For in vivo experiments, the number of replicates (n) for each group is indicated in each figure legend. In vitro experiments were conducted with three independent biological replicates and each consisting of three technical replicates.

CHAPTER 4
RESULTS

4.1 In vitro experimentation

4.1.1 Dose-dependent effects of Angiotensin II

Three concentrations of Ang II (10, 100, and 1000 nM) were tested to select a dose to induce endothelial disruption by conducting cell viability, TEER, and NaFl permeability assays (Figure 4.1).

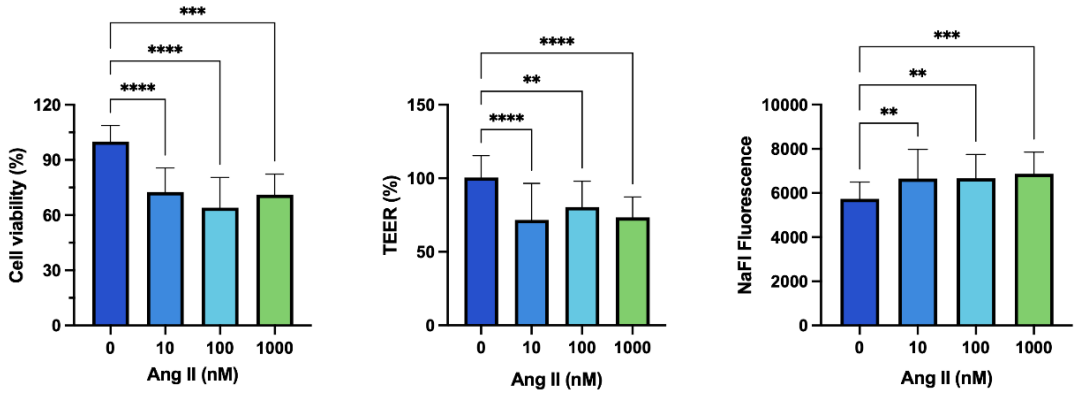

Figure 4.1 Dose-dependent effects of ANG II on bEnd.3 cells by conducting CTG assay, TEER, and NaFl permeability assay. Bars represent mean ± SD (p<0.01, *** p<0.001, **** p<0.0001).**

All the administered concentrations of Ang II significantly decreased the cell viability in bEnd.3 cells ($p<0.001$, $p<0.0001$). TEER measurements were reduced in all Ang II doses ($p<0.01$, $p<0.0001$), while the leakage of NaFl tracer was increased upon 10, 100, and 1000 nM Ang II doses ($p<0.01$, $p<0.001$). These results indicated that all Ang II doses disrupt the endothelial layer. Since 10 nM Ang II severely and significantly decreased TEER values and increased fluorescein tracer leakage compared to the control group. Hence, this dose was selected among the tested concentrations for further experiments. In addition, 10 nM was the lowest concentration that significantly reduced

cell viability. Thus, these results make 10 nM concentration for bEnd.3 impairment without inducing excessive cell death.

4.1.2 Dose-dependent effects of Resolvin D1 upon Angiotensin II disruption

bEnd.3 cells were treated with 10 nM Ang II for an hour and the cells were co-treated with 25, 50, and 75 ng/mL RvD1 for 24 hours. Afterwards, TEER, permeability, and cell viability assays were conducted to evaluate the RvD1's effect on the endothelial cell integrity (Figure 4.2).

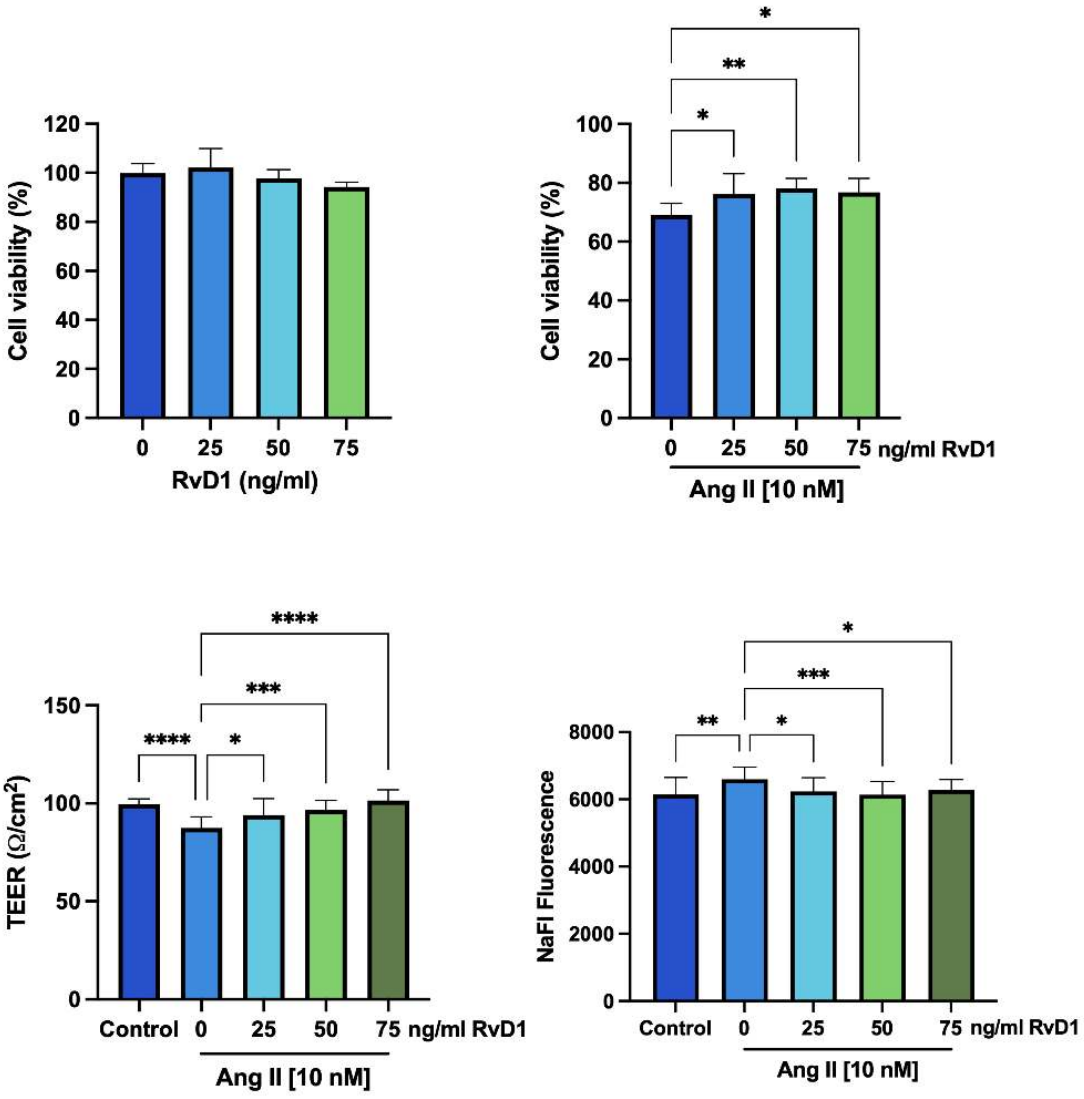

Figure 4.2 Dose-dependent effects of 25, 50, 75 ng/mL RvD1 upon Ang II administration to bend.3 cells by performing CTG assay, TEER, and NaFl permeability assay. Bars represent mean ± SD (*p<0.05, **p<0.01, *** p<0.001, **** p<0.0001).

Compared to the 10 nM Ang II-treated cells, all RvD1 doses significantly increase the cell viability upon Ang II administration (Figure 4.2, $p<0.05$, $p<0.01$). TEER measurements demonstrated that Ang II exposure decreased the TEER values compared to the control ($p<0.0001$). However, TEER values were notably elevated following 25, 50, and 75 ng/mL RvD1 treatment (Figure 4.2, $p<0.05$, $p<0.001$, $p<0.0001$). Moreover, the accumulated NaFl fluorescence in the abluminal compartment showed that Ang II administration increased the leakage across the endothelial cells, while RvD1 treatment reduced the amount of infiltrated fluorescence tracer (Figure 4.2, $p<0.05$, $p<0.01$, $p<0.001$).

Additionally, bEnd.3 cells were exposed to only RvD1 doses for 24 hours to evaluate its effect on cell viability. CTG results showed that administrated doses of RvD1 did not impair cell viability compared to the control group (Figure 4.2).

4.1.3 Immunofluorescence staining

Following Ang II and RvD1 co-treatment, the integrity across the bEnd.3 monolayer was evaluated by performing immunocytochemistry using claudin-5 antibody, one of the major TJ proteins, Cav-1, and Mfsd2a, which are key players in transcellular transport pathways (Figure 4.3,4.4 and 4.5).

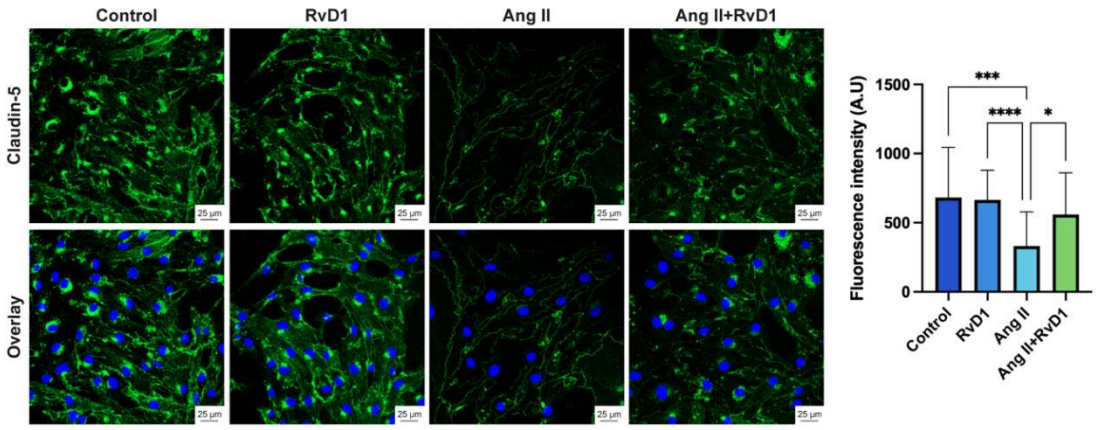

Figure 4.3 Representative images and quantitative fluorescence intensity analysis of claudin-5 in bEnd.3 cells. Bars represent mean ± SD (*p<0.05, *** p<0.001, **** p<0.0001).

Ang II administration decreased the claudin-5 levels compared to the control cells (Figure 3, $p<0.001$). Following RvD1 treatment (50 ng/mL), the fluorescence intensity of claudin-5 was significantly increased relative to the Ang II-treated group (Figure 4.3,

p<0.05).

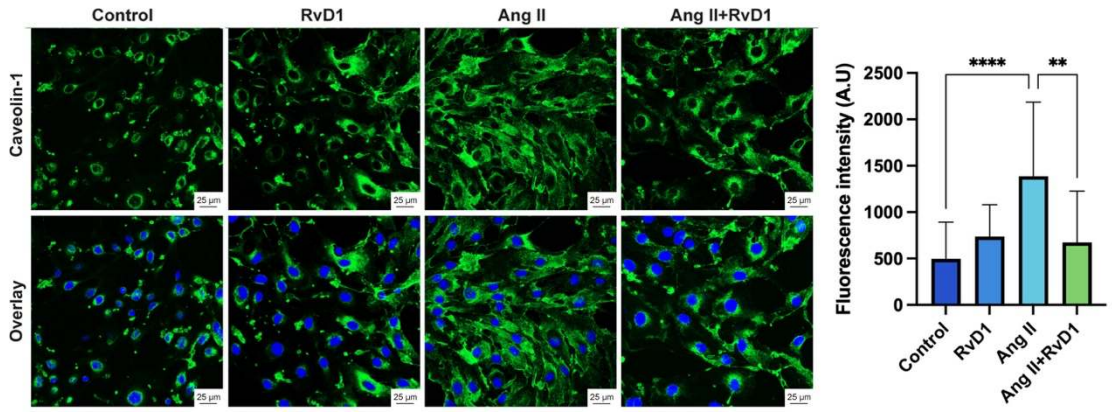

Figure 4.4. Representative images and the fluorescence intensity analysis of Cav-1 in bEnd.3 cells. Bars represent mean ± SD (p<0.01, ****p<0.0001)**

Cav-1 expression levels were remarkably increased upon Ang II administration (p<0.0001), while RvD1 treatment reduced the elevated Cav-1 intensity compared to the Ang II-exposed cells (Figure 4.4, p<0.01).

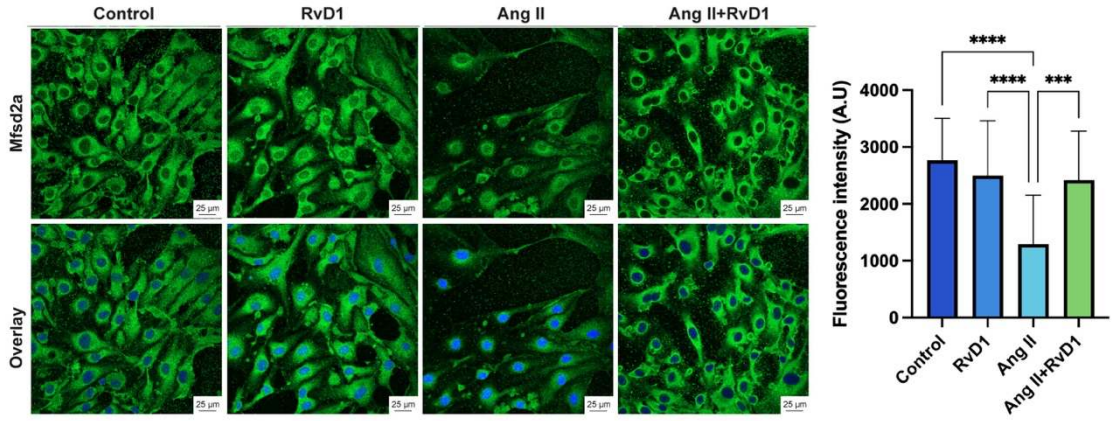

Figure 4.5. Representative images and the quantitative analysis of Mfsd2a in bEnd.3 cells. Bars represent mean ± SD (*p<0.001, ****p<0.0001)**

Compared to the control, the fluorescence intensity of Mfsd2a decreased in the Ang II group (Figure 4.5, p<0.0001). Although RvD1 treatment increased the Mfsd2a levels in Ang II-treated bEnd.3 cells (Figure 5, p<0.001).

4.2 In vivo experimentation

4.2.1 Non-invasive blood pressure measurements

All the blood pressure recording values are presented in Figure 4.6. Day 0 recordings were considered the baseline for all experimental groups.

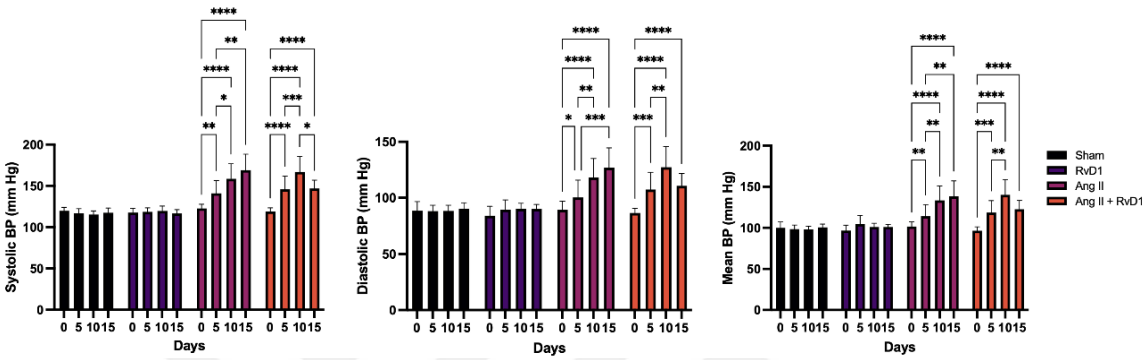

Figure 4.6. Systolic, diastolic, and mean arterial blood pressure changes among the experimental groups at day 0, 5, 10, and 15. Bars represent mean ± SD (n = 14-15 mice per group; *p<0.05, **p<0.01, ***p<0.001, ****p<0.0001).

In the Ang II-treated group, systolic, diastolic, and mean arterial pressure values significantly increased on days 5, 10, and 15 compared to the baseline values ($p<0.05$, $p<0.01$, $p<0.001$, $p<0.0001$. In the Ang II plus RvD1 cotreated group, blood pressure values also gradually increased on the 5th and 10th days compared to baseline ($p<0.01$, $p<0.001$, $p<0.0001$). Following 5 days of RvD1 administration, all systolic, diastolic, and mean blood pressure values decreased, but only the systolic blood pressure showed a significant decline compared to the values on the 10th day of Ang II-treated animals ($p<0.05$). No significant changes were observed in systolic, diastolic, and mean blood pressure values of the sham or RvD1-only group.

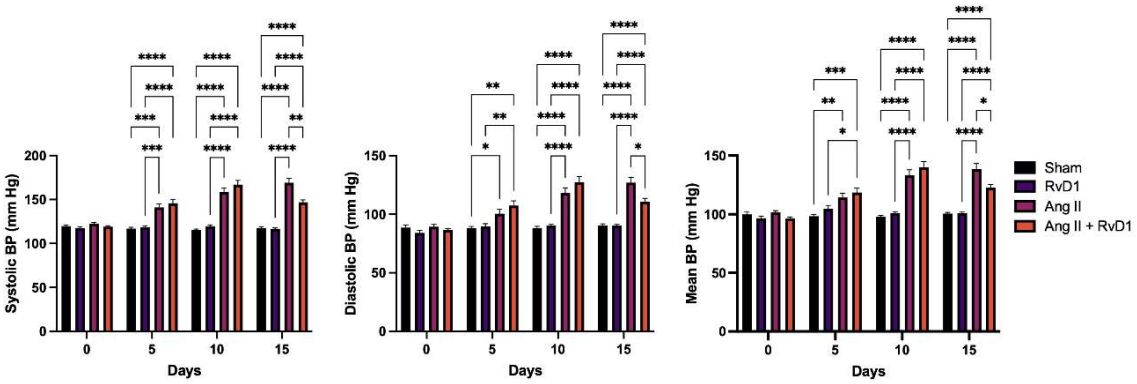

Figure 4.7. Systolic, diastolic, and mean arterial blood pressure changes in all animal groups over the experiment period. Data is represented as mean ± standard deviation; n=14-15/group, *p<0.05, **p<0.01, ***p<0.001, ****p<0.0001).

As presented in Figure 2, all systolic, diastolic, and mean blood pressure values in the Ang II group were significantly increased compared to the sham group on days 5 and 10 (Figure 4.7; $p<0.05$, $p<0.01$, $p<0.001$, $p<0.0001$). On the 15th day, all arterial blood pressure values remained significantly higher in the Ang II-treated group compared to the sham and RvD1-only groups ($p<0.0001$). Importantly, RvD1 cotreatment contributes to a significant decrease in systolic, diastolic, and mean blood pressure values compared to the Ang II group at day 15 ($p<0.05$, $p<0.01$).

4.2.2 Microhemorrhage detection using Prussian blue

Quantitative assessment of the Prussian-blue–positive area showed a significant increase in microhemorrhage content following Ang II infusion compared to the sham group (Figure 4.8, ***$p<0.001$).

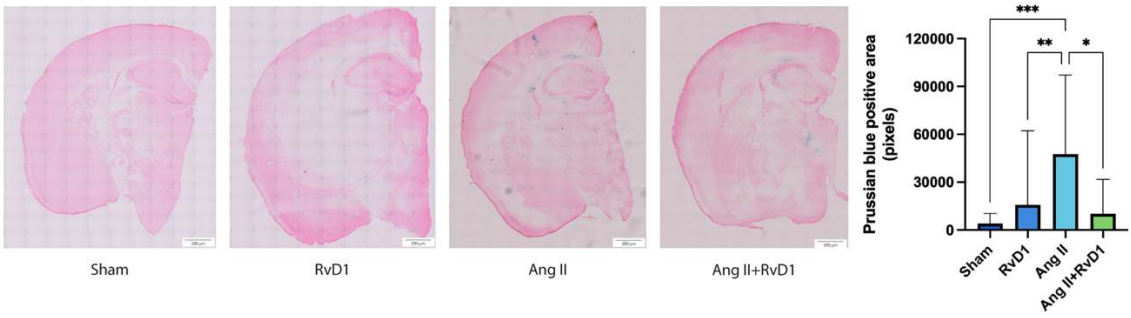

Figure 4.8. Microhemorrhage detection revealed by Prussian blue staining. Representative coronal sections show Prussian blue-positive deposits (blue) in each group. Quantification of Prussian blue-positive area per section. Bars represent mean ± SD (n = 7–8 mice per group; *p<0.05, **p<0.01, ***p<0.001)

Prussian blue staining was quantified by thresholding positive signals and analyzed for total positive pixel area using FIJI software. Notably, RvD1 administration significantly decreased Prussian blue deposition compared to the Ang II group (Figure 4.8, $p<0.05$). Hence, RvD1 treatment mitigates the Ang II-induced cerebrovascular damage.

4.2.3 Assessment of the BBB permeability using bovine serum albumin Alexa-Fluor 594 conjugate administration

BBB permeability was evaluated using Alexa Fluor 594-conjugated BSA tracer at three anatomical levels of the cerebral cortex from temporal to dorsal (P222, P273, P376) and the hippocampus levels (P273). At the P222 level, the measured fluorescence intensity of Alexa Fluor 594-conjugated BSA tracer showed a significant increase in the Ang II-treated group compared to the sham and RvD1-only treated group. Importantly, cotreatment of Ang II and RvD1 resulted in a significant decrease in the fluorescence intensity of tracer accumulation compared to the Ang II group (Figure 4.9; $p<0.0001$).

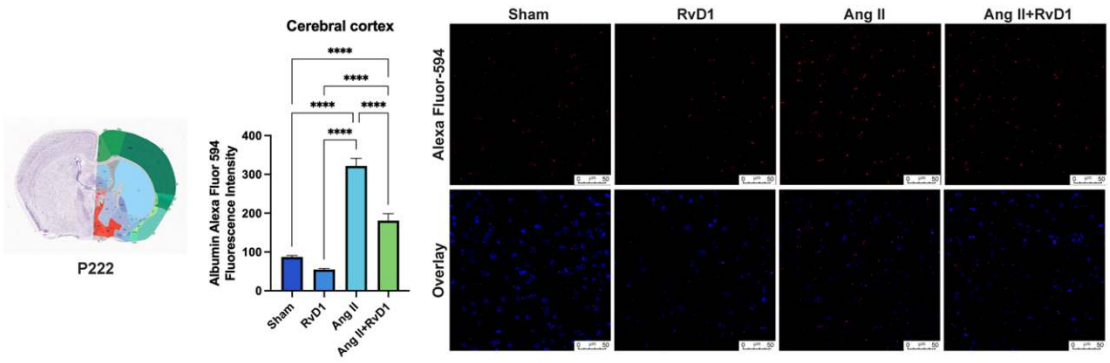

Figure 4.9. Left panel. Mouse brain p222 from the Allen brain atlas. Center panel. Quantification of Alexa Fluor 594-positive pixels within the cerebral cortex of 4 experimental groups. Right panel. Representative images for Alexa Fluor 594-conjugated BSA (red color) content in the cerebral cortex. Bars represent mean ± SD (n=5/group, ****p<0.0001).

At the P273 level of the cerebral cortex of animals, fluorescence intensity of tracer was highest in the Ang II-infused group but showed a significant decrease upon RvD1 treatment ($p<0.0001$). Similarly, the fluorescence tracer intensity in the hippocampus increased in Ang II-infused mice, but RvD1 treatment decreased the infiltrated tracer content in this region (Figure 4.10; $p<0.0001$).

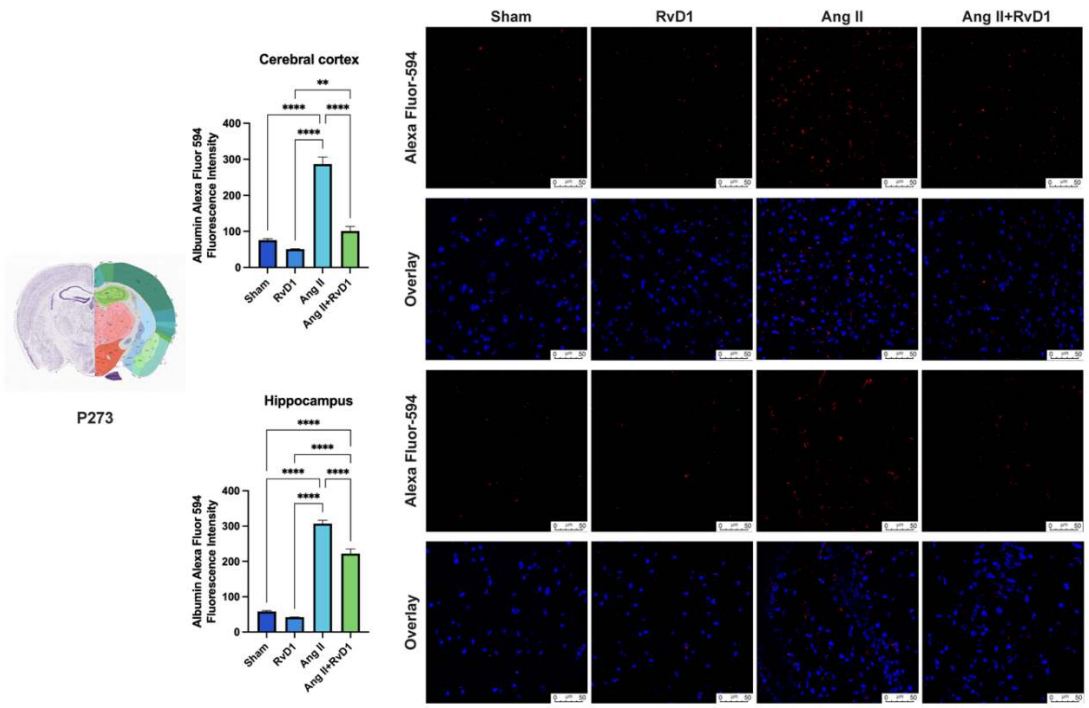

Figure 4.10: Left panel. Mouse brain p273 from the Allen brain atlas. Upper right panel. Quantification of Alexa Fluor 594 positive pixels within the cerebral cortex and representative images for Alexa Fluor 594 conjugated BSA (red color) content. Lower right panel. Quantification of Alexa Fluor 594 positive pixels within the hippocampal region and representative images for Alexa Fluor 594 conjugated BSA. Bars represent mean ± SD (n=5/group; **p<0.01, ****p<0.0001)

At the P376 section level of the cerebral cortex, fluorescent conjugated albumin tracer content was assessed. The fluorescence intensity of the tracer was significantly increased in Ang II-infused mice compared to all other experimental groups ($p<0.0001$). RvD1 treatment notably decreased the fluorescence intensity of the tracer relative to the Ang II group (Figure 4.11; $p<0.0001$).

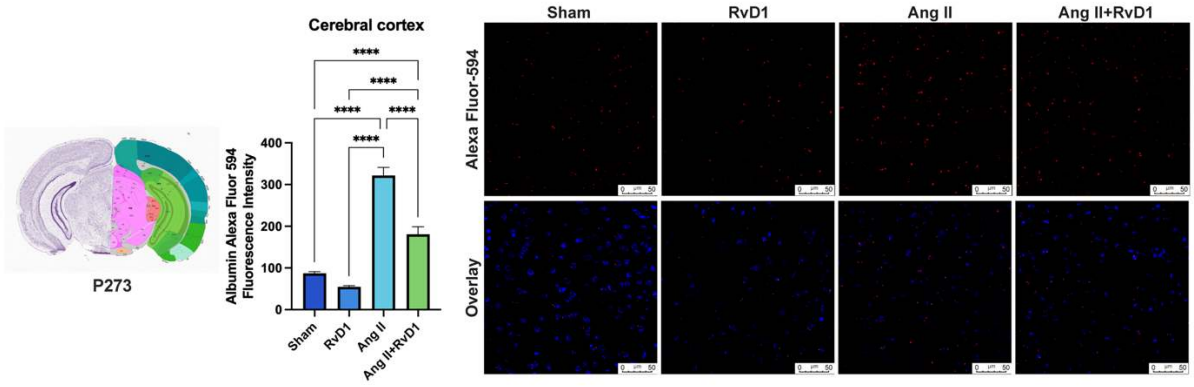

Figure 4.11: Left panel. Mouse brain p376 from the Allen brain atlas. Center panel. Quantification of Alexa Fluor 594-positive pixels within the brains of 4 experimental groups. Right panel. Representative images for Alexa Fluor 594 conjugated BSA (red color) content. Bars represent mean ± SD (n = 5 mice per group; ****p<0.0001)

4.2.4 Immunofluorescence staining of junctional and transport proteins Claudin-5

Immunofluorescence Staining

BBB integrity was evaluated by performing immunofluorescence staining with one of the major TJ proteins, claudin-5. Fluorescence intensity of claudin-5 in both the cerebral cortex and hippocampus decreased in Ang II-infused animals and increased upon 5 days of RvD1 administration compared to the Ang II group (Figure 4.12).

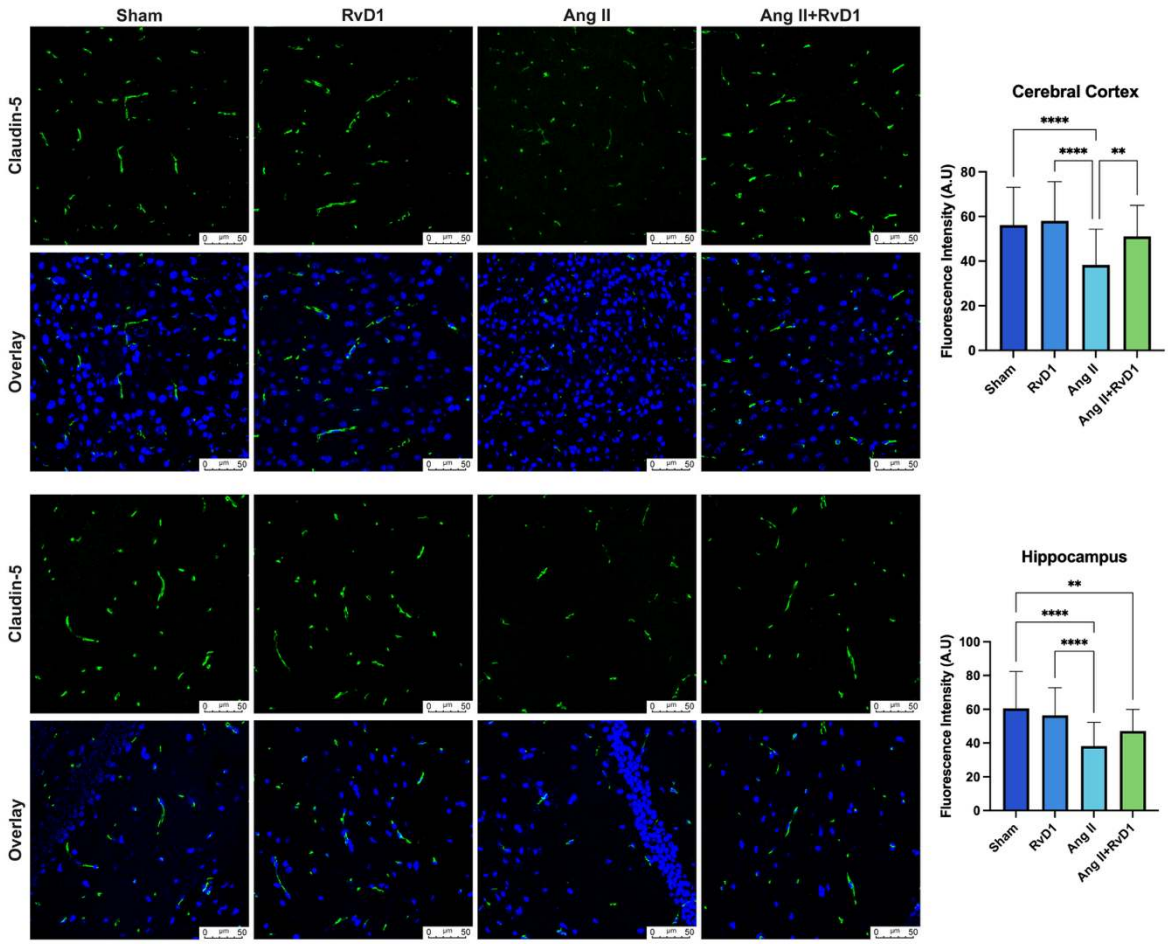

Figure 4.12: Claudin-5 immunofluorescence staining and quantitative analysis. Bars represent mean ± SD (n=5 mice/group; **p<0.01, ****p<0.0001)

Accordingly, quantification of claudin-5 immunoreactivity by image analysis showed that RvD1 treatment significantly increased the claudin-5 fluorescence intensity in the cerebral cortex of Ang II-treated animals ($p<0.01$).

4.2.5 Mfsd2a Immunofluorescence staining

BBB integrity was evaluated by performing immunofluorescence staining with Mfsd2a, which controls the expression levels of Cav-1 involved in transcellular transport. Mfsd2a fluorescence intensity in the cerebral cortex and hippocampus decreased in the Ang II-infused mice and increased following RvD1 treatment (Figure 4.13).

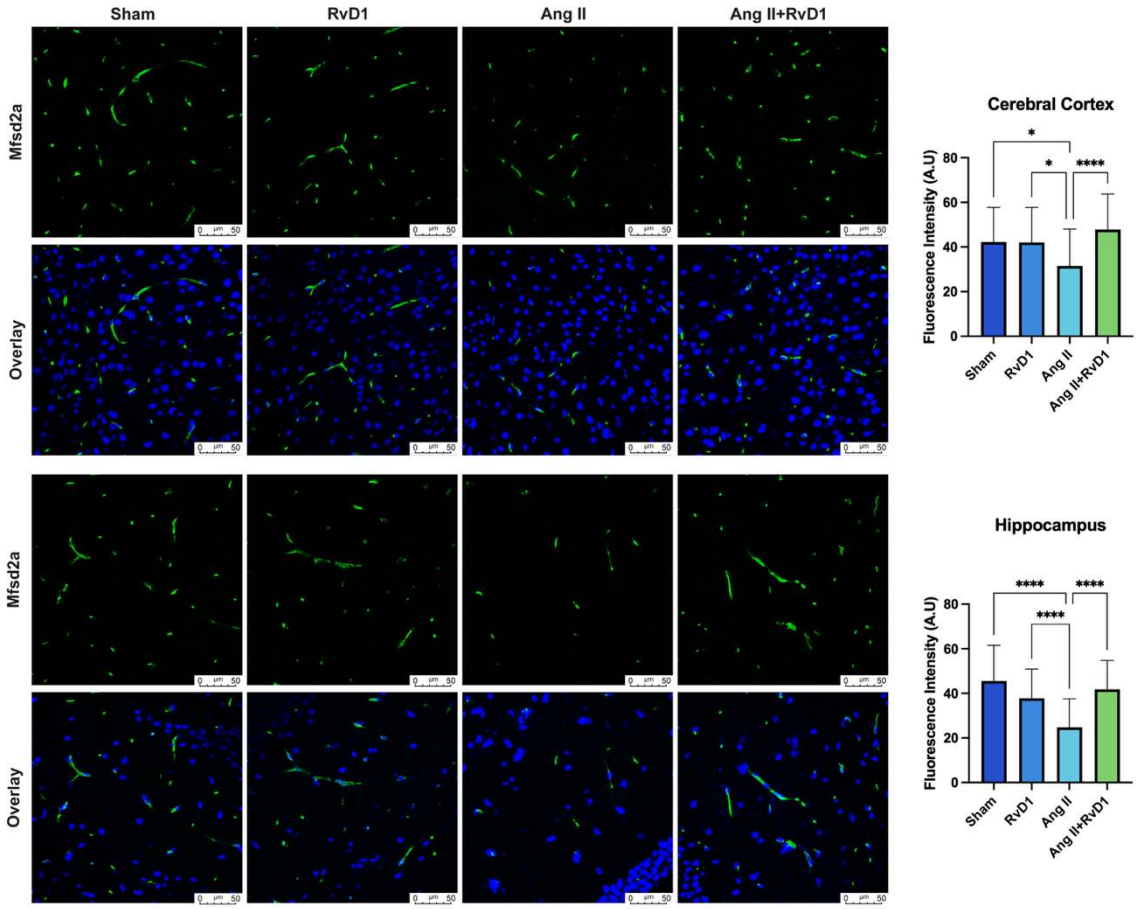

Figure 4.13: Mfsd2a immunofluorescence staining and quantitative analysis. Bars represent mean ± SD (n=5/group; *p<0.05, ****p<0.0001).

In the meantime, the quantification of Mfsd2a immunoreactivity by image analysis showed that RvD1 treatment caused overall increases in the immunofluorescence intensity of Mfsd2a in Ang II-treated animals ($p<0.05$, $p<0.0001$).

4.2.6 Caveolin-1 Immunofluorescence Staining

Cav-1 immunofluorescence intensity considerably increased in Ang II-infused animals, while administration of RvD1 decreased immunostaining of this protein in the same animals (Figure 4.14, $p<0.0001$).

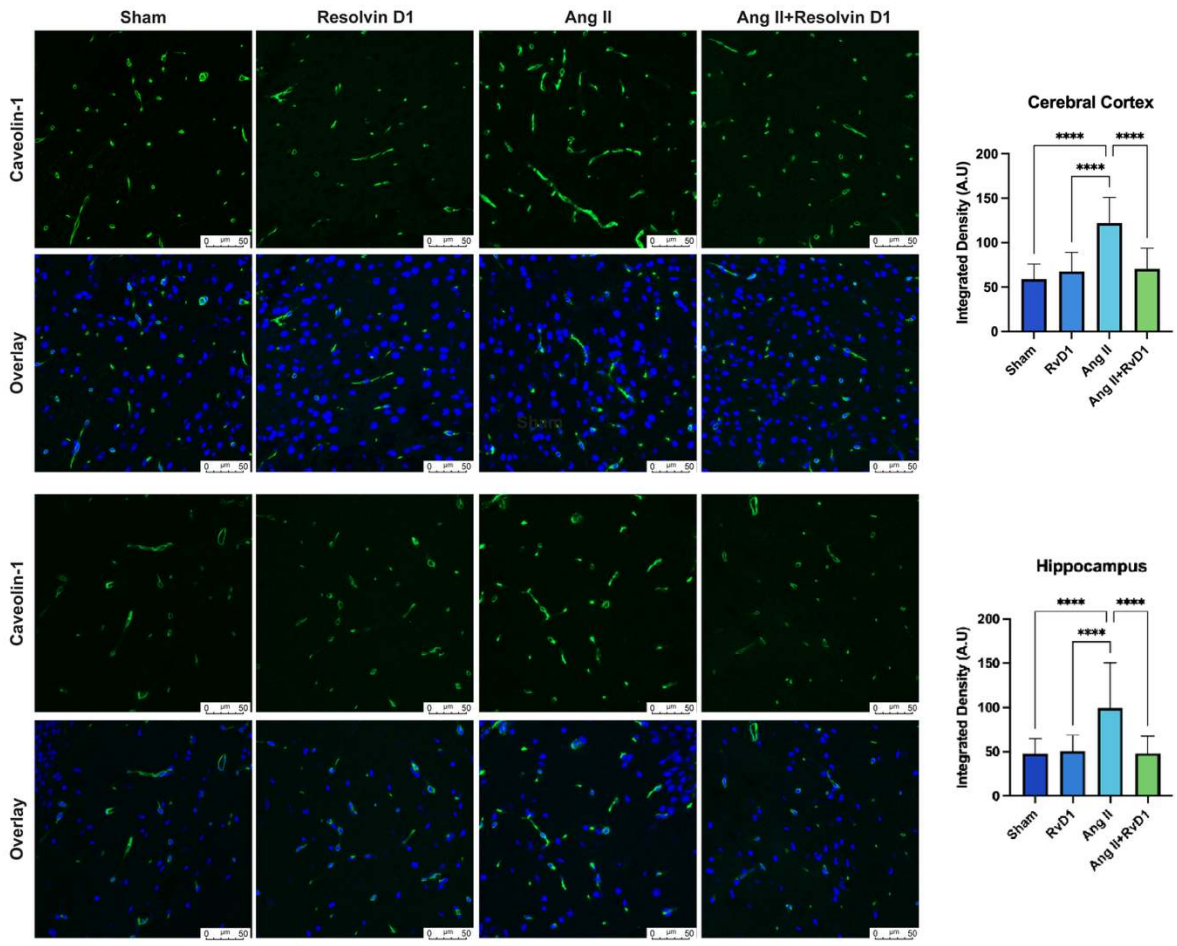

Figure 4.14: Caveolin-1 immunofluorescence staining and quantitative analysis. Bars represent mean ± SD (n=5/group, ****p<0.0001).

The quantification of Cav-1 immunoreactivity by image analysis showed that RvD1 treatment caused overall decreases in the immunofluorescence intensity of Cav-1 in animals treated with Ang II (P<0.0001).

4.2.7 Astrogliosis assessment using GFAP

The administration of Ang II to animals yielded considerably enhanced immunostaining for GFAP (Fig. 4.15).

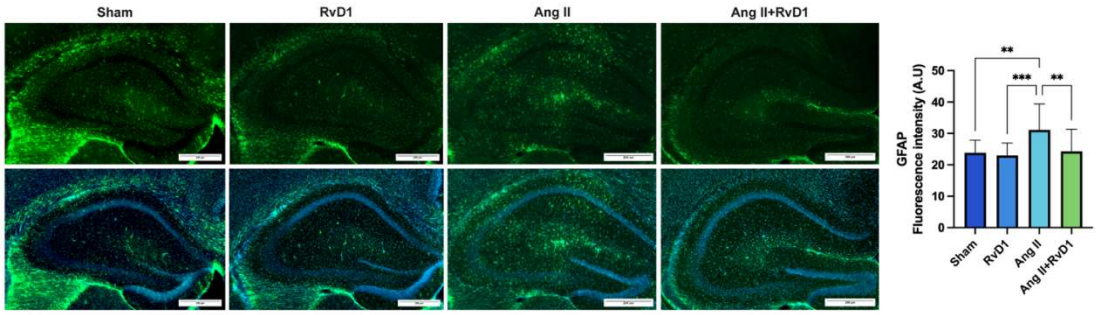

Figure 4.15: GFAP immunofluorescence staining and quantitative analysis. Bars represent mean ± SD (n=7-8/group, **p<0.01, ***p<0.001).

In parallel, the quantification of GFAP immunoreactivity by image analysis showed that RvD1 treatment significantly decreased the immunofluorescence intensity of GFAP in Ang II-treated animals ($p<0.01$).

CHAPTER 5
DISCUSSION

In this study, we investigated whether RvD1 ameliorates the disruptive effects of Ang II on the BBB integrity in an in vitro BBB model using mouse brain bEnd.3 cells and an in vivo mouse model for chronic hypertensive conditions induced by Ang II. In this study, we aimed to investigate the cellular and molecular mechanisms underlying the protective effects of RvD1 against BBB disruption in the Ang II-induced chronic hypertensive mouse model.

Our in vitro results demonstrated that Ang II administration in various doses decreased the cell viability and TEER values, whereas the NaFl infiltration into the abluminal compartment increased upon Ang II exposure. The most consistent BBB impairment was observed in the 10 nM Ang II, based on reduced cell viability, decreased endothelial resistance, and elevated fluorescent tracer passage across the bEnd.3 cell layer. CTG cell viability assay results showed that RvD1 has no cytotoxic effects alone on bEnd.3 cells only treated with a dose range of RvD1. Subsequently, RvD1 significantly increased the cell viability in all doses compared to the 10 nM Ang II-exposed cells. Additionally, TEER values in the bEnd.3 cells were remarkably elevated after RvD1 treatment compared with the only Ang II-treated group. Furthermore, RvD1 notably reduced the efflux of NaFl tracer across the endothelial barrier. Moreover, claudin-5 and Mfsd2a fluorescence intensity were reduced upon Ang II administration, and RvD1 elevated these protein levels. In contrast, RvD1 significantly decreased the Cav-1 levels, which were increased upon Ang II impairment. These results elucidate that RvD1 mitigates the destructive effects of Ang II on bEnd.3 cells by increasing cell viability, elevating TEER values, decreasing the accumulated NaFl amount in the abluminal compartment, and restoring claudin-5, Cav-1, and Mfsd2a protein levels.

In the in vivo part of our study, systolic, diastolic, and mean blood pressure were progressively increased day by day in Ang II-induced hypertensive mice. Remarkably, RvD1 treatment for 5 days alleviates the systolic, diastolic, and mean blood pressure at

day 15. Notably, RvD1 treatment significantly reduced the microhemorrhage formation within the brain, which suggests the protective role of RvD1 upon Ang II-induced cerebrovascular damage. Similarly, the accumulated Alexa Fluor 594-conjugated BSA within the various levels of brain parenchyma was reduced following RvD1 treatment. Consistently, immunofluorescence staining demonstrated that RvD1 elevated the expression of claudin-5 and Mfsd2a, and decreased Cav-1. These results indicate that RvD1 has ameliorating effects on Ang II-induced BBB disruption due to improving TJ integrity and permeability across the barrier endothelial cells. RvD1 also reduced the expression of GFAP, which is one of the most common astrogliosis markers. Overall, these findings suggest that RvD1 has remarkable protective impacts against Ang II-induced BBB disruption and cerebrovascular damage.

Hypertension is the most common risk factor for heart attack, cardiac atrophy, stroke, dementia, Alzheimer's Disease, and cerebral small vessel disease (Zhou et al., 2021). Worldwide, 1.27 billion people suffer from hypertension, and most of these people are unaware of their disease (Rossi et al., 2024). The most common risk factors that stimulate the emergence of hypertension are listed as age, higher body mass index, and excessive salt intake (Nishimoto et al., 2024; Tang et al., 2022). In Turkey, one person in every three has died because of cardiovascular diseases, largely hypertension, and nearly 4.5 % of annual deaths are caused by Alzheimer's and dementia (Yurekli et al., 2019). Although hypertension can be kept under control by taking medications, antihypertensive drugs cannot restore all damage to cardio or cerebrovascular structures (Liu et al., 2015). Considering the clinical and economic burdens associated with hypertension, the development of effective therapeutic strategies to mitigate hypertension and its destructive impacts on peripheral and cerebral vasculature is critical.

In this study, we first investigated the effect of RvD1 treatment on Ang II-induced hypertension. Successful development of hypertension was verified by the gradual blood pressure increase in only the Ang II receiving group for 15 days. All systolic, diastolic, and mean blood pressure values were significantly elevated on days 5, 10, and 15 compared to day 0 baseline values. Similarly, Ang II infusion increased the systolic blood pressure values at 490 ng/kg/min infusion rate for 14 days (Yin et al., 2022). Combination of Ang II infusion and high dose of salt intake for 5 days leads to high systolic, diastolic, and mean blood pressure in Balb/c mice (Becirovic-Agic et al., 2019). In another study, a chronic hypertensive model was established by the 1900 ng/kg/min Ang II infusion for 10 days. In the mentioned study, Ang II infusion elevated blood pressure measurements

and caused cognitive decline by the assessment of the Morris water maze test (Duchemin et al., 2013). Increased arterial blood pressure contributes to the damage to the body's vasculature and disruption of the BBB and NVU components (Boily et al., 2021; van den Kerkhof et al., 2024; Yu et al., 2025).

In our study, administration of RvD1 reduced arterial blood pressure values observed in Ang II-treated conditions. In parallel with our results, Olivares-Silva suggested that RvD1 attenuates the blood pressure elevation and mitigates the hypertension development in 1.5 mg/kg/day Ang II-infused mice for 14 days (Olivares-Silva et al., 2021). In addition, a recent study reported that daily administration of RvD1 has a restorative effect on Ang II-induced hypertensive mice by decreasing the blood pressure, vessel thickness, and collagen accumulation within the lumen (Wei et al., 2024b).

As we evaluated the microhemorrhage formation by performing Prussian blue staining, Ang II infusion contributes to the emergence of microhemorrhagic patterns, whereas RvD1 treatment reduced the Prussian-blue deposition within the brain. In a previous study, Ang II infusion led to an increase in Prussian-blue positive microhemorrhage area compared to the sham group (Xie et al., 2025). Additionally, exogenous RvD1 injections help to lower the organ injury, such as skeletal muscle damage, renal and hepatic dysfunction, following the controlled hemorrhagic shock (Sordi et al., 2021). Another recent study demonstrated that RvD1 attenuates the hemorrhage-induced neuronal injury by alleviating the neuroinflammation and promoting the recovery after intracerebral hemorrhage (Xiaoyu et al., 2024).

We evaluated the BBB integrity at 3 different anatomical levels (P222, P273, and P376) using Alexa Fluor-594 conjugated BSA for in vivo conditions. At all cortical levels, BBB permeability significantly increased upon Ang II infusion, which indicates the elevated accumulation of fluorescent conjugated albumin compared to the sham group. Following RvD1 injections, the accumulated Alexa Fluor-594 conjugated BSA was decreased in all the evaluated brain regions. Parallel with this data, BSA leakage through the BBB was increased in Ang II receiving animals, and this leakage was reduced by the RvD1 treatment in the hippocampal region at level P273. Our findings support that Ang II causes cerebrovascular damage through the BBB impairment and enhances the blood-borne substance extravasation rate across the BBB.

In a similar study, IgG leakage through the BBB was increased in the cerebral cortex and hippocampus upon Ang II infusion at a 2 μg/kg/min rate (Foulquier et al., 2018). Atis et.al demonstrated that continuous Ang II infusion (2 μg/kg/min for 14 days)

elevated the leakage of Alexa Fluor-594 conjugated BSA in both cerebral cortex and hippocampus regions (Atis et al., 2022). In similar studies, a significant increase in Evans blue-labelled albumin and horseradish-peroxidase was observed in both cerebral cortex and hippocampus regions of both acute and chronic hypertensive models (Atış et al., 2019; Vital et al., 2010; Zhang et al., 2010). In contrast, intraventricular Ang II administration restores the tightness of the barrier in angiotensinogen-deficient mice by restoring the disorganized occludin and decreasing the paracellular leakage of plasminogen and albumin in the brain capillary cells (Kakinuma et al., 1998; Wosik et al., 2007). These results suggest that sufficient amount of Ang II and its activity through the membrane receptors are essential to maintain the BBB integrity.

Besides, an infiltrated NaFl tracer was used for integrity assessment in vitro experiments using bEnd.3 cells. Our in vitro results showed that Ang II disrupts the BBB integrity by reducing cell viability, decreasing TEER to disrupt the BBB, and increasing the permeability of NaFl to the abluminal compartment. Although RvD1 treatment significantly decreases the NaFl tracer and restores the bEnd.3 integrity by elevating cell viability and TEER values. In HUVECs, Ang II exposure enhanced the permeability of 40 kDa FITC-dextran across the endothelial layer, lowered the TEER values, elevated macrophage adhesion, and trans endothelial migration (Bodor et al., 2012; Yin et al., 2022). In another study, bEnd.3 endothelial cells and BV-2 microglia were used to establish a co-culture system. In this system, both NaFl and BSA-FITC efflux across the bEnd.3 cells were elevated upon Ang II, which induced microglia activation and BBB impairment (Lu et al., 2021). Similarly, Guo et.al demonstrated that 24-hour Ang II exposure on human brain microvascular endothelial cells elevated the leakage of Alexa Fluor 488-conjugated BSA, which indicates the enhancement of the vesicular transport. Moreover, Ang II exposure contributes to the paracellular leakage by loosening tight junctional integrity in brain microvessel endothelial cells through the elevation of labelled albumin efflux, reduction in TEER values, and uneven distribution of JAM-A, ZO-1, and VE-cadherin (Fleegal-DeMotta et al., 2009; Guo et al., 2019).

Cav-1 and Mfsd2a are the critical modulators that regulate the BBB integrity and proper functioning. In this study, we found that Ang II administration significantly increased the Cav-1 immunofluorescence intensity in both in vitro and in vivo experiments, which indicates the elevated caveolar transcytosis across the brain microvascular endothelial cells. Importantly, RvD1 treatment attenuates the Ang II-induced alterations by reducing the Cav-1 expression and enhancing the Mfsd2a fluorescence intensity in both our in

vitro and in vivo models.

Mfsd2a acts as a negative regulator of endothelial transcytosis, and Mfsd2a-knockout mice contribute to continuous leakage of 10-70 kDa tracers, which indicates the necessity of Mfsd2a for the maintenance of an intact BBB integrity. Additionally, electron microscopy analysis demonstrated that the transcytosis rate increased across the BBB in Mfsd2a knockout mice, and this data suggest that Mfsd2a controls the vesicular transport rather than being involved in junctional integrity in barrier-type endothelial cells (Ben-Zvi et al., 2014). In parallel with the literature findings, our data showed that Ang II increased the Cav-1 expression through the AT1 receptor activation and elevated the rate of transcytosis across the endothelial cells. Moreover, Ang II increased the rate of transcellular traffic and endothelial transport by down-regulating the Mfsd2a and up-regulating Cav-1 (Guo et al., 2019). In hypertensive rats, elevated Cav-1 expression levels contribute to albumin leakage across the BBB. Additionally, the Cav-1 knockdown model demonstrated that downregulated Cav-1 protein increases the barrier tightness. In parallel with our results, gain-of-function experiments in bEnd.3 cells and Mfsd2a knock-in mouse model demonstrated that Mfsd2a expression suppressed the caveolar pit formation and leakiness across the barrier cells (Andreone et al., 2017). In addition to this, Ang II-treated bEnd.3 cells cause endothelial damage via increasing Cav-1 expression, reducing the expression of Mfsd2a protein, and enhancing BSA-FITC leakage (Xia et al., 2022; Xie et al., 2022). Similarly, a recent study suggests that Ang II-infusion for 2 weeks reduced the expression levels of Mfsd2a, enhanced the Cav-1 production, and decreased the claudin-5 in PVN microvessels (Yu et al., 2025). Together, reciprocal Cav-1/Mfsd2a imbalance leads to excessive transcytosis switch, barrier leakage, and finally cerebrovascular dysfunction.

Claudin-5, one of the major TJ proteins, provides full integrity of the BBB. Our data demonstrated that Ang II infusion significantly decreased claudin-5 fluorescence intensity in both the cerebral cortex and the hippocampus, while 5-day treatment of RvD1 enhanced the disrupted pattern of claudin-5. Consistently, from the results of immunofluorescence staining, claudin-5 intensity was elevated in Ang II-treated bEnd.3 cells. Moreover, Ang II exposure triggers bEnd.3 apoptosis and disrupts the TJs by downregulating the claudin-5 and ZO-1 expression (Xie et al., 2022). Ang II administration to bEnd.3 cells also enhance the inflammation by activating downstream pathways such as TLR4, MyD88, and TNF-α (Xia et al., 2022). However, 100 nM Ang II administration to brain microvessel endothelial cells for 6 hours has no effect on the

expression levels of claudin-5 or occludin (Fleegal-DeMotta et al., 2009). This study indicates the dose and time-dependent manner of Ang II disruption. Intravenous administration of RvD1 upregulates the occludin, claudin-5, and ZO-1 expressions and suppresses the MMP-9 levels after subarachnoid hemorrhage in rats (Wei et al., 2021b). These findings reported that RvD1 contributes to the protection of TJ integrity by regulating claudin-5 expression in Ang II-induced pathological conditions.

In the chronic hypertensive model, Ang II infusion caused a significant increase in GFAP immunostaining, whereas cotreatment with RvD1 remarkably alleviated the response of astrocytes. Consistent with our results, chronic Ang II infusion enhanced the GFAP expression in the hippocampus (Iulita et al., 2018; Milner et al., 2022). Tomassoni et.al enlightened that GFAP mRNA and protein levels of spontaneously hypertensive rats were increased in several brain regions such as striatum, hippocampus, frontal and occipital cortex (Tomassoni et al., 2004).

CHAPTER 6
CONCLUSION

In this study, we aimed to investigate the RvD1's potential impacts on Ang II-induced BBB disruption using an in vitro bEnd.3 cells and Ang II-infused hypertensive mice. In vitro results showed that Ang II administration induced disruption of barrier integrity in bEnd.3 cells by reducing cell viability and TEER, while increasing NaFl permeability. Additionally, Ang II altered the transcellular and paracellular transport pathways through the upregulated Cav-1 levels, downregulated expressions of claudin-5, and Mfsd2a. Following RvD1 treatment, cell viability and TEER values were increased, NaFl leakage was reduced, and paracellular and transcellular permeability across the bEnd.3 cells were restored by decreasing Cav-1, increasing claudin-5 and Mfsd2a levels.

According to in vivo results, continuous infusion of Ang II elevated the arterial blood pressure and permeability to Alexa Fluor-594 conjugated BSA, induced microhemorrhage formation, and exacerbated astrogliosis. Furthermore, Ang II exposure increased the Cav-1, decreased claudin-5, and Mfsd2a protein levels. 5-day RvD1 treatment reversed the Ang II-induced changes by lowering blood pressure, attenuating microhemorrhages and astrogliosis, inhibiting Cav-1, upregulating Mfsd2a, and restoring claudin-5 levels.

Altogether, Ang II causes BBB impairment through the enhanced caveolar transcytosis by upregulating Cav-1 with Mfsd2a downregulation and diminished TJ integrity. Therefore, RvD1 treatment altered the balance between Cav-1 and Mfsd2a, leading to the normal rate of transcytosis, enhanced claudin-5 to provide tight junctional integrity, and alleviated astrocytic inflammatory response in Ang II-induced hypertensive mice.

Our results highlighted the therapeutic potential of RvD1 in the treatment of hypertension-associated cerebrovascular impairment.

BIBLIOGRAPHY

Abbott, N. J. (2002). Astrocyte-endothelial interactions and blood-brain barrier permeability. *Journal of Anatomy*, *200*(6), 629–638. https://doi.org/10.1046/j.1469-7580.2002.00064.x

Abbott, N. J. (2013). Blood–brain barrier structure and function and the challenges for CNS drug delivery. *Journal of Inherited Metabolic Disease*, *36*(3), 437–449. https://doi.org/10.1007/s10545-013-9608-0

Abbott, N. J., Patabendige, A. A. K., Dolman, D. E. M., Yusof, S. R., & Begley, D. J. (2010a). Structure and function of the blood–brain barrier. *Neurobiology of Disease*, *37*(1), 13–25. https://doi.org/10.1016/j.nbd.2009.07.030

Abbott, N. J., Patabendige, A. A. K., Dolman, D. E. M., Yusof, S. R., & Begley, D. J. (2010b). Structure and function of the blood–brain barrier. *Neurobiology of Disease*, *37*(1), 13–25. https://doi.org/10.1016/j.nbd.2009.07.030

Abbott, N. J., & Romero, I. A. (1996). Transporting therapeutics across the blood-brain barrier. *Molecular Medicine Today*, *2*(3), 106–113. https://doi.org/10.1016/1357-4310(96)88720-x

Ajoolabady, A., Pratico, D., & Ren, J. (2024). Angiotensin II: Role in oxidative stress, endothelial dysfunction, and diseases. *Molecular and Cellular Endocrinology*, *592*, 112309. https://doi.org/10.1016/j.mce.2024.112309

Alfaro, S., Acuña, V., Ceriani, R., Cavieres, M. F., Weinstein-Oppenheimer, C. R., & Campos-Estrada, C. (2022). Involvement of Inflammation and Its Resolution in Disease and Therapeutics. *International Journal of Molecular Sciences*, *23*(18), 10719. https://doi.org/10.3390/ijms231810719

Althammer, F., Roy, R. K., Kirchner, M. K., Podpecan, Y., Helen, J., McGrath, S., Lira, E. C., & Stern, J. E. (2024). Angiotensin-II drives changes in microglia–vascular interactions in rats with heart failure. *Communications Biology*, *7*(1), 1537. https://doi.org/10.1038/s42003-024-07229-8

Alvarez, J. I., Katayama, T., & Prat, A. (2013). Glial influence on the blood brain barrier. *Glia*, *61*(12), 1939–1958. https://doi.org/10.1002/glia.22575

Amponsah-Offeh, M., Diaba-Nuhoho, P., Speier, S., & Morawietz, H. (2023). Oxidative Stress, Antioxidants and Hypertension. *Antioxidants*, *12*(2), 281. https://doi.org/10.3390/antiox12020281

Andersen, J. V., Schousboe, A., & Verkhratsky, A. (2022). Astrocyte energy and neurotransmitter metabolism in Alzheimer's disease: Integration of the glutamate/GABA-glutamine cycle. *Progress in Neurobiology*, *217*, 102331. https://doi.org/10.1016/j.pneurobio.2022.102331

Ando, K., Nagaraj, S., Küçükali, F., de Fisenne, M.-A., Kosa, A.-C., Doeraene, E., Lopez Gutierrez, L., Brion, J.-P., & Leroy, K. (2022). PICALM and Alzheimer's Disease: An Update and Perspectives. *Cells*, *11*(24), 3994. https://doi.org/10.3390/cells11243994

Andreone, B. J., Chow, B. W., Tata, A., Lacoste, B., Ben-Zvi, A., Bullock, K., Deik, A. A., Ginty, D. D., Clish, C. B., & Gu, C. (2017). Blood-Brain Barrier Permeability Is Regulated by Lipid Transport-Dependent Suppression of Caveolae-Mediated Transcytosis. *Neuron*, *94*(3), 581-594.e5. https://doi.org/10.1016/j.neuron.2017.03.043

Argaw, A. T., Asp, L., Zhang, J., Navrazhina, K., Pham, T., Mariani, J. N., Mahase, S., Dutta, D. J., Seto, J., Kramer, E. G., Ferrara, N., Sofroniew, M. V., & John, G. R. (2012). Astrocyte-derived VEGF-A drives blood-brain barrier disruption in CNS inflammatory disease. *Journal of Clinical Investigation*, *122*(7), 2454–2468. https://doi.org/10.1172/JCI60842

Arita, M., Yoshida, M., Hong, S., Tjonahen, E., Glickman, J. N., Petasis, N. A., Blumberg, R. S., & Serhan, C. N. (2005). Resolvin E1, an endogenous lipid mediator derived from omega-3 eicosapentaenoic acid, protects against 2,4,6-trinitrobenzene sulfonic acid-induced colitis. *Proceedings of the National Academy of Sciences of the United States*

of America, *102*(21), 7671–7676. https://doi.org/10.1073/pnas.0409271102
Assersen, K. B., Sumners, C., & Steckelings, U. M. (2020). The Renin-Angiotensin System in Hypertension, a Constantly Renewing Classic: Focus on the Angiotensin AT2-Receptor. *Canadian Journal of Cardiology*, *36*(5), 683–693. https://doi.org/10.1016/j.cjca.2020.02.095
Atis, M., Akcan, U., Altunsu, D., Ayvaz, E., Uğur Yılmaz, C., Sarıkaya, D., Temizyürek, A., Ahıshalı, B., Girouard, H., & Kaya, M. (2022). Targeting the blood–brain barrier disruption in hypertension by ALK5/TGF-B type I receptor inhibitor SB-431542 and dynamin inhibitor dynasore. *Brain Research*, *1794*, 148071. https://doi.org/10.1016/j.brainres.2022.148071
Atış, M., Akcan, U., Uğur Yılmaz, C., Orhan, N., Düzgün, P., Deniz Ceylan, U., Arıcan, N., Karahüseyinoğlu, S., Nur Şahin, G., Ahıshalı, B., & Kaya, M. (2019). Effects of methyl-beta-cyclodextrin on blood-brain barrier permeability in angiotensin II-induced hypertensive rats. *Brain Research*, *1715*, 148–155. https://doi.org/10.1016/j.brainres.2019.03.024
Ayloo, S., & Gu, C. (2019). Transcytosis at the blood–brain barrier. *Current Opinion in Neurobiology*, *57*, 32–38. https://doi.org/10.1016/j.conb.2018.12.014
Baggeroer, C. E., Cambronero, F. E., Savan, N. A., Jefferson, A. L., & Santisteban, M. M. (2024). Basic Mechanisms of Brain Injury and Cognitive Decline in Hypertension. *Hypertension*, *81*(1), 34–44. https://doi.org/10.1161/HYPERTENSIONAHA.123.19939
Bajwa, E., & Klegeris, A. (2022). Neuroinflammation as a mechanism linking hypertension with the increased risk of Alzheimer's disease. *Neural Regeneration Research*, *17*(11), 2342. https://doi.org/10.4103/1673-5374.336869
Baltira, C., Aronica, E., Elmquist, W. F., Langer, O., Löscher, W., Sarkaria, J. N., Wesseling, P., de Gooijer, M. C., & van Tellingen, O. (2024). The impact of ATP-binding cassette transporters in the diseased brain: Context matters. *Cell Reports Medicine*, *5*(6), 101609. https://doi.org/10.1016/j.xcrm.2024.101609
Baraldi, D., Jones, E. S., Hilliard, L. M., Del Borgo, M., Gaspari, T. A., McCarthy, C. A., Vinh, A., Welungoda, I., Aguilar, M.-I., Denton, K. M., & Widdop, R. E. (2015). AT2R, Vascular Effects, and Blood Pressure. In *The Protective Arm of the Renin Angiotensin System (RAS)* (pp. 49–55). Elsevier. https://doi.org/10.1016/B978-0-12-801364-9.00007-9
Basting, T., & Lazartigues, E. (2017). DOCA-Salt Hypertension: an Update. *Current Hypertension Reports*, *19*(4), 32. https://doi.org/10.1007/s11906-017-0731-4
Becirovic-Agic, M., Jönsson, S., Tveitarås, M. K., Skogstrand, T., Karlsen, T. V., Lidén, Å., Leh, S., Ericsson, M., Nilsson, S. K., Reed, R. K., & Hultström, M. (2019). Time course of decompensation after angiotensin II and high-salt diet in Balb/CJ mice suggests pulmonary hypertension-induced cardiorenal syndrome. *American Journal of Physiology-Regulatory, Integrative and Comparative Physiology*, *316*(5), R563–R570. https://doi.org/10.1152/ajpregu.00373.2018
Ben-Zvi, A., Lacoste, B., Kur, E., Andreone, B. J., Mayshar, Y., Yan, H., & Gu, C. (2014). Mfsd2a is critical for the formation and function of the blood–brain barrier. *Nature*, *509*(7501), 507–511. https://doi.org/10.1038/nature13324
Betsholtz, C. (2014). Double function at the blood–brain barrier. *Nature*, *509*(7501), 432–433. https://doi.org/10.1038/nature13339
Biancardi, V. C., Stranahan, A. M., Krause, E. G., de Kloet, A. D., & Stern, J. E. (2016). Cross talk between AT $_1$ receptors and Toll-like receptor 4 in microglia contributes to angiotensin II-derived ROS production in the hypothalamic paraventricular nucleus. *American Journal of Physiology-Heart and Circulatory Physiology*, *310*(3), H404–H415. https://doi.org/10.1152/ajpheart.00247.2015
Bisicchia, E., Sasso, V., Catanzaro, G., Leuti, A., Besharat, Z. M., Chiacchiarini, M., Molinari, M., Ferretti, E., Viscomi, M. T., & Chiurchiù, V. (2018). Resolvin D1 Halts Remote Neuroinflammation and Improves Functional Recovery after Focal Brain Damage Via ALX/FPR2 Receptor-Regulated MicroRNAs. *Molecular Neurobiology*, *55*(8), 6894–6905. https://doi.org/10.1007/s12035-018-0889-z

Biswas, S. K. (2016). Does the Interdependence between Oxidative Stress and Inflammation Explain the Antioxidant Paradox? *Oxidative Medicine and Cellular Longevity*, *2016*(1). https://doi.org/10.1155/2016/5698931

Bo, C., Liu, X., Liu, Y., Xu, L., & Huang, Q. (2025). Resolvin D1 accelerates resolution of neuroinflammation by inhibiting microglia activation through the BDNF/TrkB signaling pathway. *European Journal of Medical Research*, *30*(1), 189. https://doi.org/10.1186/s40001-025-02424-7

Bodor, C., Nagy, J. P., Végh, B., Németh, A., Jenei, A., MirzaHosseini, S., Sebe, A., & Rosivall, L. (2012). Angiotensin II increases the permeability and PV-1 expression of endothelial cells. *American Journal of Physiology-Cell Physiology*, *302*(1), C267–C276. https://doi.org/10.1152/ajpcell.00138.2011

Boily, M., Li, L., Vallerand, D., & Girouard, H. (2021). Angiotensin II Disrupts Neurovascular Coupling by Potentiating Calcium Increases in Astrocytic Endfeet. *Journal of the American Heart Association*, *10*(17). https://doi.org/10.1161/JAHA.120.020608

Braga, V. A., Medeiros, I. A., Ribeiro, T. P., França-Silva, M. S., Botelho-Ono, M. S., & Guimarães, D. D. (2011). Angiotensin-II-induced reactive oxygen species along the SFO-PVN-RVLM pathway: implications in neurogenic hypertension. *Brazilian Journal of Medical and Biological Research*, *44*(9), 871–876. https://doi.org/10.1590/S0100-879X2011007500088

Cerutti, C., & Ridley, A. J. (2017). Endothelial cell-cell adhesion and signaling. *Experimental Cell Research*, *358*(1), 31–38. https://doi.org/10.1016/j.yexcr.2017.06.003

Chen, E., Zhou, D., & Deng, R. (2023). Serum resolvin D1 potentially predicts neurofunctional recovery, the risk of recurrence and death in patients with acute ischemic stroke. *Biomedical Reports*, *20*(1), 10. https://doi.org/10.3892/br.2023.1698

Chen, J. J., Chen, J., Jiang, Z. X., Zhou, Z., & Zhou, C. N. (2020). Resolvin D1 alleviates cerebral ischemia/reperfusion injury in rats by inhibiting NLRP3 signaling pathway. *Journal of Biological Regulators and Homeostatic Agents*, *34*(5). https://doi.org/10.23812/20-392-A

Chen, W., Ju, X., Lu, Y., Ding, X., Miao, C., & Chen, J. (2019). Propofol improved hypoxia-impaired integrity of blood-brain barrier via modulating the expression and phosphorylation of zonula occludens-1. *CNS Neuroscience & Therapeutics*, *25*(6), 704–713. https://doi.org/10.1111/cns.13101

Cheon, E.-J. (2022). Hypertension and cognitive dysfunction: a narrative review. *Journal of Yeungnam Medical Science*. https://doi.org/10.12701/jyms.2022.00605

Cheslow, L., & Alvarez, J. I. (2016). Glial-endothelial crosstalk regulates blood–brain barrier function. *Current Opinion in Pharmacology*, *26*, 39–46. https://doi.org/10.1016/j.coph.2015.09.010

Chow, B. W., & Gu, C. (2017). Gradual Suppression of Transcytosis Governs Functional Blood-Retinal Barrier Formation. *Neuron*, *93*(6), 1325-1333.e3. https://doi.org/10.1016/j.neuron.2017.02.043

Cifuentes, D., Poittevin, M., Dere, E., Broquères-You, D., Bonnin, P., Benessiano, J., Pocard, M., Mariani, J., Kubis, N., Merkulova-Rainon, T., & Lévy, B. I. (2015). Hypertension Accelerates the Progression of Alzheimer-Like Pathology in a Mouse Model of the Disease. *Hypertension*, *65*(1), 218–224. https://doi.org/10.1161/HYPERTENSIONAHA.114.04139

Clark, L. R., Koscik, R. L., Allison, S. L., Berman, S. E., Norton, D., Carlsson, C. M., Betthauser, T. J., Bendlin, B. B., Christian, B. T., Chin, N. A., Asthana, S., & Johnson, S. C. (2019). Hypertension and obesity moderate the relationship between β-amyloid and cognitive decline in midlife. *Alzheimer's & Dementia*, *15*(3), 418–428. https://doi.org/10.1016/j.jalz.2018.09.008

Colombari, E., Biancardi, V. C., Colombari, D. S. A., Katayama, P. L., Medeiros, F. de C. de, Aitken, A. V., Xavier, C. H., Pedrino, G. R., & Bragin, D. E. (2025). Hypertension, blood–brain barrier disruption and changes in intracranial pressure. *The Journal of Physiology*, *603*(8), 2245–2261. https://doi.org/10.1113/JP285058

Cong, X., & Kong, W. (2020). Endothelial tight junctions and their regulatory signaling

pathways in vascular homeostasis and disease. *Cellular Signalling*, *66*, 109485. https://doi.org/10.1016/j.cellsig.2019.109485

Dalkara, T., & Alarcon-Martinez, L. (2015). Cerebral microvascular pericytes and neurogliovascular signaling in health and disease. *Brain Research*, *1623*, 3–17. https://doi.org/10.1016/j.brainres.2015.03.047

Dange, R. B., Agarwal, D., Teruyama, R., & Francis, J. (2015). Toll-like receptor 4 inhibition within the paraventricular nucleus attenuates blood pressure and inflammatory response in a genetic model of hypertension. *Journal of Neuroinflammation*, *12*(1), 31. https://doi.org/10.1186/s12974-015-0242-7

Dash, U. C., Bhol, N. K., Swain, S. K., Samal, R. R., Nayak, P. K., Raina, V., Panda, S. K., Kerry, R. G., Duttaroy, A. K., & Jena, A. B. (2025). Oxidative stress and inflammation in the pathogenesis of neurological disorders: Mechanisms and implications. *Acta Pharmaceutica Sinica B*, *15*(1), 15–34. https://doi.org/10.1016/j.apsb.2024.10.004

Daugherty, A. M. (2021). Hypertension-related risk for dementia: A summary review with future directions. *Seminars in Cell & Developmental Biology*. https://doi.org/10.1016/j.semcdb.2021.03.002

de Kloet, A. D., Pitra, S., Wang, L., Hiller, H., Pioquinto, D. J., Smith, J. A., Sumners, C., Stern, J. E., & Krause, E. G. (2016). Angiotensin Type-2 Receptors Influence the Activity of Vasopressin Neurons in the Paraventricular Nucleus of the Hypothalamus in Male Mice. *Endocrinology*, *157*(8), 3167–3180. https://doi.org/10.1210/en.2016-1131

de Montgolfier, O., Thorin-Trescases, N., & Thorin, E. (2020). Pathological Continuum From the Rise in Pulse Pressure to Impaired Neurovascular Coupling and Cognitive Decline. *American Journal of Hypertension*, *33*(5), 375–390. https://doi.org/10.1093/ajh/hpaa001

Dikalov, S. I., Nazarewicz, R. R., Bikineyeva, A., Hilenski, L., Lassègue, B., Griendling, K. K., Harrison, D. G., & Dikalova, A. E. (2014). Nox2-Induced Production of Mitochondrial Superoxide in Angiotensin II-Mediated Endothelial Oxidative Stress and Hypertension. *Antioxidants & Redox Signaling*, *20*(2), 281–294. https://doi.org/10.1089/ars.2012.4918

Duchemin, S., Belanger, E., Wu, R., Ferland, G., & Girouard, H. (2013). Chronic perfusion of angiotensin II causes cognitive dysfunctions and anxiety in mice. *Physiology & Behavior*, *109*, 63–68. https://doi.org/10.1016/j.physbeh.2012.10.005

Durkee, C. A., & Araque, A. (2019). Diversity and Specificity of Astrocyte–neuron Communication. *Neuroscience*, *396*, 73–78. https://doi.org/10.1016/j.neuroscience.2018.11.010

Ehrlich, P. (1885). *Das sauerstoffbedürfnis des organismus, in Eine Farbe Analytische Studie.*

Elsaafien, K., de Kloet, A. D., Krause, E. G., & Sumners, C. (2020). Brain Angiotensin Type-1 and Type-2 Receptors in Physiological and Hypertensive Conditions: Focus on Neuroinflammation. *Current Hypertension Reports*, *22*(7), 48. https://doi.org/10.1007/s11906-020-01062-0

Engelhardt, B., & Liebner, S. (2014). Novel insights into the development and maintenance of the blood–brain barrier. *Cell and Tissue Research*, *355*(3), 687–699. https://doi.org/10.1007/s00441-014-1811-2

Eser Ocak, P., Ocak, U., Sherchan, P., Gamdzyk, M., Tang, J., & Zhang, J. H. (2020). Overexpression of Mfsd2a attenuates blood brain barrier dysfunction via Cav-1/Keap-1/Nrf-2/HO-1 pathway in a rat model of surgical brain injury. *Experimental Neurology*, *326*, 113203. https://doi.org/10.1016/j.expneurol.2020.113203

Fanning, A. S., Jameson, B. J., Jesaitis, L. A., & Anderson, J. M. (1998). The Tight Junction Protein ZO-1 Establishes a Link between the Transmembrane Protein Occludin and the Actin Cytoskeleton. *Journal of Biological Chemistry*, *273*(45), 29745–29753. https://doi.org/10.1074/jbc.273.45.29745

Faraco, G., Park, L., Zhou, P., Luo, W., Paul, S. M., Anrather, J., & Iadecola, C. (2016). Hypertension enhances Aβ-induced neurovascular dysfunction, promotes β-secretase activity, and leads to amyloidogenic processing of APP. *Journal of Cerebral Blood Flow*

& Metabolism, *36*(1), 241–252. https://doi.org/10.1038/jcbfm.2015.79
Fleegal-DeMotta, M. A., Doghu, S., & Banks, W. A. (2009). Angiotensin II Modulates BBB Permeability via Activation of the AT Receptor in Brain Endothelial Cells. *Journal of Cerebral Blood Flow & Metabolism*, *29*(3), 640–647. https://doi.org/10.1038/jcbfm.2008.158
Forstermann, U., & Sessa, W. C. (2012). Nitric oxide synthases: regulation and function. *European Heart Journal*, *33*(7), 829–837. https://doi.org/10.1093/eurheartj/ehr304
Foulquier, S., Namsolleck, P., Van Hagen, B. T., Milanova, I., Post, M. J., Blankesteijn, W. M., Rutten, B. P., Prickaerts, J., Van Oostenbrugge, R. J., & Unger, T. (2018). Hypertension-induced cognitive impairment: insights from prolonged angiotensin II infusion in mice. *Hypertension Research*, *41*(10), 817–827. https://doi.org/10.1038/s41440-018-0090-9
Furuse, M., Hirase, T., Itoh, M., Nagafuchi, A., Yonemura, S., Tsukita, S., & Tsukita, S. (1993). Occludin: a novel integral membrane protein localizing at tight junctions. *The Journal of Cell Biology*, *123*(6), 1777–1788. https://doi.org/10.1083/jcb.123.6.1777
Gannon, O., Tremble, S. M., McGinn, C., Guth, R., Scoppettone, N., Hunt, R. D., Prakash, K., & Johnson, A. C. (2024). Angiotensin II-mediated hippocampal hypoperfusion and vascular dysfunction contribute to vascular cognitive impairment in aged hypertensive rats. *Alzheimer's & Dementia*, *20*(2), 890–903. https://doi.org/10.1002/alz.13491
Gao, Y., Zhang, H., Luo, L., Lin, J., Li, D., Zheng, S., Huang, H., Yan, S., Yang, J., Hao, Y., Li, H., Gao Smith, F., & Jin, S. (2017). Resolvin D1 Improves the Resolution of Inflammation via Activating NF-κB p50/p50–Mediated Cyclooxygenase-2 Expression in Acute Respiratory Distress Syndrome. *The Journal of Immunology*, *199*(6), 2043–2054. https://doi.org/10.4049/jimmunol.1700315
Ghosh, C., Gonzalez-Martinez, J., Hossain, M., Cucullo, L., Fazio, V., Janigro, D., & Marchi, N. (2010). Pattern of P450 expression at the human blood–brain barrier: Roles of epileptic condition and laminar flow. *Epilepsia*, *51*(8), 1408–1417. https://doi.org/10.1111/j.1528-1167.2009.02428.x
Goldblatt, H., Lynch, J., Hanzal, R. F., & Summerville, W. W. (1934). STUDIES ON EXPERIMENTAL HYPERTENSION. *Journal of Experimental Medicine*, *59*(3), 347–379. https://doi.org/10.1084/jem.59.3.347
Goldmann, E. E. (1912). *Vitalfärbung am Zentralnervensystem*.
Gowrisankar, Y. V., & Clark, M. A. (2016). Angiotensin II induces interleukin-6 expression in astrocytes: Role of reactive oxygen species and NF-κB. *Molecular and Cellular Endocrinology*, *437*, 130–141. https://doi.org/10.1016/j.mce.2016.08.013
Gu, C. (2016). KIR4.1: K+ Channel Illusion or Reality in the Autoimmune Pathogenesis of Multiple Sclerosis. *Frontiers in Molecular Neuroscience*, *9*. https://doi.org/10.3389/fnmol.2016.00090
Guo, S., Som, A. T., Arai, K., & Lo, E. H. (2019). Effects of angiotensin-II on brain endothelial cell permeability via PPARalpha regulation of para- and trans-cellular pathways. *Brain Research*, *1722*, 146353. https://doi.org/10.1016/j.brainres.2019.146353
Hansen, E., Grimm, D., & Wehland, M. (2022). Current Knowledge about the New Drug Firibastat in Arterial Hypertension. *International Journal of Molecular Sciences*, *23*(3), 1459. https://doi.org/10.3390/ijms23031459
Harrison, I. F., Ismail, O., Machhada, A., Colgan, N., Ohene, Y., Nahavandi, P., Ahmed, Z., Fisher, A., Meftah, S., Murray, T. K., Ottersen, O. P., Nagelhus, E. A., O'Neill, M. J., Wells, J. A., & Lythgoe, M. F. (2020). Impaired glymphatic function and clearance of tau in an Alzheimer's disease model. *Brain*, *143*(8), 2576–2593. https://doi.org/10.1093/brain/awaa179
Harrison, J. L., Rowe, R. K., Ellis, T. W., Yee, N. S., O'Hara, B. F., Adelson, P. D., & Lifshitz, J. (2015). Resolvins AT-D1 and E1 differentially impact functional outcome, post-traumatic sleep, and microglial activation following diffuse brain injury in the mouse. *Brain, Behavior, and Immunity*, *47*, 131–140. https://doi.org/10.1016/j.bbi.2015.01.001
Haskins, J., Gu, L., Wittchen, E. S., Hibbard, J., & Stevenson, B. R. (1998). ZO-3, a Novel

Member of the MAGUK Protein Family Found at the Tight Junction, Interacts with ZO-1 and Occludin. *The Journal of Cell Biology*, *141*(1), 199–208. https://doi.org/10.1083/jcb.141.1.199

Haspula, D., & Clark, M. A. (2018). Neuroinflammation and sympathetic overactivity: Mechanisms and implications in hypertension. *Autonomic Neuroscience*, *210*, 10–17. https://doi.org/10.1016/j.autneu.2018.01.002

Hawkins, B. T., & Davis, T. P. (2005). The blood-brain barrier/neurovascular unit in health and disease. *Pharmacological Reviews*, *57*(2), 173–185. https://doi.org/10.1124/pr.57.2.4

Helms, H. C., Abbott, N. J., Burek, M., Cecchelli, R., Couraud, P.-O., Deli, M. A., Förster, C., Galla, H. J., Romero, I. A., Shusta, E. V, Stebbins, M. J., Vandenhaute, E., Weksler, B., & Brodin, B. (2016). In vitro models of the blood–brain barrier: An overview of commonly used brain endothelial cell culture models and guidelines for their use. *Journal of Cerebral Blood Flow & Metabolism*, *36*(5), 862–890. https://doi.org/10.1177/0271678X16630991

Iadecola, C. (2013). The Pathobiology of Vascular Dementia. *Neuron*, *80*(4), 844–866. https://doi.org/10.1016/j.neuron.2013.10.008

Iadecola, C. (2017). The Neurovascular Unit Coming of Age: A Journey through Neurovascular Coupling in Health and Disease. *Neuron*, *96*(1), 17–42. https://doi.org/10.1016/j.neuron.2017.07.030

Iadecola, C., & Gottesman, R. F. (2019). Neurovascular and Cognitive Dysfunction in Hypertension. *Circulation Research*, *124*(7), 1025–1044. https://doi.org/10.1161/CIRCRESAHA.118.313260

Iadecola, C., Yaffe, K., Biller, J., Bratzke, L. C., Faraci, F. M., Gorelick, P. B., Gulati, M., Kamel, H., Knopman, D. S., Launer, L. J., Saczynski, J. S., Seshadri, S., & Zeki Al Hazzouri, A. (2016). Impact of Hypertension on Cognitive Function: A Scientific Statement From the American Heart Association. *Hypertension*, *68*(6). https://doi.org/10.1161/HYP.0000000000000053

Ishida, H., Takemori, K., Dote, K., & Ito, H. (2006). Expression of Glucose Transporter-1 and Aquaporin-4 in the Cerebral Cortex of Stroke-Prone Spontaneously Hypertensive Rats in Relation to the Blood-Brain Barrier Function. *American Journal of Hypertension*, *19*(1), 33–39. https://doi.org/10.1016/j.amjhyper.2005.06.023

Iulita, M. F., Vallerand, D., Beauvillier, M., Haupert, N., A. Ulysse, C., Gagné, A., Vernoux, N., Duchemin, S., Boily, M., Tremblay, M.-È., & Girouard, H. (2018). Differential effect of angiotensin II and blood pressure on hippocampal inflammation in mice. *Journal of Neuroinflammation*, *15*(1), 62. https://doi.org/10.1186/s12974-018-1090-z

Jasmin, J.-F., Malhotra, S., Singh Dhallu, M., Mercier, I., Rosenbaum, D. M., & Lisanti, M. P. (2007). Caveolin-1 Deficiency Increases Cerebral Ischemic Injury. *Circulation Research*, *100*(5), 721–729. https://doi.org/10.1161/01.RES.0000260180.42709.29

Jesaitis, L., & Goodenough, D. (1994). Molecular characterization and tissue distribution of ZO-2, a tight junction protein homologous to ZO-1 and the Drosophila discs-large tumor suppressor protein. *The Journal of Cell Biology*, *124*(6), 949–961. https://doi.org/10.1083/jcb.124.6.949

Johnson, R. J., Rodríguez-Iturbe, B., Schreiner, G. F., & Herrera-Acosta, J. (2002). Hypertension: a microvascular and tubulointerstitial disease. *Journal of Hypertension. Supplement : Official Journal of the International Society of Hypertension*, *20*(3), S1-7.

Jurga, A. M., Paleczna, M., & Kuter, K. Z. (2020). Overview of General and Discriminating Markers of Differential Microglia Phenotypes. *Frontiers in Cellular Neuroscience*, *14*. https://doi.org/10.3389/fncel.2020.00198

Kadlecova, Z., Spielman, S. J., Loerke, D., Mohanakrishnan, A., Reed, D. K., & Schmid, S. L. (2017). Regulation of clathrin-mediated endocytosis by hierarchical allosteric activation of AP2. *Journal of Cell Biology*, *216*(1), 167–179. https://doi.org/10.1083/jcb.201608071

Kadry, H., Noorani, B., & Cucullo, L. (2020). A blood–brain barrier overview on structure,

function, impairment, and biomarkers of integrity. *Fluids and Barriers of the CNS*, *17*(1), 69. https://doi.org/10.1186/s12987-020-00230-3

Kakinuma, Y., Hama, H., Sugiyama, F., Yagami, K., Goto, K., Murakami, K., & Fukamizu, A. (1998). Impaired blood–brain barrier function in angiotensinogen-deficient mice. *Nature Medicine*, *4*(9), 1078–1080. https://doi.org/10.1038/2070

Kalayci, R., Kaya, M., Elmas, I., Arican, N., Ahishali, B., Uzun, H., Bilgic, B., Kucuk, M., & Kudat, H. (2005). Effects of atorvastatin on blood-brain barrier permeability during L-NAME hypertension followed by angiotensin-II in rats. *Brain Research*, *1042*(2), 184–193. https://doi.org/10.1016/j.brainres.2005.02.044

Kaur, C., & Ling, E.-A. (2017). The circumventricular organs. *Histology and Histopathology*, *32*(9), 879–892. https://doi.org/10.14670/HH-11-881

Kaya, M., Kalayci, R., Arican, N., Küçük, M., & Elmas, I. (2003). Effect of Aluminum on the Blood-Brain Barrier Permeability During Nitric Oxide-Blockade-Induced Chronic Hypertension in Rats. *Biological Trace Element Research*, *92*(3), 221–230. https://doi.org/10.1385/BTER:92:3:221

Kerkhofs, D., van Hagen, B. T., Milanova, I. V., Schell, K. J., van Essen, H., Wijnands, E., Goossens, P., Blankesteijn, W. M., Unger, T., Prickaerts, J., Biessen, E. A., van Oostenbrugge, R. J., & Foulquier, S. (2020). Pharmacological depletion of microglia and perivascular macrophages prevents vascular Cognitive Impairment in Ang II-induced Hypertension. *Theranostics*, *10*(21), 9512–9527. https://doi.org/10.7150/thno.44394

Kisler, K., Nelson, A. R., Montagne, A., & Zlokovic, B. V. (2017). Cerebral blood flow regulation and neurovascular dysfunction in Alzheimer disease. *Nature Reviews Neuroscience*, *18*(7), 419–434. https://doi.org/10.1038/nrn.2017.48

Koizumi, T., Herckenrath, E. M., Taguchi, K., Mizuta, I., Mizuno, T., & Tanaka, M. (2025). CCL2/CCR2 signaling-mediated microglial migration leads to cerebral small vessel dysfunction in chronic hypertension model rats. *Experimental Neurology*, *387*, 115192. https://doi.org/10.1016/j.expneurol.2025.115192

Komarova, Y. A., Kruse, K., Mehta, D., & Malik, A. B. (2017). Protein Interactions at Endothelial Junctions and Signaling Mechanisms Regulating Endothelial Permeability. *Circulation Research*, *120*(1), 179–206. https://doi.org/10.1161/CIRCRESAHA.116.306534

Kopincová, J., Púzserová, A., & Bernátová, I. (2012). L-NAME in the cardiovascular system – nitric oxide synthase activator? *Pharmacological Reports*, *64*(3), 511–520. https://doi.org/10.1016/S1734-1140(12)70846-0

Kraehling, J. R., & Sessa, W. C. (2017). Contemporary Approaches to Modulating the Nitric Oxide–cGMP Pathway in Cardiovascular Disease. *Circulation Research*, *120*(7), 1174–1182. https://doi.org/10.1161/CIRCRESAHA.117.303776

Krishnamoorthy, S., Recchiuti, A., Chiang, N., Yacoubian, S., Lee, C.-H., Yang, R., Petasis, N. A., & Serhan, C. N. (2010). Resolvin D1 binds human phagocytes with evidence for proresolving receptors. *Proceedings of the National Academy of Sciences*, *107*(4), 1660–1665. https://doi.org/10.1073/pnas.0907342107

Kuczeriszka, M., & Wąsowicz, K. (2022). Animal models of hypertension: The status of nitric oxide and oxidative stress and the role of the renal medulla. *Nitric Oxide*, *125–126*, 40–46. https://doi.org/10.1016/j.niox.2022.06.003

Lacoste, B., Comin, C. H., Ben-Zvi, A., Kaeser, P. S., Xu, X., Costa, L. da F., & Gu, C. (2014). Sensory-Related Neural Activity Regulates the Structure of Vascular Networks in the Cerebral Cortex. *Neuron*, *83*(5), 1117–1130. https://doi.org/10.1016/j.neuron.2014.07.034

Lampugnani, M. G. (2012). Endothelial Cell-to-Cell Junctions: Adhesion and Signaling in Physiology and Pathology. *Cold Spring Harbor Perspectives in Medicine*, *2*(10), a006528–a006528. https://doi.org/10.1101/cshperspect.a006528

Langen, U. H., Ayloo, S., & Gu, C. (2019). Development and Cell Biology of the Blood-Brain Barrier. *Annual Review of Cell and Developmental Biology*, *35*(1), 591–613. https://doi.org/10.1146/annurev-cellbio-100617-062608

Lavoie, J. L., & Sigmund, C. D. (2003). Minireview: Overview of the Renin-Angiotensin System—An Endocrine and Paracrine System. *Endocrinology*, *144*(6), 2179–2183. https://doi.org/10.1210/en.2003-0150

Lee, H., Lee, S., Cho, I.-H., & Joong Lee, S. (2013). Toll-Like Receptors: Sensor Molecules for Detecting Damage to the Nervous System. *Current Protein & Peptide Science*, *14*(1), 33–42. https://doi.org/10.2174/1389203711314010006

Lee, H.-G., Lee, J.-H., Flausino, L. E., & Quintana, F. J. (2023). Neuroinflammation: An astrocyte perspective. *Science Translational Medicine*, *15*(721). https://doi.org/10.1126/scitranslmed.adi7828

Leong, X.-F., Ng, C.-Y., & Jaarin, K. (2015). Animal Models in Cardiovascular Research: Hypertension and Atherosclerosis. *BioMed Research International*, *2015*, 528757. https://doi.org/10.1155/2015/528757

Lerman, L. O., Kurtz, T. W., Touyz, R. M., Ellison, D. H., Chade, A. R., Crowley, S. D., Mattson, D. L., Mullins, J. J., Osborn, J., Eirin, A., Reckelhoff, J. F., Iadecola, C., & Coffman, T. M. (2019). Animal Models of Hypertension: A Scientific Statement From the American Heart Association. *Hypertension*, *73*(6). https://doi.org/10.1161/HYP.0000000000000090

Li, P., & Fan, H. (2023). Pericyte Loss in Diseases. *Cells*, *12*(15), 1931. https://doi.org/10.3390/cells12151931

Liebner, S., Dijkhuizen, R. M., Reiss, Y., Plate, K. H., Agalliu, D., & Constantin, G. (2018). Functional morphology of the blood–brain barrier in health and disease. *Acta Neuropathologica*, *135*(3), 311–336. https://doi.org/10.1007/s00401-018-1815-1

Liu, G.-J., Tao, T., Zhang, X.-S., Lu, Y., Wu, L.-Y., Gao, Y.-Y., Wang, H., Dai, H.-B., Zhou, Y., Zhuang, Z., Hang, C.-H., & Li, W. (2021). Resolvin D1 Attenuates Innate Immune Reactions in Experimental Subarachnoid Hemorrhage Rat Model. *Molecular Neurobiology*, *58*(5), 1963–1977. https://doi.org/10.1007/s12035-020-02237-1

Liu, J., Wang, T., Dong, J., & Lu, Y. (2025a). The blood–brain barriers: novel nanocarriers for central nervous system diseases. *Journal of Nanobiotechnology*, *23*(1), 146. https://doi.org/10.1186/s12951-025-03247-8

Liu, J., Wang, T., Dong, J., & Lu, Y. (2025b). The blood–brain barriers: novel nanocarriers for central nervous system diseases. *Journal of Nanobiotechnology*, *23*(1), 146. https://doi.org/10.1186/s12951-025-03247-8

Liu, K., Colangelo, L. A., Daviglus, M. L., Goff, D. C., Pletcher, M., Schreiner, P. J., Sibley, C. T., Burke, G. L., Post, W. S., Michos, E. D., & Lloyd-Jones, D. M. (2015). Can Antihypertensive Treatment Restore the Risk of Cardiovascular Disease to Ideal Levels? *Journal of the American Heart Association*, *4*(9). https://doi.org/10.1161/JAHA.115.002275

Liu, L., Liu, J., Bao, J., Bai, Q., & Wang, G. (2020). Interaction of Microglia and Astrocytes in the Neurovascular Unit. *Frontiers in Immunology*, *11*. https://doi.org/10.3389/fimmu.2020.01024

Liu, X.-J., Yu, X.-J., Su, Y.-K., Qiao, J.-A., Sun, Y.-J., Bai, X.-J., Zhang, N., Yang, H.-Y., Yin, L.-X., Kang, Y.-M., & Yang, Z.-M. (2023). Minocycline and Pyrrolidine Dithiocarbamate Attenuate Hypertension via Suppressing Activation of Microglia in the Hypothalamic Paraventricular Nucleus. *The Tohoku Journal of Experimental Medicine*, *259*(2), 2022.J102. https://doi.org/10.1620/tjem.2022.J102

Loewenstein, D., & Rabbat, M. (2021). Neurological complications of systemic hypertension. *Handbook of Clinical Neurology*, *177*, 253–259. https://doi.org/10.1016/B978-0-12-819814-8.00018-4

Longden, T. A., Dabertrand, F., Koide, M., Gonzales, A. L., Tykocki, N. R., Brayden, J. E., Hill-Eubanks, D., & Nelson, M. T. (2017). Capillary K+-sensing initiates retrograde hyperpolarization to increase local cerebral blood flow. *Nature Neuroscience*, *20*(5), 717–726. https://doi.org/10.1038/nn.4533

Lopez-Candales, A., Hernández Burgos, P. M., Hernandez-Suarez, D. F., & Harris, D. (2017). Linking Chronic Inflammation with Cardiovascular Disease: From Normal Aging to the Metabolic Syndrome. *Journal of Nature and Science*, *3*(4).

Low, A., van Winden, S., Cai, L., Kessels, R. P. C., Maas, M. C., Morris, R. G., Nus, M., Tozer, D. J., Tuladhar, A., van der Kolk, A., Wolters, R., Mallat, Z., Riksen, N. P., Markus, H., & de Leeuw, F. (2024). Immune regulation and blood–brain barrier permeability in cerebral small vessel disease: study protocol of the INflammation and Small Vessel Disease (INSVD) study – a multicentre prospective cohort study. *BMJ Open*, *14*(2), e084303. https://doi.org/10.1136/bmjopen-2024-084303

Lu, Y., Hao, R., Hu, Y., Wei, Y., Xie, Y., Shen, Y., Rui, Q., & Yu, G. (2021). Harpagide alleviate neuronal apoptosis and blood-brain barrier leakage by inhibiting TLR4/MyD88/NF-κB signaling pathway in Angiotensin II-induced microglial activation in vitro. *Chemico-Biological Interactions*, *348*, 109653. https://doi.org/10.1016/j.cbi.2021.109653

Lu, Z.-Y., Qi, J., Yang, B., Cao, H.-L., Wang, R.-Y., Wang, X., Chi, R.-F., Guo, C.-L., Yang, Z.-M., Liu, H.-M., & Li, B. (2020). Diallyl Trisulfide Suppresses Angiotensin II–Induced Vascular Remodeling Via Inhibition of Mitochondrial Fission. *Cardiovascular Drugs and Therapy*, *34*(5), 605–618. https://doi.org/10.1007/s10557-020-07000-1

Ma, X., Zhang, H., Pan, Q., Zhao, Y., Chen, J., Zhao, B., & Chen, Y. (2013). Hypoxia/Aglycemia-Induced Endothelial Barrier Dysfunction and Tight Junction Protein Downregulation Can Be Ameliorated by Citicoline. *PLoS ONE*, *8*(12), e82604. https://doi.org/10.1371/journal.pone.0082604

Mamo, J. C. L., Lam, V., Giles, C., Coulson, S. H., Fimognari, N., Mooranian, A., Al-Salami, H., & Takechi, R. (2017). Antihypertensive agents do not prevent blood-brain barrier dysfunction and cognitive deficits in dietary-induced obese mice. *International Journal of Obesity (2005)*, *41*(6), 926–934. https://doi.org/10.1038/ijo.2017.57

Mapunda, J. A., Tibar, H., Regragui, W., & Engelhardt, B. (2022). How Does the Immune System Enter the Brain? *Frontiers in Immunology*, *13*. https://doi.org/10.3389/fimmu.2022.805657

Marchetti, L., Francisco, D., Soldati, S., Haghayegh Jahromi, N., Barcos, S., Gruber, I., Pareja, J. R., Thiriot, A., von Andrian, U., Deutsch, U., Lyck, R., Bruggmann, R., & Engelhardt, B. (2022). ACKR1 favors transcellular over paracellular T-cell diapedesis across the blood-brain barrier in neuroinflammation in vitro. *European Journal of Immunology*, *52*(1), 161–177. https://doi.org/10.1002/eji.202149238

Martìn-Padura, I., Lostaglio, S., Schneemann, M., Williams, L., Romano, M., Fruscella, P., Panzeri, C., Stoppacciaro, A., Ruco, L., Villa, A., Simmons, D., & Dejana, E. (1998). Junctional Adhesion Molecule, a Novel Member of the Immunoglobulin Superfamily That Distributes at Intercellular Junctions and Modulates Monocyte Transmigration. *The Journal of Cell Biology*, *142*(1), 117–127. https://doi.org/10.1083/jcb.142.1.117

Massagué, J., & Sheppard, D. (2023). TGF-β signaling in health and disease. *Cell*, *186*(19), 4007–4037. https://doi.org/10.1016/j.cell.2023.07.036

McConnell, H. L., & Mishra, A. (2022). *Cells of the Blood–Brain Barrier: An Overview of the Neurovascular Unit in Health and Disease* (pp. 3–24). https://doi.org/10.1007/978-1-0716-2289-6_1

Miller, A. J., & Arnold, A. C. (2019). The renin–angiotensin system in cardiovascular autonomic control: recent developments and clinical implications. *Clinical Autonomic Research*, *29*(2), 231–243. https://doi.org/10.1007/s10286-018-0572-5

Miller, D. S. (2015). *Regulation of ABC Transporters Blood–Brain Barrier* (pp. 43–70). https://doi.org/10.1016/bs.acr.2014.10.002

Milner, T. A., Chen, R. X., Welington, D., Rubin, B. R., Contoreggi, N. H., Johnson, M. A., Mazid, S., Marques-Lopes, J., Marongiu, R., & Glass, M. J. (2022). Angiotensin II differentially affects hippocampal glial inflammatory markers in young adult male and female mice. *Learning & Memory*, *29*(9), 265–273. https://doi.org/10.1101/lm.053507.121

Miners, J. S., Kehoe, P. G., Love, S., Zetterberg, H., & Blennow, K. (2019). CSF evidence of pericyte damage in Alzheimer's disease is associated with markers of blood-brain barrier dysfunction and disease pathology. *Alzheimer's Research & Therapy*, *11*(1), 81. https://doi.org/10.1186/s13195-019-0534-8

Mogi, M. (2024). Small vessels cause big problems. *Hypertension Research*, *47*(10), 2930–

2932. https://doi.org/10.1038/s41440-024-01811-7
Mohi-ud-Din, R., Mir, R. H., Mir, P. A., Banday, N., Shah, A. J., Sawhney, G., Bhat, M. M., Batiha, G. E., & Pottoo, F. H. (2022). Dysfunction of ABC Transporters at the Surface of BBB: Potential Implications in Intractable Epilepsy and Applications of Nanotechnology Enabled Drug Delivery. *Current Drug Metabolism*, *23*(9), 735–756. https://doi.org/10.2174/1389200223666220817115003
Morita, S., & Miyata, S. (2012). Different vascular permeability between the sensory and secretory circumventricular organs of adult mouse brain. *Cell and Tissue Research*, *349*(2), 589–603. https://doi.org/10.1007/s00441-012-1421-9
Moskal, J., & Michalak, S. (2025). Tight junction proteins in glial tumors development and progression. *Frontiers in Cellular Neuroscience*, *19*. https://doi.org/10.3389/fncel.2025.1541885
Mowry, F. E., Peaden, S. C., Stern, J. E., & Biancardi, V. C. (2021). TLR4 and AT1R mediate blood-brain barrier disruption, neuroinflammation, and autonomic dysfunction in spontaneously hypertensive rats. *Pharmacological Research*, *174*, 105877. https://doi.org/10.1016/j.phrs.2021.105877
Muñoz Maniega, S., Chappell, F. M., Valdés Hernández, M. C., Armitage, P. A., Makin, S. D., Heye, A. K., Thrippleton, M. J., Sakka, E., Shuler, K., Dennis, M. S., & Wardlaw, J. M. (2017). Integrity of normal-appearing white matter: Influence of age, visible lesion burden and hypertension in patients with small-vessel disease. *Journal of Cerebral Blood Flow & Metabolism*, *37*(2), 644–656. https://doi.org/10.1177/0271678X16635657
Nabika, T., Ohara, H., Kato, N., & Isomura, M. (2012). The stroke-prone spontaneously hypertensive rat: still a useful model for post-GWAS genetic studies? *Hypertension Research*, *35*(5), 477–484. https://doi.org/10.1038/hr.2012.30
Nagata, S., & Yamasaki, R. (2024). The Involvement of Glial Cells in Blood–Brain Barrier Damage in Neuroimmune Diseases. *International Journal of Molecular Sciences*, *25*(22), 12323. https://doi.org/10.3390/ijms252212323
Nasdala, I., Wolburg-Buchholz, K., Wolburg, H., Kuhn, A., Ebnet, K., Brachtendorf, G., Samulowitz, U., Kuster, B., Engelhardt, B., Vestweber, D., & Butz, S. (2002). A Transmembrane Tight Junction Protein Selectively Expressed on Endothelial Cells and Platelets. *Journal of Biological Chemistry*, *277*(18), 16294–16303. https://doi.org/10.1074/jbc.M111999200
Nezu, T., Hosomi, N., Aoki, S., Kubo, S., Araki, M., Mukai, T., Takahashi, T., Maruyama, H., Higashi, Y., & Matsumoto, M. (2015). Endothelial dysfunction is associated with the severity of cerebral small vessel disease. *Hypertension Research*, *38*(4), 291–297. https://doi.org/10.1038/hr.2015.4
Nishimoto, M., Griffin, K. A., Wynne, B. M., & Fujita, T. (2024). Salt-Sensitive Hypertension and the Kidney. *Hypertension*, *81*(6), 1206–1217. https://doi.org/10.1161/HYPERTENSIONAHA.123.21369
Nitta, T., Hata, M., Gotoh, S., Seo, Y., Sasaki, H., Hashimoto, N., Furuse, M., & Tsukita, S. (2003). Size-selective loosening of the blood-brain barrier in claudin-5–deficient mice. *The Journal of Cell Biology*, *161*(3), 653–660. https://doi.org/10.1083/jcb.200302070
Norden, D. M., Fenn, A. M., Dugan, A., & Godbout, J. P. (2014). TGFβ produced by IL-10 redirected astrocytes attenuates microglial activation. *Glia*, *62*(6), 881–895. https://doi.org/10.1002/glia.22647
Nozoe, M., Hirooka, Y., Koga, Y., Araki, S., Konno, S., Kishi, T., Ide, T., & Sunagawa, K. (2008). Mitochondria-derived reactive oxygen species mediate sympathoexcitation induced by angiotensin II in the rostral ventrolateral medulla. *Journal of Hypertension*, *26*(11), 2176–2184. https://doi.org/10.1097/HJH.0b013e32830dd5d3
Ohtsuki, S., Sato, S., Yamaguchi, H., Kamoi, M., Asashima, T., & Terasaki, T. (2007). Exogenous expression of claudin-5 induces barrier properties in cultured rat brain capillary endothelial cells. *Journal of Cellular Physiology*, *210*(1), 81–86. https://doi.org/10.1002/jcp.20823
Olivares-Silva, F., De Gregorio, N., Espitia-Corredor, J., Espinoza, C., Vivar, R., Silva, D.,

Osorio, J. M., Lavandero, S., Peiró, C., Sánchez-Ferrer, C., & Díaz-Araya, G. (2021). Resolvin-D1 attenuation of angiotensin II-induced cardiac inflammation in mice is associated with prevention of cardiac remodeling and hypertension. *Biochimica et Biophysica Acta (BBA) - Molecular Basis of Disease*, *1867*(12), 166241. https://doi.org/10.1016/j.bbadis.2021.166241

Olivera-Perez, H. M., Lam, L., Dang, J., Jiang, W., Rodriguez, F., Rigali, E., Weitzman, S., Porter, V., Rubbi, L., Morselli, M., Pellegrini, M., & Fiala, M. (2017). Omega-3 fatty acids increase the unfolded protein response and improve amyloid-β phagocytosis by macrophages of patients with mild cognitive impairment. *The FASEB Journal*, *31*(10), 4359–4369. https://doi.org/10.1096/fj.201700290R

Pajewski, N. M., Elahi, F. M., Tamura, M. K., Hinman, J. D., Nasrallah, I. M., Ix, J. H., Miller, L. M., Launer, L. J., Wright, C. B., Supiano, M. A., Lerner, A. J., Sudduth, T. L., Killeen, A. A., Cheung, A. K., Reboussin, D. M., Wilcock, D. M., & Williamson, J. D. (2022). Plasma amyloid beta, neurofilament light chain, and total tau in the Systolic Blood Pressure Intervention Trial (SPRINT). *Alzheimer's & Dementia*, *18*(8), 1472–1483. https://doi.org/10.1002/alz.12496

Panigrahy, D., Gilligan, M. M., Serhan, C. N., & Kashfi, K. (2021). Resolution of inflammation: An organizing principle in biology and medicine. *Pharmacology & Therapeutics*, *227*, 107879. https://doi.org/10.1016/j.pharmthera.2021.107879

Pardridge, W. M. (2023). Brain gene therapy with Trojan horse lipid nanoparticles. *Trends in Molecular Medicine*, *29*(5), 343–353. https://doi.org/10.1016/j.molmed.2023.02.004

Paulis, L., Zicha, J., Kunes, J., Hojna, S., Behuliak, M., Celec, P., Kojsova, S., Pechanova, O., & Simko, F. (2008). Regression of L-NAME–Induced Hypertension: The Role of Nitric Oxide and Endothelium-Derived Constricting Factor. *Hypertension Research*, *31*(4), 793–803. https://doi.org/10.1291/hypres.31.793

Persidsky, Y., Ramirez, S. H., Haorah, J., & Kanmogne, G. D. (2006). Blood–brain Barrier: Structural Components and Function Under Physiologic and Pathologic Conditions. *Journal of Neuroimmune Pharmacology*, *1*(3), 223–236. https://doi.org/10.1007/s11481-006-9025-3

Petty, M. A., & Lo, E. H. (2002). Junctional complexes of the blood–brain barrier: permeability changes in neuroinflammation. *Progress in Neurobiology*, *68*(5), 311–323. https://doi.org/10.1016/S0301-0082(02)00128-4

Pfau, S. J., Langen, U. H., Fisher, T. M., Prakash, I., Nagpurwala, F., Lozoya, R. A., Lee, W.-C. A., Wu, Z., & Gu, C. (2024). Characteristics of blood–brain barrier heterogeneity between brain regions revealed by profiling vascular and perivascular cells. *Nature Neuroscience*, *27*(10), 1892–1903. https://doi.org/10.1038/s41593-024-01743-y

Poulet, R., Gentile, M. T., Vecchione, C., Distaso, M., Aretini, A., Fratta, L., Russo, G., Echart, C., Maffei, A., De Simoni, M. G., & Lembo, G. (2006). Acute Hypertension Induces Oxidative Stress in Brain Tissues. *Journal of Cerebral Blood Flow & Metabolism*, *26*(2), 253–262. https://doi.org/10.1038/sj.jcbfm.9600188

Prado, A. F., Batista, R. I. M., Tanus-Santos, J. E., & Gerlach, R. F. (2021). Matrix Metalloproteinases and Arterial Hypertension: Role of Oxidative Stress and Nitric Oxide in Vascular Functional and Structural Alterations. *Biomolecules*, *11*(4), 585. https://doi.org/10.3390/biom11040585

Presa, J. L., Saravia, F., Bagi, Z., & Filosa, J. A. (2020). Vasculo-Neuronal Coupling and Neurovascular Coupling at the Neurovascular Unit: Impact of Hypertension. *Frontiers in Physiology*, *11*. https://doi.org/10.3389/fphys.2020.584135

Prinz, M., Jung, S., & Priller, J. (2019). Microglia Biology: One Century of Evolving Concepts. *Cell*, *179*(2), 292–311. https://doi.org/10.1016/j.cell.2019.08.053

Puddu, A., Montecucco, F., & Maggi, D. (2023). Caveolin-1 and Atherosclerosis: Regulation of LDLs Fate in Endothelial Cells. *International Journal of Molecular Sciences*, *24*(10), 8869. https://doi.org/10.3390/ijms24108869

Pueyo, M. E., Gonzalez, W., Nicoletti, A., Savoie, F., Arnal, J.-F., & Michel, J.-B. (2000). Angiotensin II Stimulates Endothelial Vascular Cell Adhesion Molecule-1 via Nuclear

Factor-κB Activation Induced by Intracellular Oxidative Stress. *Arteriosclerosis, Thrombosis, and Vascular Biology*, *20*(3), 645–651. https://doi.org/10.1161/01.ATV.20.3.645

Pulgar, V. M. (2019). Transcytosis to Cross the Blood Brain Barrier, New Advancements and Challenges. *Frontiers in Neuroscience*, *12*. https://doi.org/10.3389/fnins.2018.01019

Rajanathan, R., Pedersen, T. M., Thomsen, M. B., Botker, H. E., & Matchkov, V. V. (2022). Phenylephrine-Induced Cardiovascular Changes in the Anesthetized Mouse: An Integrated Assessment of in vivo Hemodynamics Under Conditions of Controlled Heart Rate. *Frontiers in Physiology*, *13*. https://doi.org/10.3389/fphys.2022.831724

Rasmussen, M. K., Mestre, H., & Nedergaard, M. (2022). Fluid transport in the brain. *Physiological Reviews*, *102*(2), 1025–1151. https://doi.org/10.1152/physrev.00031.2020

Recchiuti, A., Krishnamoorthy, S., Fredman, G., Chiang, N., & Serhan, C. N. (2011). MicroRNAs in resolution of acute inflammation: identification of novel resolvin D1-miRNA circuits. *FASEB Journal : Official Publication of the Federation of American Societies for Experimental Biology*, *25*(2), 544–560. https://doi.org/10.1096/fj.10-169599

Ren, Y.-Z., Zhang, B.-Z., Zhao, X.-J., & Zhang, Z.-Y. (2020). Resolvin D1 ameliorates cognitive impairment following traumatic brain injury via protecting astrocytic mitochondria. *Journal of Neurochemistry*, *154*(5), 530–546. https://doi.org/10.1111/jnc.14962

Rey, C., Nadjar, A., Buaud, B., Vaysse, C., Aubert, A., Pallet, V., Layé, S., & Joffre, C. (2016a). Resolvin D1 and E1 promote resolution of inflammation in microglial cells in vitro. *Brain, Behavior, and Immunity*, *55*, 249–259. https://doi.org/10.1016/j.bbi.2015.12.013

Rey, C., Nadjar, A., Buaud, B., Vaysse, C., Aubert, A., Pallet, V., Layé, S., & Joffre, C. (2016b). Resolvin D1 and E1 promote resolution of inflammation in microglial cells in vitro. *Brain, Behavior, and Immunity*, *55*, 249–259. https://doi.org/10.1016/j.bbi.2015.12.013

Ribeiro Vitorino, T., Ferraz do Prado, A., Bruno de Assis Cau, S., & Rizzi, E. (2023). MMP-2 and its implications on cardiac function and structure: Interplay with inflammation in hypertension. *Biochemical Pharmacology*, *215*, 115684. https://doi.org/10.1016/j.bcp.2023.115684

Rossi, G. P., Bagordo, D., Rossi, F. B., Pintus, G., Rossitto, G., & Seccia, T. M. (2024). 'Essential' arterial hypertension: time for a paradigm change. *Journal of Hypertension*, *42*(8), 1298–1304. https://doi.org/10.1097/HJH.0000000000003767

Rowsthorn, E., Pham, W., Nazem-Zadeh, M.-R., Law, M., Pase, M. P., & Harding, I. H. (2023). Imaging the neurovascular unit in health and neurodegeneration: a scoping review of interdependencies between MRI measures. *Fluids and Barriers of the CNS*, *20*(1), 97. https://doi.org/10.1186/s12987-023-00499-0

Santisteban, M. M., Ahmari, N., Carvajal, J. M., Zingler, M. B., Qi, Y., Kim, S., Joseph, J., Garcia-Pereira, F., Johnson, R. D., Shenoy, V., Raizada, M. K., & Zubcevic, J. (2015). Involvement of Bone Marrow Cells and Neuroinflammation in Hypertension. *Circulation Research*, *117*(2), 178–191. https://doi.org/10.1161/CIRCRESAHA.117.305853

Santos, G. S. P., Magno, L. A. V., Romano-Silva, M. A., Mintz, A., & Birbrair, A. (2019). Pericyte Plasticity in the Brain. *Neuroscience Bulletin*, *35*(3), 551–560. https://doi.org/10.1007/s12264-018-0296-5

Santos, Sampaio, W. O., Alzamora, A. C., Motta-Santos, D., Alenina, N., Bader, M., & Campagnole-Santos, M. J. (2018). The ACE2/Angiotensin-(1–7)/MAS Axis of the Renin-Angiotensin System: Focus on Angiotensin-(1–7). *Physiological Reviews*, *98*(1), 505–553. https://doi.org/10.1152/physrev.00023.2016

Sargurupremraj, M., Suzuki, H., Jian, X., Sarnowski, C., Evans, T. E., Bis, J. C., Eiriksdottir, G., Sakaue, S., Terzikhan, N., Habes, M., Zhao, W., Armstrong, N. J., Hofer, E., Yanek, L. R., Hagenaars, S. P., Kumar, R. B., van den Akker, E. B., McWhirter, R. E., Trompet,

S., … Debette, S. (2020). Cerebral small vessel disease genomics and its implications across the lifespan. *Nature Communications*, *11*(1), 6285. https://doi.org/10.1038/s41467-020-19111-2

Scalisi, J., Balau, B., Deneyer, L., Bouchat, J., Gilloteaux, J., & Nicaise, C. (2021). Blood-brain barrier permeability towards small and large tracers in a mouse model of osmotic demyelination syndrome. *Neuroscience Letters*, *746*, 135665. https://doi.org/10.1016/j.neulet.2021.135665

Schaeffer, S., & Iadecola, C. (2021). Revisiting the neurovascular unit. *Nature Neuroscience*, *24*(9), 1198–1209. https://doi.org/10.1038/s41593-021-00904-7

Serhan, C. N. (2014). Pro-resolving lipid mediators are leads for resolution physiology. *Nature*, *510*(7503), 92–101. https://doi.org/10.1038/nature13479

Serhan, C. N., Chiang, N., & Nshimiyimana, R. (2024). Low-dose pro-resolving mediators temporally reset the resolution response to microbial inflammation. *Molecular Medicine*, *30*(1), 153. https://doi.org/10.1186/s10020-024-00877-w

Serhan, C. N., Chiang, N., & Van Dyke, T. E. (2008). Resolving inflammation: dual anti-inflammatory and pro-resolution lipid mediators. *Nature Reviews. Immunology*, *8*(5), 349–361. https://doi.org/10.1038/nri2294

Serhan, C. N., Gotlinger, K., Hong, S., & Arita, M. (2004). Resolvins, docosatrienes, and neuroprotectins, novel omega-3-derived mediators, and their aspirin-triggered endogenous epimers: an overview of their protective roles in catabasis. *Prostaglandins & Other Lipid Mediators*, *73*(3–4), 155–172. https://doi.org/10.1016/j.prostaglandins.2004.03.005

Serhan, C. N., Hong, S., Gronert, K., Colgan, S. P., Devchand, P. R., Mirick, G., & Moussignac, R.-L. (2002). Resolvins: a family of bioactive products of omega-3 fatty acid transformation circuits initiated by aspirin treatment that counter proinflammation signals. *The Journal of Experimental Medicine*, *196*(8), 1025–1037. https://doi.org/10.1084/jem.20020760

Serhan, C. N., & Levy, B. D. (2018). Resolvins in inflammation: emergence of the pro-resolving superfamily of mediators. *Journal of Clinical Investigation*, *128*(7), 2657–2669. https://doi.org/10.1172/JCI97943

Shalini, S.-M., Ho, C. F.-Y., Ng, Y.-K., Tong, J.-X., Ong, E.-S., Herr, D. R., Dawe, G. S., & Ong, W.-Y. (2018). Distribution of Alox15 in the Rat Brain and Its Role in Prefrontal Cortical Resolvin D1 Formation and Spatial Working Memory. *Molecular Neurobiology*, *55*(2), 1537–1550. https://doi.org/10.1007/s12035-017-0413-x

Shanaki-Bavarsad, M., Almolda, B., González, B., & Castellano, B. (2022). Astrocyte-targeted Overproduction of IL-10 Reduces Neurodegeneration after TBI. *Experimental Neurobiology*, *31*(3), 173–195. https://doi.org/10.5607/en21035

Shekhar, S., Liu, R., Travis, O. K., Roman, R. J., & Fan, F. (2017). Cerebral Autoregulation in Hypertension and Ischemic Stroke: A Mini Review. *Journal of Pharmaceutical Sciences and Experimental Pharmacology*, *2017*(1), 21–27.

Shi, P., Diez-Freire, C., Jun, J. Y., Qi, Y., Katovich, M. J., Li, Q., Sriramula, S., Francis, J., Sumners, C., & Raizada, M. K. (2010). Brain Microglial Cytokines in Neurogenic Hypertension. *Hypertension*, *56*(2), 297–303. https://doi.org/10.1161/HYPERTENSIONAHA.110.150409

Siddiqui, H., Yevstigneyev, N., Madani, G., & McCormick, S. (2022). Approaches to Visualising Endocytosis of LDL-Related Lipoproteins. *Biomolecules*, *12*(2), 158. https://doi.org/10.3390/biom12020158

Silver, J., & Miller, J. H. (2004). Regeneration beyond the glial scar. *Nature Reviews Neuroscience*, *5*(2), 146–156. https://doi.org/10.1038/nrn1326

Singh, N., & Ecker, G. F. (2018). Insights into the Structure, Function, and Ligand Discovery of the Large Neutral Amino Acid Transporter 1, LAT1. *International Journal of Molecular Sciences*, *19*(5), 1278. https://doi.org/10.3390/ijms19051278

Sofroniew, M. V. (2015). Astrocyte barriers to neurotoxic inflammation. *Nature Reviews Neuroscience*, *16*(5), 249–263. https://doi.org/10.1038/nrn3898

Solé-Guardia, G., Janssen, A., Wolters, R., Dohmen, T., Küsters, B., Claassen, J. A., Leeuw,

F.-E. de, Wiesmann, M., Gutierrez, J., & Kiliaan, A. J. (2025a). Impact of hypertension on cerebral small vessel disease: A post-mortem study of microvascular pathology from normal-appearing white matter into white matter hyperintensities. *Journal of Cerebral Blood Flow & Metabolism*. https://doi.org/10.1177/0271678X251333256

Solé-Guardia, G., Janssen, A., Wolters, R., Dohmen, T., Küsters, B., Claassen, J. A., Leeuw, F.-E. de, Wiesmann, M., Gutierrez, J., & Kiliaan, A. J. (2025b). Impact of hypertension on cerebral small vessel disease: A post-mortem study of microvascular pathology from normal-appearing white matter into white matter hyperintensities. *Journal of Cerebral Blood Flow & Metabolism*. https://doi.org/10.1177/0271678X251333256

Soliman, A. M., Soliman, M., Shah, S. S. H., Baig, H. A., Gouda, N. S., Alenezi, B. T., Alenezy, A., Hegazy, A. M. S., Jan, M., & Eltom, E. H. (2025). Molecular dynamics of inflammation resolution: therapeutic implications. *Frontiers in Cell and Developmental Biology*, *13*. https://doi.org/10.3389/fcell.2025.1600149

Song, J., Wu, C., Korpos, E., Zhang, X., Agrawal, S. M., Wang, Y., Faber, C., Schäfers, M., Körner, H., Opdenakker, G., Hallmann, R., & Sorokin, L. (2015). Focal MMP-2 and MMP-9 Activity at the Blood-Brain Barrier Promotes Chemokine-Induced Leukocyte Migration. *Cell Reports*, *10*(7), 1040–1054. https://doi.org/10.1016/j.celrep.2015.01.037

Sordi, R., Chiazza, F., Collotta, D., Migliaretti, G., Colas, R. A., Vulliamy, P., Brohi, K., Dalli, J., Collino, M., & Thiemermann, C. (2021). Resolvin D1 Attenuates the Organ Injury Associated With Experimental Hemorrhagic Shock. *Annals of Surgery*, *273*(5), 1012–1021. https://doi.org/10.1097/SLA.0000000000003407

Sorets, A. G., Rosch, J. C., Duvall, C. L., & Lippmann, E. S. (2020). Caveolae-mediated transport at the injured blood–brain barrier as an underexplored pathway for central nervous system drug delivery. *Current Opinion in Chemical Engineering*, *30*, 86–95. https://doi.org/10.1016/j.coche.2020.08.009

Sorriento, D., De Luca, N., Trimarco, B., & Iaccarino, G. (2018). The Antioxidant Therapy: New Insights in the Treatment of Hypertension. *Frontiers in Physiology*, *9*. https://doi.org/10.3389/fphys.2018.00258

Sousa, A. B., & Barbosa, J. N. (2023). The Use of Specialized Pro-Resolving Mediators in Biomaterial-Based Immunomodulation. *Journal of Functional Biomaterials*, *14*(4), 223. https://doi.org/10.3390/jfb14040223

Stern, J. E., Son, S., Biancardi, V. C., Zheng, H., Sharma, N., & Patel, K. P. (2016). Astrocytes Contribute to Angiotensin II Stimulation of Hypothalamic Neuronal Activity and Sympathetic Outflow. *Hypertension*, *68*(6), 1483–1493. https://doi.org/10.1161/HYPERTENSIONAHA.116.07747

Stevenson, B. R., Siliciano, J. D., Mooseker, M. S., & Goodenough, D. A. (1986). Identification of ZO-1: a high molecular weight polypeptide associated with the tight junction (zonula occludens) in a variety of epithelia. *The Journal of Cell Biology*, *103*(3), 755–766. https://doi.org/10.1083/jcb.103.3.755

Sumitomo-Ueda, Y., Aihara, K., Ise, T., Yoshida, S., Ikeda, Y., Uemoto, R., Yagi, S., Iwase, T., Ishikawa, K., Hirata, Y., Akaike, M., Sata, M., Kato, S., & Matsumoto, T. (2010). Heparin Cofactor II Protects Against Angiotensin II-Induced Cardiac Remodeling Via Attenuation of Oxidative Stress in Mice. *Hypertension*, *56*(3), 430–436. https://doi.org/10.1161/HYPERTENSIONAHA.110.152207

Sun, Q., Yan, H., Chen, F., Jiang, F., Chen, W., Li, D., & Guo, Y. (2021). Restoration of Proresolution Pathway with Exogenous Resolvin D1 Prevents Sevoflurane-Induced Cognitive Decline by Attenuating Neuroinflammation in the Hippocampus in Rats with Type 2 Diabetes Mellitus. *Frontiers in Pharmacology*, *12*. https://doi.org/10.3389/fphar.2021.720249

Sweeney, M. D., Zhao, Z., Montagne, A., Nelson, A. R., & Zlokovic, B. V. (2019a). Blood-Brain Barrier: From Physiology to Disease and Back. *Physiological Reviews*, *99*(1), 21–78. https://doi.org/10.1152/physrev.00050.2017

Sweeney, M. D., Zhao, Z., Montagne, A., Nelson, A. R., & Zlokovic, B. V. (2019b). Blood-Brain Barrier: From Physiology to Disease and Back. *Physiological Reviews*, *99*(1), 21–

78. https://doi.org/10.1152/physrev.00050.2017
Takata, F., Nakagawa, S., Matsumoto, J., & Dohgu, S. (2021). Blood-Brain Barrier Dysfunction Amplifies the Development of Neuroinflammation: Understanding of Cellular Events in Brain Microvascular Endothelial Cells for Prevention and Treatment of BBB Dysfunction. *Frontiers in Cellular Neuroscience*, *15*. https://doi.org/10.3389/fncel.2021.661838
Tang, N., Ma, J., Tao, R., Chen, Z., Yang, Y., He, Q., Lv, Y., Lan, Z., & Zhou, J. (2022). The effects of the interaction between BMI and dyslipidemia on hypertension in adults. *Scientific Reports*, *12*(1), 927. https://doi.org/10.1038/s41598-022-04968-8
te Riet, L., van Esch, J. H. M., Roks, A. J. M., van den Meiracker, A. H., & Danser, A. H. J. (2015). Hypertension. *Circulation Research*, *116*(6), 960–975. https://doi.org/10.1161/CIRCRESAHA.116.303587
Terrando, N., Gómez-Galán, M., Yang, T., Carlström, M., Gustavsson, D., Harding, R. E., Lindskog, M., & Eriksson, L. I. (2013). Aspirin-triggered resolvin D1 prevents surgery-induced cognitive decline. *The FASEB Journal*, *27*(9), 3564–3571. https://doi.org/10.1096/fj.13-230276
Tomassoni, D., Avola, R., Di Tullio, M. A., Sabbatini, M., Vitaioli, L., & Amenta, F. (2004). Increased Expression of Glial Fibrillary Acidic Protein in the Brain of Spontaneously Hypertensive Rats. *Clinical and Experimental Hypertension*, *26*(4), 335–350. https://doi.org/10.1081/CEH-120034138
Tornavaca, O., Chia, M., Dufton, N., Almagro, L. O., Conway, D. E., Randi, A. M., Schwartz, M. A., Matter, K., & Balda, M. S. (2015). ZO-1 controls endothelial adherens junctions, cell–cell tension, angiogenesis, and barrier formation. *Journal of Cell Biology*, *208*(6), 821–838. https://doi.org/10.1083/jcb.201404140
Ungvari, Z., Toth, P., Tarantini, S., Prodan, C. I., Sorond, F., Merkely, B., & Csiszar, A. (2021). Hypertension-induced cognitive impairment: from pathophysiology to public health. *Nature Reviews Nephrology*, *17*(10), 639–654. https://doi.org/10.1038/s41581-021-00430-6
Valko, M., Leibfritz, D., Moncol, J., Cronin, M. T. D., Mazur, M., & Telser, J. (2007). Free radicals and antioxidants in normal physiological functions and human disease. *The International Journal of Biochemistry & Cell Biology*, *39*(1), 44–84. https://doi.org/10.1016/j.biocel.2006.07.001
van den Kerkhof, M., de Jong, J. J. A., Voorter, P. H. M., Postma, A. A., Kroon, A. A., van Oostenbrugge, R. J., Jansen, J. F. A., & Backes, W. H. (2024). Blood-Brain Barrier Integrity Decreases With Higher Blood Pressure: A 7T DCE-MRI Study. *Hypertension*, *81*(10), 2162–2172. https://doi.org/10.1161/HYPERTENSIONAHA.123.22617
van Vliet, E. A., da Costa Araujo, S., Redeker, S., van Schaik, R., Aronica, E., & Gorter, J. A. (2007). Blood-brain barrier leakage may lead to progression of temporal lobe epilepsy. *Brain*, *130*(2), 521–534. https://doi.org/10.1093/brain/awl318
Verkhratsky, A., & Nedergaard, M. (2018). Physiology of Astroglia. *Physiological Reviews*, *98*(1), 239–389. https://doi.org/10.1152/physrev.00042.2016
Vital, S. A., Terao, S., Nagai, M., & Granger, D. N. (2010). Mechanisms Underlying the Cerebral Microvascular Responses to Angiotensin II-Induced Hypertension. *Microcirculation*, *17*(8), 641–649. https://doi.org/10.1111/j.1549-8719.2010.00060.x
Wang, F., Cao, Y., Ma, L., Pei, H., Rausch, W. D., & Li, H. (2018). Dysfunction of Cerebrovascular Endothelial Cells: Prelude to Vascular Dementia. *Frontiers in Aging Neuroscience*, *10*. https://doi.org/10.3389/fnagi.2018.00376
Wang, H., Xu, Z., Xia, Z., Rallo, M., Duffy, A., & Matise, M. P. (2021). Inactivation of Hedgehog signal transduction in adult astrocytes results in region-specific blood–brain barrier defects. *Proceedings of the National Academy of Sciences*, *118*(34). https://doi.org/10.1073/pnas.2017779118
Wang, M. J., Zhou, L., Wu, J., Wang, Y., Ren, T., Yin, Y. F., Cao, J., & Cheng, T. (2025). [The clinical significance of resolvin D1 in patients with systemic lupus erythematosus treated with Belimumab]. *Zhonghua Yi Xue Za Zhi*, *105*(5), 358–363. https://doi.org/10.3760/cma.j.cn112137-20240717-01640

Wang, M., Pan, W., Xu, Y., Zhang, J., Wan, J., & Jiang, H. (2022). Microglia-Mediated Neuroinflammation: A Potential Target for the Treatment of Cardiovascular Diseases. *Journal of Inflammation Research*, *Volume 15*, 3083–3094. https://doi.org/10.2147/JIR.S350109

Wang, R., Wang, M., Du, D., Shan, Z., Bi, L., & Chen, Q.-H. (2025). Brain-Targeted Reactive Oxygen Species in Hypertension: Unveiling Subcellular Dynamics, Immune Cross-Talk, and Novel Therapeutic Pathways. *Antioxidants*, *14*(4), 408. https://doi.org/10.3390/antiox14040408

Wang, X., Deckert, M., Xuan, N. T., Nishanth, G., Just, S., Waisman, A., Naumann, M., & Schlüter, D. (2013). Astrocytic A20 ameliorates experimental autoimmune encephalomyelitis by inhibiting NF-κB- and STAT1-dependent chemokine production in astrocytes. *Acta Neuropathologica*, *126*(5), 711–724. https://doi.org/10.1007/s00401-013-1183-9

Wanner, I. B., Anderson, M. A., Song, B., Levine, J., Fernandez, A., Gray-Thompson, Z., Ao, Y., & Sofroniew, M. V. (2013). Glial Scar Borders Are Formed by Newly Proliferated, Elongated Astrocytes That Interact to Corral Inflammatory and Fibrotic Cells via STAT3-Dependent Mechanisms after Spinal Cord Injury. *Journal of Neuroscience*, *33*(31), 12870–12886. https://doi.org/10.1523/JNEUROSCI.2121-13.2013

Wei, B., Cheng, G., Bi, Q., Lu, C., Sun, Q., Li, L., Chen, N., Hu, M., Lu, H., Xu, X., Mao, G., Wan, S., Hu, Z., Gu, Y., Zheng, J., Zhao, L., Shen, X. Z., Liu, X., & Shi, P. (2024a). Microglia in the hypothalamic paraventricular nucleus sense hemodynamic disturbance and promote sympathetic excitation in hypertension. *Immunity*, *57*(9), 2030-2042.e8. https://doi.org/10.1016/j.immuni.2024.07.011

Wei, B., Cheng, G., Bi, Q., Lu, C., Sun, Q., Li, L., Chen, N., Hu, M., Lu, H., Xu, X., Mao, G., Wan, S., Hu, Z., Gu, Y., Zheng, J., Zhao, L., Shen, X. Z., Liu, X., & Shi, P. (2024b). Microglia in the hypothalamic paraventricular nucleus sense hemodynamic disturbance and promote sympathetic excitation in hypertension. *Immunity*, *57*(9), 2030-2042.e8. https://doi.org/10.1016/j.immuni.2024.07.011

Wei, C., Guo, S., Liu, W., Jin, F., Wei, B., Fan, H., Su, H., Liu, J., Zhang, N., Fang, D., Li, G., Shu, S., Li, X., He, X., Zhang, X., & Duan, C. (2021a). Resolvin D1 ameliorates Inflammation-Mediated Blood-Brain Barrier Disruption After Subarachnoid Hemorrhage in rats by Modulating A20 and NLRP3 Inflammasome. *Frontiers in Pharmacology*, *11*. https://doi.org/10.3389/fphar.2020.610734

Wei, C., Guo, S., Liu, W., Jin, F., Wei, B., Fan, H., Su, H., Liu, J., Zhang, N., Fang, D., Li, G., Shu, S., Li, X., He, X., Zhang, X., & Duan, C. (2021b). Resolvin D1 ameliorates Inflammation-Mediated Blood-Brain Barrier Disruption After Subarachnoid Hemorrhage in rats by Modulating A20 and NLRP3 Inflammasome. *Frontiers in Pharmacology*, *11*. https://doi.org/10.3389/fphar.2020.610734

Wei, C., Zhang, J., Peng, S., Liu, J., Xu, Y., Zhao, M., Xu, S., Pan, W., Yin, Z., Zheng, Z., Qin, J.-J., Wan, J., & Wang, M. (2024a). Resolvin D1 attenuates Ang II-induced hypertension in mice by inhibiting the proliferation, migration and phenotypic transformation of vascular smooth muscle cells by blocking the RhoA/mitogen-activated protein kinase pathway. *Journal of Hypertension*, *42*(3), 420–431. https://doi.org/10.1097/HJH.0000000000003610

Wei, C., Zhang, J., Peng, S., Liu, J., Xu, Y., Zhao, M., Xu, S., Pan, W., Yin, Z., Zheng, Z., Qin, J.-J., Wan, J., & Wang, M. (2024b). Resolvin D1 attenuates Ang II-induced hypertension in mice by inhibiting the proliferation, migration and phenotypic transformation of vascular smooth muscle cells by blocking the RhoA/mitogen-activated protein kinase pathway. *Journal of Hypertension*, *42*(3), 420–431. https://doi.org/10.1097/HJH.0000000000003610

Weiss, N., Miller, F., Cazaubon, S., & Couraud, P.-O. (2009). The blood-brain barrier in brain homeostasis and neurological diseases. *Biochimica et Biophysica Acta (BBA) - Biomembranes*, *1788*(4), 842–857. https://doi.org/10.1016/j.bbamem.2008.10.022

Wigner, P., Dziedzic, A., Synowiec, E., Miller, E., Bijak, M., & Saluk-Bijak, J. (2022). Variation of genes encoding nitric oxide synthases and antioxidant enzymes as potential

risks of multiple sclerosis development: a preliminary study. *Scientific Reports*, *12*(1), 10603. https://doi.org/10.1038/s41598-022-14795-6

Williams, B., Mancia, G., Spiering, W., Agabiti Rosei, E., Azizi, M., Burnier, M., Clement, D. L., Coca, A., de Simone, G., Dominiczak, A., Kahan, T., Mahfoud, F., Redon, J., Ruilope, L., Zanchetti, A., Kerins, M., Kjeldsen, S. E., Kreutz, R., Laurent, S., … Brady, A. (2018). 2018 ESC/ESH Guidelines for the management of arterial hypertension. *European Heart Journal*, *39*(33), 3021–3104. https://doi.org/10.1093/eurheartj/ehy339

Winklewski, P. J., Radkowski, M., Wszedybyl-Winklewska, M., & Demkow, U. (2015). Brain inflammation and hypertension: the chicken or the egg? *Journal of Neuroinflammation*, *12*(1), 85. https://doi.org/10.1186/s12974-015-0306-8

Wolburg, H., Wolburg-Buchholz, K., Kraus, J., Rascher-Eggstein, G., Liebner, S., Hamm, S., Duffner, F., Grote, E.-H., Risau, W., & Engelhardt, B. (2003). Localization of claudin-3 in tight junctions of the blood-brain barrier is selectively lost during experimental autoimmune encephalomyelitis and human glioblastoma multiforme. *Acta Neuropathologica*, *105*(6), 586–592. https://doi.org/10.1007/s00401-003-0688-z

Woodburn, S. C., Bollinger, J. L., & Wohleb, E. S. (2021). The semantics of microglia activation: neuroinflammation, homeostasis, and stress. *Journal of Neuroinflammation*, *18*(1), 258. https://doi.org/10.1186/s12974-021-02309-6

Wosik, K., Cayrol, R., Dodelet-Devillers, A., Berthelet, F., Bernard, M., Moumdjian, R., Bouthillier, A., Reudelhuber, T. L., & Prat, A. (2007). Angiotensin II Controls Occludin Function and Is Required for Blood–Brain Barrier Maintenance: Relevance to Multiple Sclerosis. *The Journal of Neuroscience*, *27*(34), 9032–9042. https://doi.org/10.1523/JNEUROSCI.2088-07.2007

Wu, K. L., Chan, S. H., & Chan, J. Y. (2012). Neuroinflammation and oxidative stress in rostral ventrolateral medulla contribute to neurogenic hypertension induced by systemic inflammation. *Journal of Neuroinflammation*, *9*(1), 212. https://doi.org/10.1186/1742-2094-9-212

Xanthos, D. N., & Sandkühler, J. (2014). Neurogenic neuroinflammation: inflammatory CNS reactions in response to neuronal activity. *Nature Reviews Neuroscience*, *15*(1), 43–53. https://doi.org/10.1038/nrn3617

Xia, Y., Lu, Y. W., Hao, R. J., & Yu, G. R. (2022). Catalpol relieved angiotensin II-induced blood–brain barrier destruction via inhibiting the TLR4 pathway in brain endothelial cells. *Pharmaceutical Biology*, *60*(1), 2210–2218. https://doi.org/10.1080/13880209.2022.2142801

Xiaoyu, L., Dandan, L., Tianzhao, O., Ziyou, Z., Zhenlin, L., Zhuang, L., Mingrui, L., Yusong, H., Yangyang, Z., Yanjiao, L., Chun, S., Siqi, W., Tong, L., & Bensi, Z. (2024). Resolvin D1 combined with exercise rehabilitation alleviates neurological injury in mice with intracranial hemorrhage via the BDNF/TrkB/PI3K/AKT pathway. *Scientific Reports*, *14*(1), 31447. https://doi.org/10.1038/s41598-024-83019-w

Xie, D. F., Fang, C., Crouzet, C., Hung, Y.-H., Vallejo, A., Lee, D., Liu, J., Liu, H., Muvvala, S., Paganini-Hill, A., Lau, W. L., Cribbs, D. H., Choi, B., & Fisher, M. (2025). Development of cerebral microhemorrhages in a mouse model of hypertension. *Journal of Neuroinflammation*, *22*(1), 67. https://doi.org/10.1186/s12974-025-03378-7

Xie, Y. Y., Lu, Y. W., & Yu, G. R. (2022). The protective effects of hyperoside on Ang II-mediated apoptosis of bEnd.3 cells and injury of blood-brain barrier model in vitro. *BMC Complementary Medicine and Therapies*, *22*(1), 157. https://doi.org/10.1186/s12906-022-03635-9

Xing, Z., Liu, J., Cai, J., Jiang, X., Liang, J., Fujio, M., Hadler-Olsen, E., Wang, J., Kantarci, A., & Xue, Y. (2024). The Application of Resolvin D1-Loaded Gelatin Methacrylate in a Rat Periodontitis Model. *Pharmaceutics*, *17*(1), 16. https://doi.org/10.3390/pharmaceutics17010016

Xu, L., & Sved, A. F. (2002). Acute sympathoexcitatory action of angiotensin II in conscious baroreceptor-denervated rats. *American Journal of Physiology-Regulatory, Integrative and Comparative Physiology*, *283*(2), R451–R459. https://doi.org/10.1152/ajpregu.00648.2001

Xue, T., Song, Y., Zhao, J., Fan, G., & Liu, Z. (2025). Inhibition of S100A4 decreases neurotoxic astrocyte reactivity and attenuates neuropathic pain via the TLR4/NF-κB pathway in a rat model of spinal nerve ligation. *The Journal of Headache and Pain*, *26*(1), 97. https://doi.org/10.1186/s10194-025-02045-9

Yang, K., Li, Q., Ruan, Y., Xia, Y., & Fang, Z. (2025). Caveolae-Mediated Transcytosis and Its Role in Neurological Disorders. *Biomolecules*, *15*(4), 456. https://doi.org/10.3390/biom15040456

Yang, Wang, Z., Guo, M., Du, M., Wen, X., Geng, L., Yu, F., Liu, L., Li, Y., Feng, L., & Zhou, T. (2021). UPLC-MS-Based Serum Metabolomics Reveals Potential Biomarkers of Ang II-Induced Hypertension in Mice. *Frontiers in Cardiovascular Medicine*, *8*. https://doi.org/10.3389/fcvm.2021.683859

Yanoshita, M., Hirose, N., Nishiyama, S., Tsuboi, E., Kubo, N., Kita, D., & Tanimoto, K. (2025). Resolvin D1 suppresses inflammation in human fibroblast-like synoviocytes via the p-38, NF-κB, and AKT signaling pathways. *In Vitro Cellular & Developmental Biology - Animal*, *61*(3), 331–339. https://doi.org/10.1007/s11626-024-01008-9

Yao, L., Kan, E. M., Lu, J., Hao, A., Dheen, S. T., Kaur, C., & Ling, E.-A. (2013). Toll-like receptor 4 mediates microglial activation and production of inflammatory mediators in neonatal rat brain following hypoxia: role of TLR4 in hypoxic microglia. *Journal of Neuroinflammation*, *10*(1), 785. https://doi.org/10.1186/1742-2094-10-23

Yao, Y., Chen, Y., Tomer, R., & Silver, R. (2025). Capillary connections between sensory circumventricular organs and adjacent parenchyma enable local volume transmission. *Journal of Neuroendocrinology*, *37*(4). https://doi.org/10.1111/jne.13490

Yazdani, S., Jaldin-Fincati, J. R., Pereira, R. V. S., & Klip, A. (2019). Endothelial cell barriers: Transport of molecules between blood and tissues. *Traffic*, *20*(6), 390–403. https://doi.org/10.1111/tra.12645

Yin, L., Bai, J., Yu, W.-J., Liu, Y., Li, H.-H., & Lin, Q.-Y. (2022). Blocking VCAM-1 Prevents Angiotensin II-Induced Hypertension and Vascular Remodeling in Mice. *Frontiers in Pharmacology*, *13*. https://doi.org/10.3389/fphar.2022.825459

Yu, S., He, J., & Xie, K. (2023). Zonula Occludens Proteins Signaling in Inflammation and Tumorigenesis. *International Journal of Biological Sciences*, *19*(12), 3804–3815. https://doi.org/10.7150/ijbs.85765

Yu, Y., Xue, B., Tong, L., Bassuk, A. G., Johnson, A. K., & Wei, S. (2025). RORγt Mediates Angiotensin II-Induced Pressor Responses, Microglia Activation, and Neuroinflammation by Disrupting the Blood–Brain Barrier in Rats. *Journal of the American Heart Association*, *14*(5). https://doi.org/10.1161/JAHA.124.040461

Yue, Q., & Man Hoi, M. (2023). Emerging roles of astrocytes in blood-brain barrier disruption upon amyloid-beta insults in Alzheimer's disease. *Neural Regeneration Research*, *0*(0), 0. https://doi.org/10.4103/1673-5374.367832

Yurekli, A. A., Bilir, N., & Husain, M. J. (2019). Projecting burden of hypertension and its management in Turkey, 2015-2030. *PLOS ONE*, *14*(9), e0221556. https://doi.org/10.1371/journal.pone.0221556

Zaragozá, R. (2020). Transport of Amino Acids Across the Blood-Brain Barrier. *Frontiers in Physiology*, *11*. https://doi.org/10.3389/fphys.2020.00973

Zhang, Kimura, S., Nishiyama, A., Shokoji, T., Rahman, M., & Abe, Y. (2004). ROS During the Acute Phase of Ang II Hypertension Participates in Cardiovascular MAPK Activation But Not Vasoconstriction. *Hypertension*, *43*(1), 117–124. https://doi.org/10.1161/01.HYP.0000105110.12667.F8

Zhang, M., Mao, Y., Ramirez, S. H., Tuma, R. F., & Chabrashvili, T. (2010). Angiotensin II induced cerebral microvascular inflammation and increased blood–brain barrier permeability via oxidative stress. *Neuroscience*, *171*(3), 852–858. https://doi.org/10.1016/j.neuroscience.2010.09.029

Zhang, R. M., McNerney, K. P., Riek, A. E., & Bernal-Mizrachi, C. (2021). Immunity and Hypertension. *Acta Physiologica*, *231*(1). https://doi.org/10.1111/apha.13487

Zhang, W., Xiao, D., Mao, Q., & Xia, H. (2023). Role of neuroinflammation in neurodegeneration development. *Signal Transduction and Targeted Therapy*, *8*(1),

267. https://doi.org/10.1038/s41392-023-01486-5
Zhang, Y., Qi, Y., Gao, Y., Chen, W., Zhou, T., Zang, Y., & Li, J. (2023). Astrocyte metabolism and signaling pathways in the CNS. *Frontiers in Neuroscience*, *17*. https://doi.org/10.3389/fnins.2023.1217451
Zhao, Y., Gan, L., Ren, L., Lin, Y., Ma, C., & Lin, X. (2022). Factors influencing the blood-brain barrier permeability. *Brain Research*, *1788*, 147937. https://doi.org/10.1016/j.brainres.2022.147937
Zhao, Z., & Zlokovic, B. V. (2014). Blood-Brain Barrier: A Dual Life of MFSD2A? *Neuron*, *82*(4), 728–730. https://doi.org/10.1016/j.neuron.2014.05.012
Zhou, B., Perel, P., Mensah, G. A., & Ezzati, M. (2021). Global epidemiology, health burden and effective interventions for elevated blood pressure and hypertension. *Nature Reviews Cardiology*, *18*(11), 785–802. https://doi.org/10.1038/s41569-021-00559-8
Zhou, Y., Ariotti, N., Rae, J., Liang, H., Tillu, V., Tee, S., Bastiani, M., Bademosi, A. T., Collins, B. M., Meunier, F. A., Hancock, J. F., & Parton, R. G. (2021). Caveolin-1 and cavin1 act synergistically to generate a unique lipid environment in caveolae. *Journal of Cell Biology*, *220*(3). https://doi.org/10.1083/jcb.202005138
Zlokovic, B. V. (2011). Neurovascular pathways to neurodegeneration in Alzheimer's disease and other disorders. *Nature Reviews Neuroscience*, *12*(12), 723–738. https://doi.org/10.1038/nrn3114
Zubcevic, J., Santisteban, M. M., Perez, P. D., Arocha, R., Hiller, H., Malphurs, W. L., Colon-Perez, L. M., Sharma, R. K., de Kloet, A., Krause, E. G., Febo, M., & Raizada, M. K. (2017). A Single Angiotensin II Hypertensive Stimulus Is Associated with Prolonged Neuronal and Immune System Activation in Wistar-Kyoto Rats. *Frontiers in Physiology*, *8*. https://doi.org/10.3389/fphys.2017.00592